INFORMATION TO USERS

This manuscript has been reproduced from the microfilm master. UMI films the text directly from the original or copy submitted. Thus, some thesis and dissertation copies are in typewriter face, while others may be from any type of computer printer.

The quality of this reproduction is dependent upon the quality of the copy submitted. Broken or indistinct print, colored or poor quality illustrations and photographs, print bleedthrough, substandard margins, and improper alignment can adversely affect reproduction.

In the unlikely event that the author did not send UMI a complete manuscript and there are missing pages, these will be noted. Also, if unauthorized copyright material had to be removed, a note will indicate the deletion.

Oversize materials (e.g., maps, drawings, charts) are reproduced by sectioning the original, beginning at the upper left-hand corner and continuing from left to right in equal sections with small overlaps.

Photographs included in the original manuscript have been reproduced xerographically in this copy. Higher quality 6" x 9" black and white photographic prints are available for any photographs or illustrations appearing in this copy for an additional charge. Contact UMI directly to order.

Bell & Howell Information and Learning
300 North Zeeb Road, Ann Arbor, MI 48106-1346 USA
800-521-0600

Université d'Ottawa · University of Ottawa

INTERPRETATION OF MULTI-MEDIA GEOCHEMICAL DATASETS USING GIS: APPLICATION TO SW CAPE BRETON ISLAND

by
John L. Buckle

A thesis submitted to the School of Graduate Studies
In Partial Fulfillment of the requirements of the Degree of Masters in Earth Sciences

Ottawa-Carleton Geoscience Centre
University of Ottawa
Ottawa, Ontario, Canada

Abstract

A multimedia geochemical data set, collected in SW Cape Breton Island, was spatially and statistically analyzed to enhance the geochemical understanding and to evaluate the mineral potential of the area. The data sets, which include stream water and balsam fir twig surveys, along with the bedrock geology and the topography with drainage, were integrated and spatially analyzed in a geographic information system. Although stream sediment geochemistry is a well-established sample media in mineral exploration, little work on the statistical analysis of stream water has been done to determine the controls of the geochemistry of the water and to aid mineral exploration.

Catchment basin and statistical analysis, using box plots, of the stream water geochemical survey demonstrated that dominant lithology and pH are the main factors affecting the concentrations of metallic elements in the survey. Multiple regression experiments showed that for these elements pH combined with Fe and Mn explain between 26 and 82 % of the total variation of the metallic element concentrations. The effects of lithology are subordinate to the effects of pH combined with Fe and Mn for all elements except Sr, U, As and Mo which are not correlated with Fe and Mn oxides and hydroxides. Copper and zinc residuals, after removing the combined effects of lithology, pH and Fe and Mn as compared to known mineral occurrences provide better predictors of occurrences than the uncorrected data.

Yule's coefficient was used in two attempts, each with different zones of influence, to compare the stream water and the balsam fir twig survey. Generally it has been shown that the two surveys are not comparable but it has been determined from the results that the zone of influence used to represent each sample point is the most important factor affecting the comparison of the two surveys. As well the stability of each element in solution is an important factor as to whether the two surveys are comparable. Only for elements Fe, Mn and Al, which are unstable in solution and quickly form oxides and hydroxides, were the anomalous values for both surveys comparable when the catchment basin was used to represent the stream water sample points and the smaller zone of influence was used to represent the balsam fir twigs.

The weights of evidence technique is a probability based approach for locating mineral potential using the spatial distribution of known mineral occurrences. The

explanatory variables used to produce a mineral potential map included the underlying bedrock geology, copper residuals from the stream water geochemical survey and the proximity to structural faults. This approach calculates a weight for each class in the multi-class catchment basin maps for copper. These weights show that the maps of residuals, produced using linear regression, are more useful in predicting mineral occurrences than the maps of copper in the raw data. Seven of the fourteen copper occurrences found within catchments are located in the 75^{th} percentile and above class for Cu residuals compared to three of the fourteen are found in the same percentile interval for the raw copper data. A mineral potential map created using the weights of evidence approach was used to produce a map of relative potential (favorability) for locating potential copper mineral occurrences. This map identifies several areas of higher probability of finding an occurrence and could be used as a preliminary step in an exploration program.

Résumé

Un échantillon géochimique multimédia, pris dans le sud-oeust de l'Île du Cap-Breton, a été analysé tant au niveau spatial que statistique afin de contribuer à la compréhension géochimique de la région ainsi qu'à son potentiel en minerais. Comptant des échantillons d'eau de ruisseau et des branches de sapin, et tenant compte de la géologie du socle et de la topographie du drainage, l'échantillon géochimique multimédia, dont la nature spatiale a été analysée, a été intégré dans un système d'informations géographiques. Quoique l'analyse géochimique des sédiments de ruisseau soit une pratique d'échantillonnage bien établie dans le domaine d'exploration minière, peu de travail dans le domaine d'analyse statistique des eaux de ruisseau a été fait afin de premièrement déterminer les contrôles géochimiques de cette eau et secondement aider à l'exploration minière.

Les bassins hydrographiques et l'analyse statistique des échantillons géochimiques d'eau de ruisseau, qui ont été pris à l'aide de 'box plots', démontrent que les principaux facteurs affectant les concentrations des éléments métaliques dans les échantillons sont la lithologie dominante et le pH. Multiple expériences de régression ont démontré que pour ces éléments, le pH combiné avec le Fe et le Mn expliquerait entre 26 et 82 pour-cent de la variation totale des concentrations de l'élément métallique. Les effets de la lithologie sont subordonnés aux effets du pH combiné avec le Fe et le Mn pour tous les éléments sauf le Sr, l'U, le As et le Mo qui eux ne sont pas corrélatifs avec les oxides et les hydroxides de Fe et de Mn. Comparés aux occurences minérales connues, les résidus de cuivre et de zinc, après y avoir fait abstraction des effets combinés de la lithologie, du pH, du Fe et du Mn, sont de meilleurs indicateurs d'occurences que les données non-corrigées.

Le coefficient de Yule a éte utilisé dans deux expériences, chacune ayant une zone d'influence différente, afin de comparer les échantillons d'eau de ruisseau et des branches de sapin. De façon générale, cela a été démontré que les deux échantillons ne peuvent pas être comparés. À partir des résultats il a toutefois été déterminé que la zone d'influence utilisée pour représenter chaque endroit où l'échantillon a été pris est le

facteur le plus important qui affecte la comparaison des deux échantillons. De plus, la stabilité de chacun des éléments en solution est un facteur important quant à savoir si les deux échantillons peuvent être comparés. Seulement pour les éléments Fe, Mn et Al, qui sont instables en solution et qui forment rapidement des oxides et des hydroxides, est-ce que les valeurs anormales des deux échantillons peuvent être utilisées. Il doit être précisé que ceci s'applique seulement lorsque le bassin hydrographique a été utilisé pour représenter les points de prélèvement d'eau de ruisseau et que la plus petite zone d'influence a été utilisée pour représenter les branches de sapin.

La modélisation à pondération de donnees est une approche basée sur la probabilité d'identifier géographiquement les régions pouvant contenir des minerais en distribuant de façon spatiale les occurences connues de minerais. Les variables utilisées afin de produire une carte d'une région pouvant contenir des minerais sont la géologie du socle, les résidus de cuivre contenus dans l'échantillon géochimique de l'eau du ruisseau et la proximité de la région à une faille structurale. Cette approche calcule de pondération pour chacune des catégories dans un bassin hydrographique à multiple catégories le nuveau d'occurrence de cuivre à représentes sur la carte. Ces de pondération démontrent que les cartes de résidus, produites à partir des régressions linéaires, sont plus utiles à prédire les occurences de minerais que des cartes de cuivre dessinées à partir d'information non-traitées. Sept des quatorze occurences de cuivre identifiées à l'intérieur des bassins hydrographiques se situent dans la catégorie de 75 pour-cent et plus pour les résidus de Cu comparé à trois des quatorze occurences qui out été identifiérs à partier de donnés de cuivre non-analysiés. Une carte à potentiel minéral a été dessinée à partir du modélisation à pondération de donnees. Cette carte a ensuite servi afin d'en créer une seconde démontrant le potentiel relatif favorable à la localisation d'occurences potentielles de minerais de cuivre. Cette seconde carte identifie plusieurs régions où il y aurait haute probabilité de trouver une occurrence et elle pourrait servir d'étape préliminaire dans un programme d'exploration.

Table of Contents

List of Figures

List of Tables

List of Equations

Acknowledgments

I would first of all like to thank Dr. Graeme Bonham-Carter, my thesis supervisor, who I was very fortunate to have worked with, who provided the opportunity to partake in this project and took the time to discuss and help solve many problems.

From the Geological Survey of Canada I would like to thank Gwendy Hall who provided the initial financial support for this project and for her encouragement and helpful advice throughout the completion of this work. Dr. Al Sangster who provided insight to the regional geology and mineral deposit data of the study area, through discussions with Al many of my results were interpretable. Deb Kliza, my office mate and field partner, who showed me the ropes at the GSC and was always available for advice. To Danny Wright whose GIS knowledge and willingness to help provided me with solutions to numerous GIS problems. Thanks to Pierre Pelchat who helped with the field methodology and the quality control of the stream water samples.

I would like to express my gratitude to fellow graduate student Mark Mihalasky who taught me how to use Spans and provided continual insight through many discussions and conversations.

Thanks to my fellow students who took courses with me and tolerated my point and click approach to GIS, especially Brad Sim, Alice Deschamps and Simone Riopel. Thanks to other graduate students who helped make the last couple of years memorable, especially to Brian Luinstra, Julie Brown, Kelli Powis and Sean McClenaghan.

Very big thanks to Dave Cherry and Bridgett Malon whose outlook on life made apres thesis time very enjoyable.

Special thanks to my parents, my first teachers, whose continual support and encouragement provided all possible opportunities to further my education and complete this project.

A final extra special thanks to Andrea without whose support, faith and love this achievement would not have been possible.

1. Introduction

Geographic information systems (GIS) are used in mineral exploration to combine different types of spatial data in order to describe and analyze their interactions, and to make predictions with mineral exploration models for the purpose of locating exploration targets. Mineral exploration involves the collection, analysis, and integration of data from numerous sources. Traditionally the exploration geologist has manually, with the aid of a light table, integrated these data sources to define areas of interest or exploration targets. The results produced were often subjective and difficult to reproduce. Today, much of the integration work is done on a computer using a GIS, which allows numerous data layers to be incorporated and compared more efficiently than by traditional methods. Also a mineral exploration model can be used to guide the integration of geological data within the GIS to produce a mineral potential map of a study area.

Regional geochemical surveys involve the use of different sample media and analysis techniques, often resulting in several different data sets from the same study area. It has been shown in numerous studies that surficial geochemical media such as sediment and water from streams and lakes, soils, glacial tills, and vegetation can reflect the variation in underlying bedrock geology and are effective tools in locating the presence of mineral deposits. Spatial and statistical analysis is an essential step in the interpretation of a geochemical data set to locate trends and anomalies.

Recent developments in the use of GIS in earth sciences coupled with traditional statistical analysis have provided new ways to evaluate geological data. Catchment basin analysis facilitated by GIS, has enabled the linking of stream and lake sediment geochemistry to underlying bedrock and surficial geology so that statistical relationships can be shown. Catchment basin and regression analysis has been effectively used to determine the major controls, such as lithology, pH, and Fe and Mn oxides and hydroxides, on the geochemistry of stream sediments and subsequently to remove the effects of these controls in identifying potential mineral anomalies (Bonham-Carter and Goodfellow, 1986; Bonham-Carter et al., 1987). GIS are useful in the comparison of different data sets because they provide tools for visualization. In contrast, tools such as Pearson's correlation coefficient (r) are unsuitable because 1) they ignore spatial locations, and 2) data values are equally weighted over the entire range instead of focusing mainly on anomalous values. GIS facilitates the construction of binary maps (based on various methods of threshold selection) for pairs of continuous geochemical maps which can then be compared by the amount of spatial overlap (Bonham-Cater, 1994).

A GIS can also be used to incorporate geochemical surveys with other geological data to predict the mineral potential of an area. Previous mineral potential studies using this method include the prediction of Cu deposits in Chisel Lake-Anderson Lake Manitoba (Wright and Bonham-Carter, 1996) and in the location of gold mineralization in Nova Scotia (Wright, 1996).

Southwestern Cape Breton Island is a major region of mineral exploration in Eastern Canada. In the summer of 1995 detailed stream water and balsam fir twig geochemical surveys (Dunn and Balma, 1997) were conducted in Southwest Cape Breton Island. The study area overlies three litho-tectonic terranes, the Mira terrane, the Bras d'Or terrane, and the Aspy terrane (Figure 1.1). Within the study area there are numerous mineral showings and several deposits, most notably the Lime Hill Zinc Deposit, the Jubilee Lead Zinc deposit, and the Upper Glenco Iron Deposit. Excellent regional and surficial geological databases with extensive stream water and balsam fir geochemical surveys make this study area an ideal location for a statistical and GIS data integration study. Although previous studies have used the catchment basin approach to analyze stream sediment geochemistry, this study uses catchment basins to analyze stream water geochemical data. This study focused on the integration of stream water and balsam fir geochemical and geological data sets to better understand the factors that control the geochemistry of stream water and to predict the mineral potential of the area.

1.2 Objectives

The objectives of this study were:

1) To determine the physical and chemical factors controlling the geochemistry of the metallic elements in the stream water survey.

2) To use multiple linear regression analysis to show the variability of the water geochemistry caused by the underlying bedrock geology, pH, and Fe and Mn oxides and

hydroxides and to remove these background effects to locate potential mineral anomalies or other controlling factors.

3) To test a new method, using Yule's coefficient, for comparing the similarity between geochemical maps.

4) To use the weights of evidence method (Bonham-Carter, 1994, ch. 9) to produce a mineral potential map for copper in the study area and to show the effectiveness of linear regression to remove the background effects on the stream water geochemistry.

1.3 Location of Field Area

The study area is located in Southwestern Cape Breton Island (Figure 1.1). It comprises map sheets 11F/10, 11F/11, 11F/14, and 11F/15, and portions of 11K/2 and 11K/3. This area covers a total area of approximately 2,000 square kilometers. The Strait of Canso represents the western boundary and the eastern boundary extends along longitude 60° 45'. The southern boundary extends along latitude 45° 30' and the northern boundary extends along latitude 46° 05'.

1.4 Geological Setting of the Study Area

The study area is underlain by 3 litho-tectonic terranes of the Appalachian Orogeny, the Mira, Bras d'Or and the Aspy. The Mira terrane has been correlated to the Avalon zone in Newfoundland (Barr and Raeside, 1989) and is predominantly comprised of Late Precambrian sedimentary and volcanic rocks overlain by Cambrian to Early Ordovician

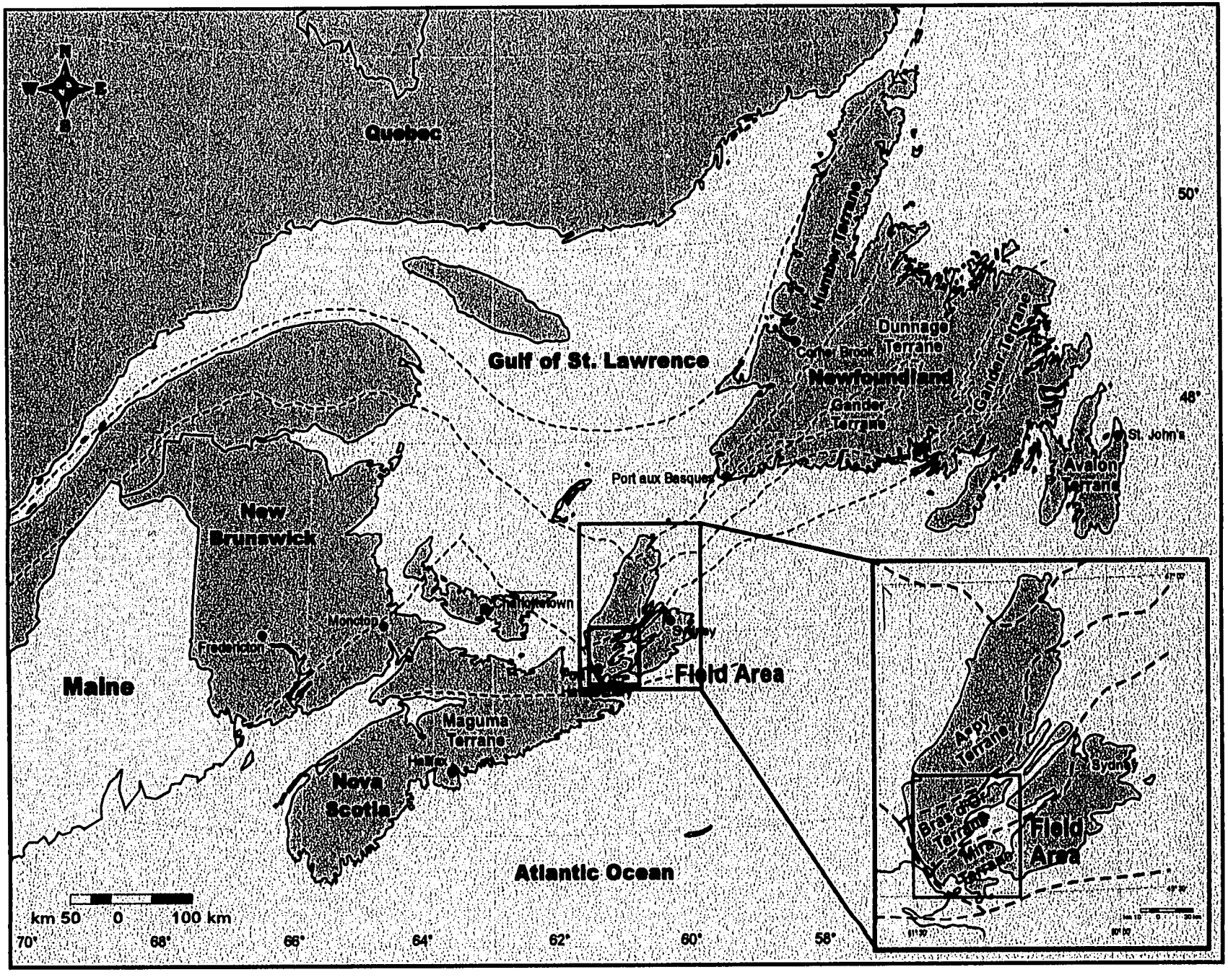

Figure 1.1. Location of field area in Eastern Canada with litho-tectonic terrane boundaries (Modified after Williams et al., 1988).

shales and sandstones. The Bras d'Or terrane is correlated with the Gander terrane in Newfoundland and is comprised of Neoproterozoic rocks, which are low pressure cordierite-andalusite gneissic units in faulted contact with low- to high-grade metasedimentary and minor meta-volcanic rocks, intruded by dioritic to granitic rocks, and Late Cambrian to Early Ordovician granitic plutons (Raeside and Barr, 1990). The Aspy terrane is composed of fragments of Bras d'Or crust and is equivalent to components of the Gander and Dunnage terranes of Newfoundland. The rocks consist of Ordovician and Silurian sedimentary and volcanic units which were intruded and metamorphosed by Silurian and Devonian granitic plutonism. The earliest post-orogenic sedimentary rocks consisted of Lower to Middle Devonian redbed conglomerates, arkosic sandstones and mudstones, locally with intercalated felsic and/or mafic volcanic flows, the Horton Group. In the Middle Carboniferous, sedimentation increased producing extensive deposits of red and grey terrigenous clastic, oil shales, coal, carbonates, and evaporites.

The Mira terrane is comprised of a series of volcanic-sedimentary-plutonic belts of different Neoproterozoic ages, separated by faults and younger cover sequences (Barr et al., 1996). The oldest units are from the Stirling belt, not found in the study area, (680 Ma; (Bevier et al., 1993)) which include mafic to felsic flows and pyroclastic rocks interbedded with tuffaceous sedimentary rocks, probably formed in a rift basin within a volcanic arc (MacDonald and Barr, 1993). High pottasium calc-alkalic rocks, (units Hcgd, Hd, Hgd and HDg) (Figure 1-3) in the field area, believed to have formed at a continental margin subduction zone (Barr, 1993) are dated to be 620 Ma, and are comprised of volcanic and

volcaniclastic rocks and cogenetic dioritic to granitic plutons. Major faults within and between the Neoproterozoic belts in the Mira terrane have unknown amount of offset, hence the origin of the belts relative to one another is uncertain making the Mira terrane a Neoproterozoic composite terrane.

The Bras d'Or terrane is characterized by Neoproterozoic rocks. Late Proterozoic rocks in the Bras d'Or zone include gneissic and lower grade metasedimentary and metavolcanic rocks, as well as plutonic rocks. Granitoid rocks dated by Dunning et al. (1990) are extensive in this zone and together with cogenetic metavolcanic rocks, have petrochemical characteristics of a continental-margin subduction zone (Raeside and Barr, 1990). Metamorphism of the metavolcanic units is dated to be 637 Ma. (Keppie, 1993). The plutonic rocks which have intruded the metamorphic rocks are dated to be 575 Ma. (Dunning et al., 1990). The Neoproterozoic rocks are overthrust by Silurian volcano-sedimentary successions of the Aspy terrane. The Bras d'Or zone is separated from the Aspy terrane by the Eastern Highlands Shear zone, a mainly ductile zone up to 800 m wide.

The Aspy terrane is characterized by Ordovician and Silurian sedimentary and volcanic rocks, which were affected by Silurian and Devonian granitic plutonism and metamorphism. The metamorphic rocks include greenschist- and amphibolite-facies phyllites and schists derived from volcanic and clastic protoliths, upper-amphibolites-facies paragneisses of similar composition and granitoid orthogneiss. These rocks form a belt of mafic volcanic rocks overlain by felsic pyroclastic rocks that inter-finger with clastic sedimentary rocks (Jamieson et al., 1986). The centre of felsic volcanism appears to have

been in the southeastern Aspy terrane, and the relative proportion of sedimentary rocks increases to the north and west. Deformation and metamorphism, combined with poor exposure, make it difficult to determine whether tectonic or stratigraphic breaks exist within the meta-volcanic-metasedimentary belt, and the relation of the phyllites and schists to the gneisses is controversial. Orthogneisses in the Aspy terrane are predominantly granitic to tonalitic in composition. The metamorphic rocks of the Aspy terrane are bounded on the southwest by the Cheticamp pluton and associate diorite and gneiss (Barr et al., 1998).

Within the study area the post orogenic sedimentary rocks consist of four main groups, the Horton Group, the Windsor Group, the Mabou Group and the Cumberland Group. The Horton Group (units CHA, CHS, CHJ, DCHC, DCH, DCFB and DCF, Figure 1-2) is of Late-Devonian to Early Carboniferous in age. It is comprised of red and grey-green conglomerates, arkosic sandstones, mudstones, oil shales, and minor non-marine evaporites. Conformably overlying this unit is the Windsor Group (units CWU, CWL and CM, Figure 1-2) of Early Carboniferous age. This group is comprised of marine limestones, evaporites, and intercalated redbeds. The Windsor Group grades upwards into the Mabou Group (units CMU, CML and CM, Figure 1-2) of Early-Middle Carboniferous age. This unit was deposited following the final marine withdrawal and is comprised of red and grey terrestrial strata. The Cumberland Group (unit Cc and CCPHL Figure 1-2) conformably overlies the Mabou Group and is Middle Carboniferous in age. The Cumberland Group consists of red and grey fluvial conglomerates and sandstones.

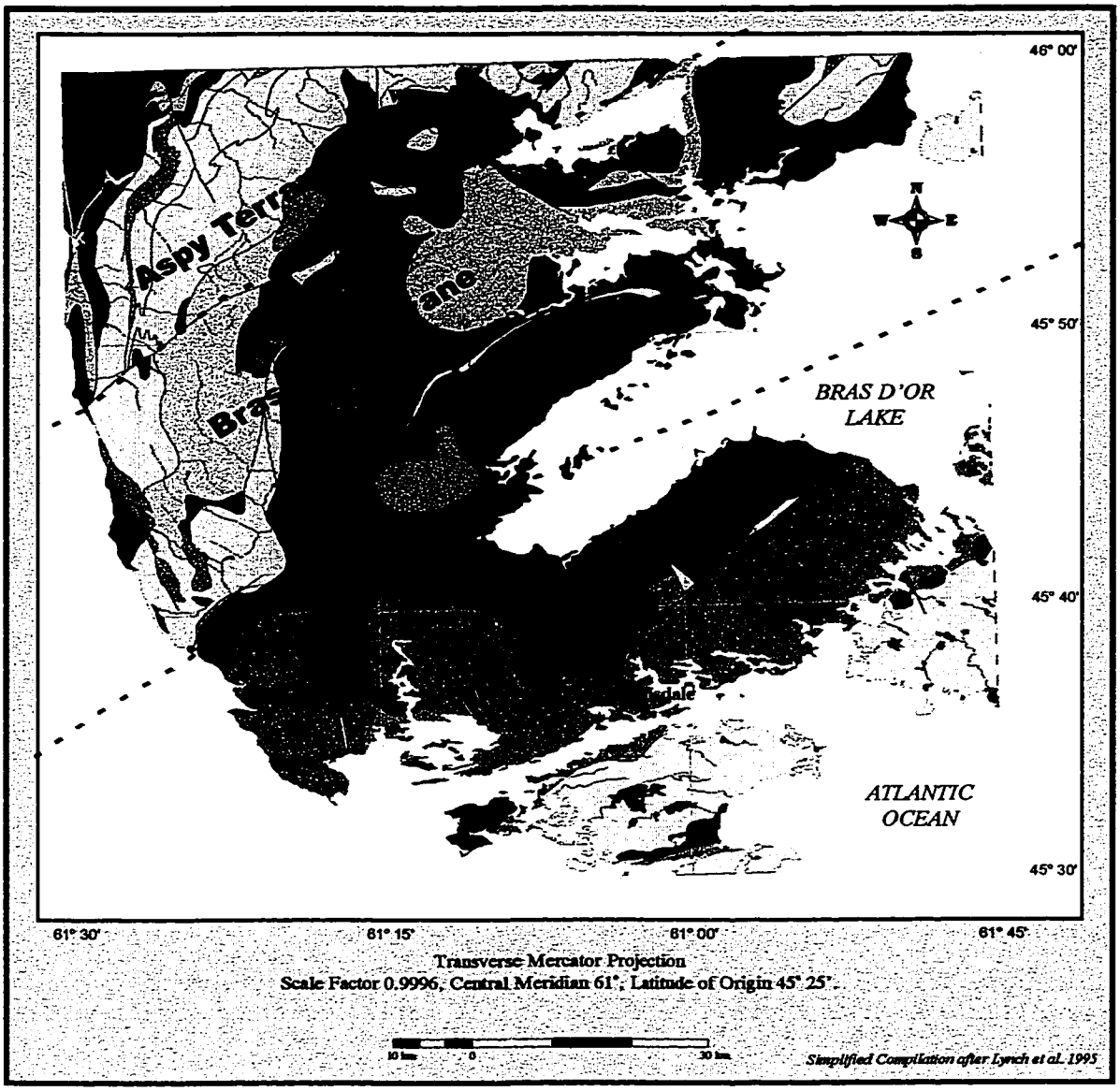

Figure 1.2. Bedrock geology of study area with mineral deposits and approximate terrane boundaries.

WESTPHALIAN-STEPHANIAN

CUMBERLAND GROUP
Lower Port Hood Formation: channelized sandstone deposits, siltstone, shale

cross-bedded and trough cross-bedded white medium sand arkose, minor siltstone, shale, and coal, equivalent to *Port Hood Formation*

NAMURIAN

gabbro, diabase

MABOU GROUP

Upper member including *Pomquet Formation*: red and green siltstone and sandstone, minor conglomerates

Lower member including *Hastings Formation*: shale and siltstone, dolomitic siltstone, and thin stromatolitic dolostone beds

undifferentiated Mabou Group

VISEAN

WINDSOR GROUP

CWU — Upper member including *Herbert River* limestone: red siltstone and sandstone with intercalated shallow marine limestone, dolostone, gypsum and halite

Lower member: limestone variably dolomitic and fossiliferous, red siltstone and thick units of gypsum and halite

CW — undifferentiated Windsor Group

LATE DEVONIAN TO CARBONIFEROUS FAMENNIAN-TOURNASIAN

HORTON GROUP

CHA — *Ainsle Formation*: cross-bedded sandstone and conglomerate, siltstone, mostly fluviatile deposits

CHS — *Strathlorne Formation*: grey and red siltstone, sandstone, micritic limestone, conglomerate with carbonate clasts

CHJ — *Judique Formation*: red cross-bedded medium to coarse sand lithic arkose, sandstone, minor conglomerate

DCHC — *Craignish Formation*: dominantly conglomerate with red and grey sandstone, thick and thinly bedded, alluvial fan facies

DCH — undifferentiated Horton Group

Fisset Brook Formation, basalt member: vesicular porphyritic basalt and andesite, with minor interbedded redbed siltstone and conglomerate

Fisset Brook Formation: vesicular basalt, rhyolite, red siltstone, sandstone, conglomerate

UNCERTAIN AGE

mylonitic granite, diorite, and mylonitic gneiss, biotite-garnet schist

HDG — medium grained variably foliated granite

diorite

amphibolite

ORDOVICIAN

monzogranite

NEOPROTEROZOIC-CAMBRIAN

medium grained granodiorite (includes Capelin Cove pluton)

LATE NEOPROTEROZOIC

gneiss

granodiorite

PRINGLE MOUNTAIN GROUP

varied basaltic to rhyolitic lapilli tuff and ash tuff, minor rhyolite flows

NEOPROTEROZOIC-PALEOPROTEROZOIC

GEORGE RIVER GROUP

limestone, marble, dolostone, calc-silicate rock, quartzite, feldspathic arenite, wacke, minor mafic metavolcanic rocks

marble, calc-silicate rock, gneiss, minor quartzite

quartzite, psammitic schist, quartzo-feldspathic gneiss,minor calc-silicate rock and amphibolite

biotite and chlorite schist, metawacke, marble, dolostone
Clac-silicate rock, quartzite, gneiss, schist, mafic metavolcanic rocks, amphibolite

POLLETS COVE RIVER GROUP

monzonite, diorite, gabbro

Figure 1.3. Legend for regional geology

The 30-unit geology map was reclassified to four main units in order to simplify calculations in later sections (Figure 1.4). With fewer groups the complex relationships between the minor units are obscured but this reclassification reveals the major trends in the data. The reclassification scheme was based on the following major litho-tectonic divisions; basement rock, the Horton Group, the Windsor Group and Carboniferous Clastics.

1.5 Mineral Deposits

Cape Breton Island has a rich history of mineral exploration and mining. In south-west Cape Breton Island there are three main deposit types: Precambrian metamorphosed carbonate-hosted strata-bound sulphide deposits, gold deposits, and carbonate-hosted base metal deposits. Swinden and Dunsworth (1995) have described these deposit types in detail. The Lime Hill Zinc deposit, located in the central part of the field area (Figure 1.2) on the shores of Bras d'Or Lake, is a carbonate-hosted strata-bound sulphide deposit. This deposit is hosted in Precambrian marble of the Lime Hill gneissic complex (Justino and Sangster, 1987) and consists of bands of massive and disseminated sphalerite, and minor pyrrhotite and pyrite, in serpentine dolomite and pure dolomite marble. Sangster, et al. (1990a) interpreted this deposit as a carbonate-hosted strata-bound sulphide deposit and suggested it may be a fault block of Grenville basement rock.

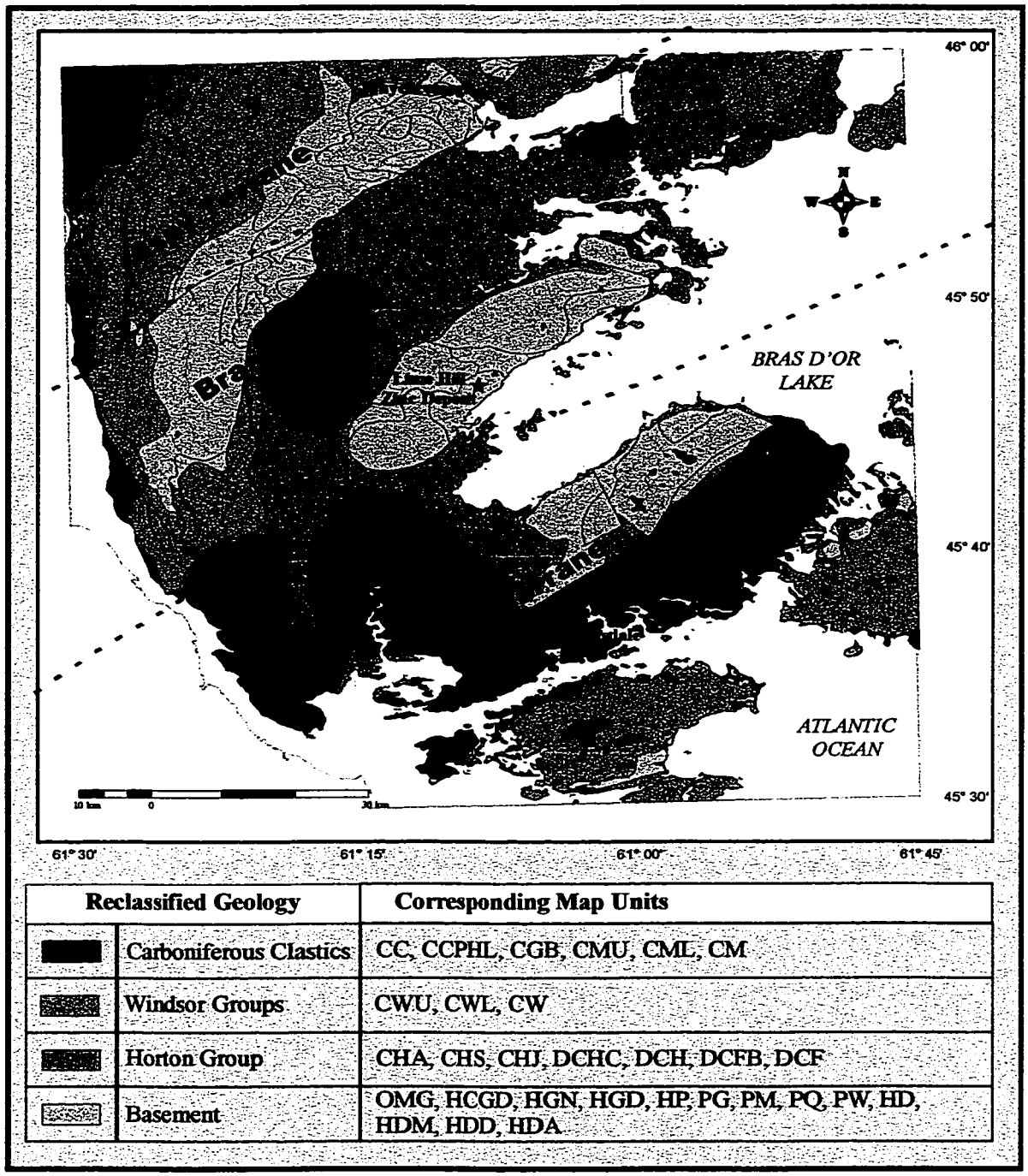

Reclassified Geology		Corresponding Map Units
	Carboniferous Clastics	CC, CCPHL, CGB, CMU, CML, CM
	Windsor Groups	CWU, CWL, CW
	Horton Group	CHA, CHS, CHJ, DCHC, DCH, DCFB, DCF
	Basement	OMG, HCGD, HGN, HGD, HP, PG, PM, PQ, PW, HD, HDM, HDD, HDA

Figure 1.4. Reclassified bedrock geology of study area with mineral deposits and approximate terrane boundaries.

The second type of mineral deposit in the field area consists of structurally controlled mesothermal vein-type gold occurrences. These occurrences are found in the Bras d'Or and Aspy terranes (Sangster et al., 1990b). The occurrences are found in narrow shear veins and extension gash veins associated with north trending fault zones which cut Cambrian granitoid intrusions and dacite tuff (MacDonald and Barr, 1985).

The third mineral deposit type comprises carbonate-hosted base metal deposits, such as the Jubilee Lead Zinc deposit (Figure 1.2). These deposits are restricted to the base of the Windsor Group, occurring in cyclic marine evaporites. The Horton Group, composed of siliciclastics (dominantly redbeds), underlies the Windsor Group. This contact, interpreted as a marine/terrestrial transition, is the location of numerous base metal, pyrite, siderite and barite occurrences (Kirkham, 1985). The Cu-Pb-Zn sulphides are believed to have been deposited at the base of the Windsor Group, where there was a redox boundary. The concentration and deposition of sulphides occurred where upward moving metalliferous brines from the underlying redbeds infiltrated anoxic carbonaceous strata (Figure 1.5) (Kirkham, 1985).

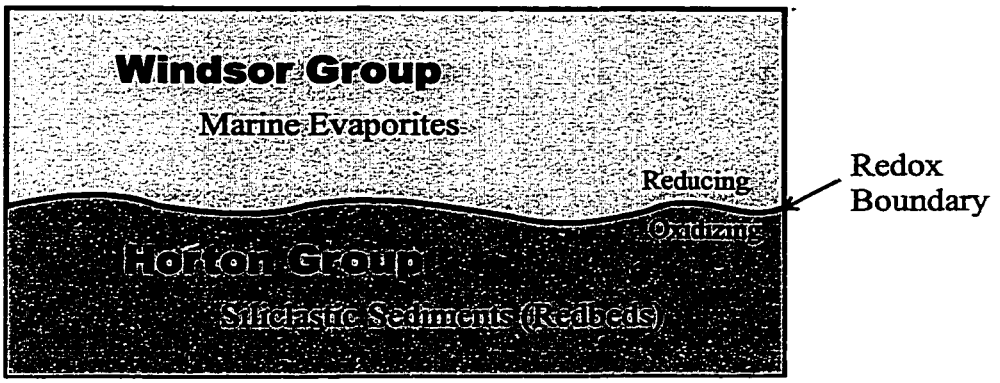

Figure 1.5. Schematic model of environment for carbonate-hosted base metal deposition (After Kirkham, 1985).

2 The GIS Study Area

The GIS software used in this study were Spans GIS (Tydac Inc, 1997), TYDIG (Tydac Inc., 1995), ArcView (ArcView, 1999), MapInfo (Mapinfo Corporation, 1996), and Vertical Mapper (Northwood Geosciences, 1998). Spans was the main GIS used for the preliminary data compilation and analysis. MapInfo and Vertical Mapper were used to contour and grid the geochemical data which was then transferred back to Spans. ArcView was used to model and map the mineral potential of the area, using an Avenue extension (ArcWofe) and Spatial Analyst (ESRI, 1999).

2.1.1 Projection

The details of the projection used in the GIS study area for this project are:

Universal Transverse Mercator	
Datum	1866, Clarke, North America.
UTM Zone	20
Central Meridian	63°W
Latitude of Origin	0° N
Scale Factor	0.9996
X-coordinate of false origin	500000 m
Y-coordinate of false origin	0 m

This projection was chosen to minimize distortion for the map scale used in this study.

2.1.2 Resolution

For the Cape Breton study area, the maximum attainable cell resolution Spans, in raster format, is 6.6395 m x 6.6395 m. This is because Spans uses a hierarchical compression data structure termed a quadtree (Bonham-Carter, 1994, Ch. 3). A Spans study area (termed a "Universe") is successively divided into quadrants. The length of the side of a universe is 2^0 X 2^0 or 1 X 1 quads. After subdivision at the first level the universe has 2^1 X 2^1 = 2 X 2 quads at level 1. After fifteen hierarchical subdivisions (the maximum in Spans), the universe has 2^{15} X 2^{15} = 32768 X 32768 quads at level 15. Notice at level X, the quads are 4 times smaller than at level X-1. In this study area a quad level of 14 was used, where the quad size (equivalent to 1 pixel at this resolution) is 13.279 m x 13.279 m, a resolution that was more than adequate for the data.

2.1.3 Extents

The geographical extents of the four corners of the Spans study area are:

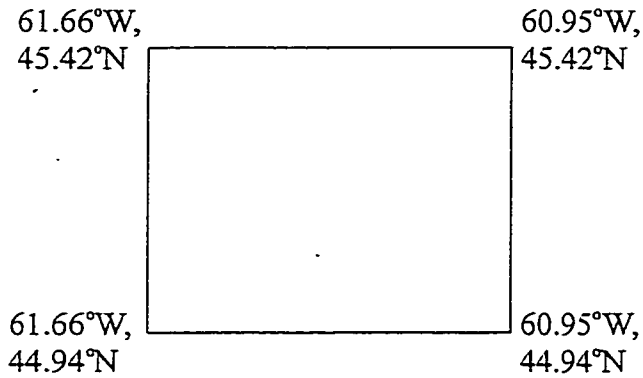

2.2 GIS Database

2.2.1 Stream Water Geochemistry

A regional stream water geochemical survey was conducted in Southwest Cape Breton Island in the summer of 1995. The samples were collected over a one month period. This resulted in the collection of 343 water samples. The samples were collected at least 5m from roads to decrease the chance of contamination. High-density polyethylene sample bottles were rinsed twice before the collection of the sample. 250 ml and 125 ml of water was collected for cation and anion analyses, respectively. All samples were filtered with a 0.45-micrometer millipore filter and cation samples were acidified with 0.4% nitric acid. One duplicate sample was collected in every 10. These samples were analyzed for alkalinity and over 35 major and trace constituents at the Geological Survey of Canada. This study focused on the metallic elements, such as Fe, Mg, Hg, Mn, Al, Cr, Co, Cu, Zn, As, and Sb, although other elements included Na, K, Ca, Si, Li, Be, Ti, V, Y, Ba, La, Ce, Pr, Nd, Sm, Eu, Gd, Tb, Dy, Ho, Er, Yb, SO_4, and Cl. A summary of the analytical methods used is outlined in Table 2.1. Analytical results with detection limits can be found in Appendix A. Results of general statistical analyses including mean, median, mode, and standard deviation for each element can be found in Table 2.2.

In order to link these data to the GIS database, the geographical coordinates of the sampling sites were determined from 1:50,000 scale National Topographic Series (NTS) maps. The entire data set was then imported into the Spans study area for further data analyses.

Stream Water Survey	
Elements	Method
Na, K, Ca	AAS
Fe, Hg, Mn, Al, Li, Be, Ti, V, Cr, Co, Cu, Zn, As, Y, Mo, Sb, Ba, La, Ce, Pr, Nd, Sm, Eu, Gd, Tb, Dy, Ho, Er, Yb, Pb, U	ICP-MS
Si, Mg	ICP-ES
SO_4, Cl	DIC
Balsam Fir Twig Survey	
Elements	Method
As, Au, Ba, Br, Ca, Ce, Co, Cr, Cs, Eu, Fe, Hf, K, La, Lu, Mo, Na, Nd, Rb, Sb, Sc, Sm, Sr, Th, U, Yb, Zn	INAA
Al, B, Cd, Cu, Li, Mg, Mn, Ni, P, Pb, V	ICP-ES
AAS – Atomic Absorption Spectroscopy ICP-MS – Inductively Coupled Plasma Mass Spectrometry ICP-ES – Inductively Coupled Emission Spectrometry DIC – Dionex Ion Chromatography INAA – Instrumental Neutron Activation Analysis	

Table 2-1. Stream water and balsam fir twigs were analyzed for major and minor elements by methods listed above.

Element	Detection Limit	Min value	Max value	Mean	Median	Standard Deviation
Fe	5.0	5.0	1113.0	160.9	123.0	152.0
Mg	50	348.0	9126.0	1158.6	820.0	1061.0
Mn	0.1	0.2	255.4	15.2	7.9	24.5
Al	2.0	3.0	626.0	162.4	129.0	121.0
Ti	0.5	0.5	7.7	1.7	1.5	0.8
Cr	0.1	0.1	1.1	0.3	.03	0.3
Co	0.05	0.05	0.6	0.1	0.09	.08
Cu	0.1	0.1	2.3	0.5	0.5	0.3
Zn	0.5	0.5	11.0	1.7	1.3	1.2
As	0.1	0.1	3.3	0.4	0.3	0.28
Sr	0.5	4.1	1943.7	53.7	13.4	0.2
Mo	0.1	0.1	1.6	0.2	0.1	0.15
Sb	0.01	0.01	0.1	0.02	0.02	0.01
Pb	0.1	0.1	1.5	0.3	0.1	0.1
U	.005	.005	0.8	0.07	0.04	0.09
Units in PPB						

Table 2-2. Summary statistics of the stream water geochemistry

2.2.2 Quality Control

As part of this study, quality control on the stream water geochemical data was carried out according to specifications outlined by the Geological Survey of Canada. Detailed descriptions of field collection methods are given in Friske and Hornbrook (1991) and descriptions of analytical accuracy and precision are given by Garrett (1991). To

evaluate the accuracy of the analytical results in-house reference samples were analyzed over 60 times throughout the analysis of the stream water samples. Results of the stream water geochemistry can be found in Appendix A. The accuracy of the geochemical analysis was calculated using the following equation:

Accuracy = absolute value ((Expected – Average) / Expected) * 100%

where the expected value is the known concentration of the reference sample and the average is the average concentration of the element for the standards run during the analyses (Garrett, 1991). In general, the analytical results are accepted if the results from the above equation are less than 10%. For the metallic elements used in this study the accuracy was close to or less than 10%.

The coefficient of variation of the reference sample was used to evaluate the precision of the analytical results.

Coefficient of variation = (standard deviation / average of reference samples) * 100.

The coefficients of variation of the reference sample for the metallic elements used in this study range from 4% to 29% (Table 2.3). As a result, the analytical results were considered to be acceptable and all metallic elements were used in this study.

The precision of field duplicates was determined graphically by a method proposed by Thompson and Howarth (1978) Appendix B. This method produces a log-log plot of difference between duplicate analysis (Y-axis) against their mean (x-axis) (Figure 2.1). Control lines are also plotted on these graphs to show various levels of precision. In this study lines for the 95th confidence limit for two levels of precision, +/- 10% and +/- 20%,

were plotted. The idea is to find the confidence limit (line) at which 95% of the duplicate pairs occur below the line. Conversely, at the selected confidence level (line) only 5% of the pairs should occur above the line.

	Coefficient of Variation
Fe_ppm_ms	4.74
Mg_ppm_es	0.35
Mn_ppM_ms	4.74
Al_ppm_ms	9.43
Ti_ppm_ms	11.40
Cr_ppm_ms	11.80
Co_ppM_ms	22.20
Cu_ppM_ms	21.50
Zn_ppM_ms	23.30
As_ppm_ms	29.10
Sr_ppm_ms	7.59
Mo_ppm_ms	14.50
Sb_ppm_ms	9.83
Pb_ppm_ms	14.30
U_ppm_ms	8.00

Table 2-3. Coefficient of variation calculated to estimate precision of analytical results of the reference sample analyzed during the analyses of the water data.

Thompson-Howarth plots were constructed for the metallic elements used in this study in order to estimate the level of precision. The results show that the precision for elements Fe, Mg, Mn, Al, Ti, Cr, Co, Zn, Cu, Sr, Mo, Pb and U was good. For elements Hg, Sb and As the precision was poor.

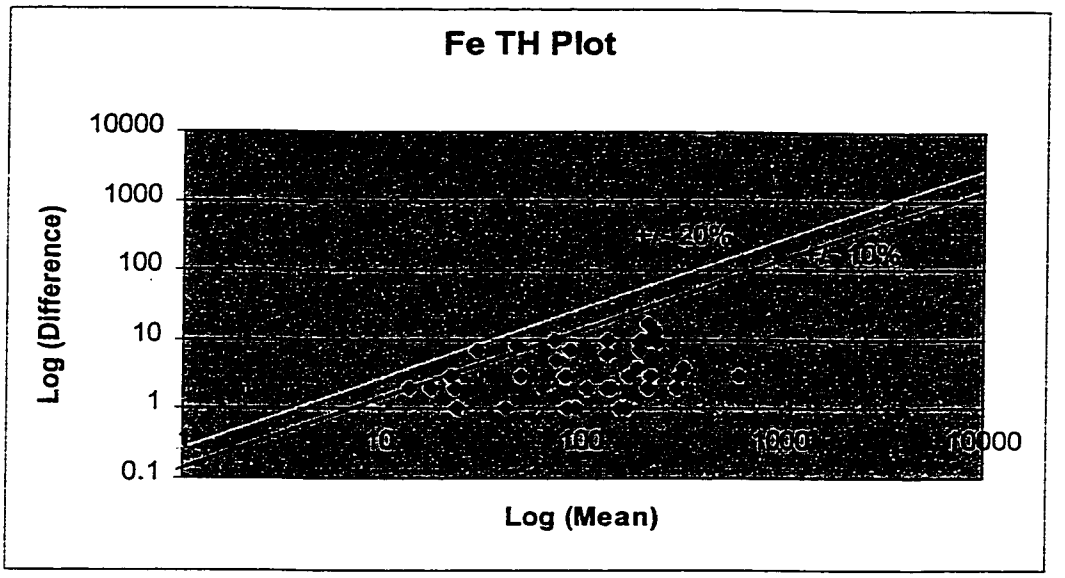

Figure 2-1. Thompson-Howarth plot for Fe. The top line is the 95th percentile with 20% error, the second line is for 10% error. All sample points plot below the 20% error line, and about 3 points occur on or above the 10% line. Given n=35 pairs, 5% is equal to 2-3. Thus the precision is close to +/- 10%.

2.2.3 Balsam Fir Twig Geochemistry

In conjunction with the stream water survey Dunn and Balma (1997) carried out a regional balsam fir twig survey in Southwest Cape Breton Island during the summer of 1995. This survey resulted in the collection of 365 samples, which were analyzed for over 30 constituents at the Geological Survey of Canada. The samples taken consisted of twigs and needles representing 5 –7 years of growth, all twig samples had a similar diameter and bark to wood ratio. Of those analyzed the metallic elements were used to compare results from the stream water survey. Analytical results with detection limits can be found in Appendix

C. A summary of the analytical methods used is outlined in Table 2.1 and a summary of the statistics can be found in Table 2.4.

In order to link these data to the GIS database, the geographical coordinates of the sampling sites were determined from 1:50,000 scale National Topographic Series (NTS) maps. The entire table of analyses was then imported into the Spans database for spatial analyses.

Summary Statistics						
Element	Detection Limit	Min value	Max value	Mean	Median	Standard Deviation
As	0.5	0.5	6.0	1.8	1.8	1.0
Co	1.0	1.0	15.0	4.7	4.0	2.2
Cr	1.0	1.0	100.0	25.2	18.0	20.0
Fe	500.0	500.0	14400.0	3060.5	2400.0	1960.1
Sb	0.1	0.1	1.9	0.4	0.4	0.15
Sr	300.0	300.0	5800.0	803.2	780.0	631.3
Zn	20.0	960.0	4200.0	1963.4	1900.0	502.3
Al	0.1	0.1	14300.0	5336.4	5200.0	2126.1
Cu	1.0	99.0	244.0	150.4	148.0	33.4
Mg	10.0	10.0	48400.0	25495.3	26000.0	6397.2
Mn	1.0	1407.0	84622.0	22911.2	20759.0	11728.3
Pb	3.0	14.0	124.0	51.2	48.0	20.9
Values in ppm						

Table 2-4. Summary statistics for the balsam fir twig survey.

2.2.4 Geological Data

The bedrock geology for this study area was obtained as a simplified digital version, in e00 format at 1:250,000 scale, of a geological map (Dunn and Balma, 1997) of Cape

Breton Island produced by Lynch et al. (1995). This map was imported into the study area with the lithological attribute data. The geological map was further simplified to four main groups of units in order to reduce the complexity of analysis (Table 2.5). The map units were used in the regression study, whereas the reclassified units were used in the box plots (see next chapter).

Reclassified Unit	Map Units
Carboniferous Clastics	CC, CCPHL, CGB, CMU, CML, CM
Windsor Group	CWU, CWL, CW
Horton Group	CHA, CHS, CHJ, DCHC, DCH, DCFB, DCF
Basement Rock	OMG, HCGD, HGN, HGD, HP, PG, PM, PQ, PW, HD, HDM, HDD, HDA

Table 2-5. Reclassification scheme used to simplify the bedrock geology.

2.2.5 Mineral Occurrence Data

The mineral occurrence data were obtained from the Nova Scotia Department of Mines and Energy Mineral Occurrence Database (NSDNR, 1996). This table was imported into the Spans database as a point data set. The table contains 78 metallic mineral occurrences, comprised of deposits, occurrences, and showings. Of importance are the Upper Glenco Fe deposit and the Lime Hill Zinc deposit (Appendix D).

2.2.6 Topographic Data

The topographic data include contours, the road network, the coastline, and the drainage. The data were obtained in DXF digital format from Geomatics Canada of the Department of Natural Resources. The digital base was produced by joining four 1:50,000, NAD 27, Universal Transverse Mercator zone 20 bases (11F/10, 11F/11, 11F/14, 11F/15).

2.2.7 Catchment Basins

The upstream segments of catchment basins for the stream water sample locations were manually digitized using Tydig from 1:50,000 NTS maps (11F/10, 11F/11, 11F/14, and 11F/15). These watershed basins were then imported into Spans and treated as polygon objects. The stream water data table was appended so that each geochemical sample location has a watershed associated with it. The basins could then be considered as the zones of influence for the sample points. The representation of the sample points as areas enables other map layers to be overlain and resampled, thereby providing a link between the stream water geochemistry and the bedrock geology.

3 Analysis of Stream Water Geochemical Data

3.1 Introduction

The goals of this section are to describe the characteristics of the stream water geochemical variables and to determine the physical and chemical controls of the variables using spatial and statistical analyses. Catchment basin analysis was used to show the distribution of the elements and relate the geochemistry to the underlying geology. Box plots (Tukey, 1977) were used to show the effects of lithology, pH and Fe and Mn oxides on the distribution of the elements.

In this study the stream water geochemistry was represented on maps using catchment basins as the zone of influence for each sample. Each catchment is assigned the geochemical attributes from the corresponding sample site. This is an alternative to representing the data as points or as interpolated grids. Catchment basins have been used to study the relationship between mapped geology and stream sediment geochemistry by various authors. For example, Rose, Dahlberg and Keith (1970) used linear regression to study the effects of changes in the areal proportions of lithological units within a catchment basin on the geochemistry of stream sediment in southeastern Pennsylvania. Bonham-Carter and Goodfellow (1986) also used this approach in the Nahanni River area, Yukon, to remove the effects of lithology and Fe and Mn oxides on the geochemistry of stream sediment to isolate anomalous catchment basins. This approach has also been used in the Cobequid Highlands, Nova Scotia (Bonham-Carter et al., 1987). The main advantage to using catchment basins is that the basins are considered the spatial zones of influence of the samples. The basins can

then be used to resample other maps, such as bedrock geology or mineral deposit data, in order to evaluate the spatial relationships between factors such as lithology and mineralization on the geochemical variables.

This approach has been used here to sample maps of bedrock geology, surficial geology and mineral occurrence data using the stream water catchments as the areal sampling units. Data from these maps were appended to the attribute table for each catchment. The attribute table consisted of a location identifier and a list of descriptive variables associated with each location. In this study each catchment basin was thus described in terms of its geochemical composition, geological composition, percentage of mapped lithology (and reclassified units) within each basin, and the presence/absence of mineral occurrences. In the later sections, the "dominant" lithology is simply the map unit with the largest area in a particular basin.

3.2 Stream Water Geochemistry

3.2.1 Box Plots

The box plot provides a graphical display of the distribution of an element within a data set. The plot shows the median value (50th percentile), the 25th percentile, 75thpercentile, hinge lines representing 1.5 X the 25th and 75th percentile, outliers and the 95th confidence interval on the median (notch) for the data set (Figure 3.1). In some cases the 95th confidence interval on the mean is greater than hinge the line, a feature seen, for example, in Figure 3.2 in the group pH = 8. By grouping the data according to a predefined attribute, dominant

lithology or pH for instance, the data can be quickly scanned and relationships between the element and the group attribute can easily be seen. The 95th confidence interval demonstrates whether the median of one sample group is significantly different from another. In this section box plots are used to reveal the main factors affecting the concentration of metallic elements within the stream water geochemical survey.

Previous studies by Simpson, et al. (1993), Davenport (1990) and Finch et al. (1993) have statistically shown that the geochemistry of stream water is partially controlled by the underlying bedrock geology, pH, and Fe and Mn oxides. The underlying bedrock geology is responsible for influencing the chemistry as the water flows over and erodes the geology. pH controls the precipitation of Fe and Mn oxides and hydroxides, which in turn control the content of some of the metallic elements by preferential sorption to the surface of the oxides (Drever, 1997). Box plots have been constructed for the metallic elements grouped by dominant lithology within each catchment and by the pH of the stream water to determine the control of these factors on the distribution of these elements.

3.2.2 Results

Grouping the distributions of metallic elements by pH in the box plots demonstrates that pH is an important factor in controlling the concentration of these elements. Three main trends are revealed; 1) elements which increase in concentration with increasing pH, 2) elements which decrease in concentration with increasing pH, and 3) those elements which show no significant relationship with pH.

Elements such as Sr, Mg, and U fall into the first trend, increasing element concentrations with increasing pH (Figure 3.2 and figures in Appendix E). In the study area there are numerous lithologic units, which contain substantial amounts of carbonate in the form of limestone and dolomite, particularly in the Windsor Group. Elements Sr and U are known to substitute for Ca because of the similar ionic charge and radius. Mg is a major element in dolomite ($CaMg(CO_3)_2$) which is found in units CWL, CWU, and PG. With the dissolution of the carbonate rich lithologic units, CO_3^{2-} along with Ca, Mg, Sr, and U ions are added to solution. The increase in CO_3^{2-} increases the buffering capacity of the water and thus increases the pH of the water, resulting in a direct relationship between pH and the concentration of Ca, Mg, Sr, and U, as shown in the plots.

Elements Fe, Mn, Pb, Zn, Cr, Ti, Cu and Al are found in the second trend, decreasing element content with increasing pH. Figure 3.3 demonstrates this trend using Al. Other box plots showing this trend can be found in Appendix E. In surface waters the precipitation of Fe and Mn oxides is pH dependent. As pH increases Fe and Mn precipitate to form oxides and hydroxides. These substances then provide sites to which other metallic elements such as Zn, Pb, Al, Cr, and Ti can preferentially sorb, thus reducing their concentration in solution and explaining their relationship with pH.

Elements such as As, Sb and Mo show no relationship to pH demonstrating that the distribution of these elements are controlled by other factors, possibly bedrock geology (Figure 3.4 and figures in Appendix E).

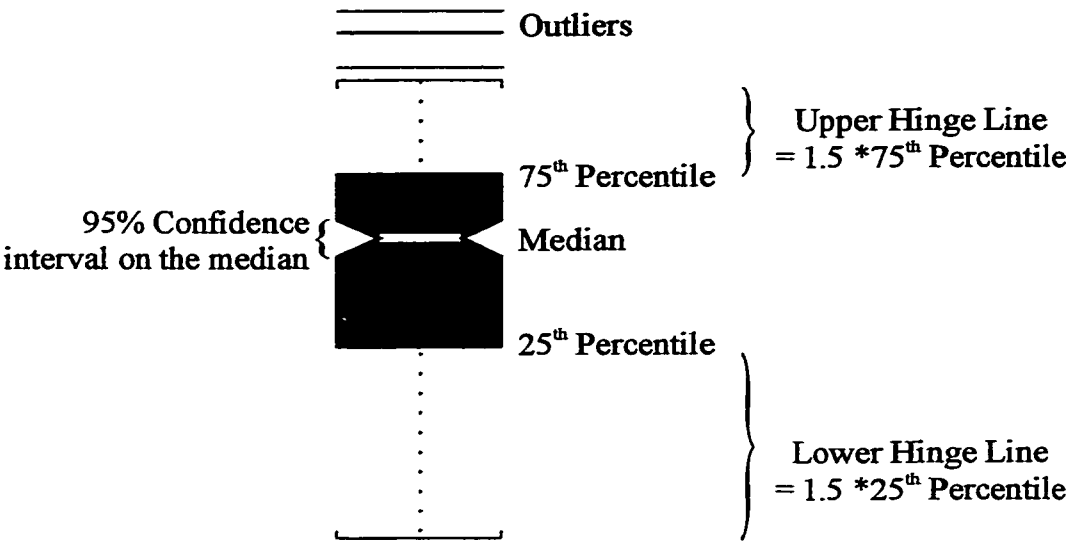

Figure 3.1. Box plot definition diagram.

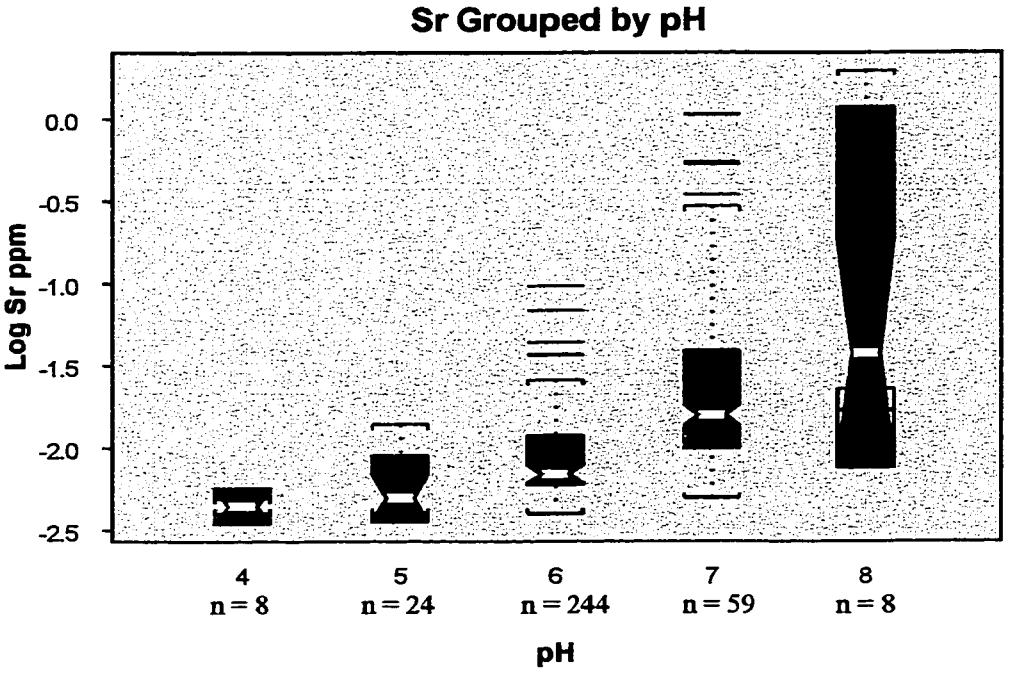

Figure 3.2 Box plot, showing Sr ppm grouped by pH, demonstrating trend 1, increasing concentration with increasing pH. N = the number of samples in each group.

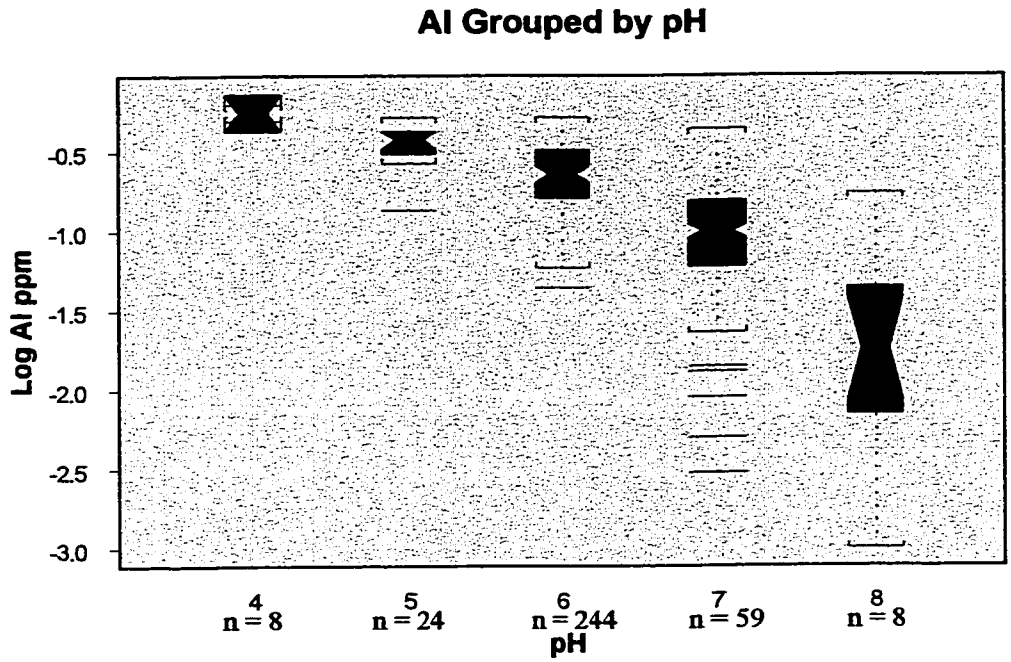

Figure 3.3 Box plot, showing Al ppm grouped by pH, demonstrating trend 2, decreasing concentration with increasing pH.

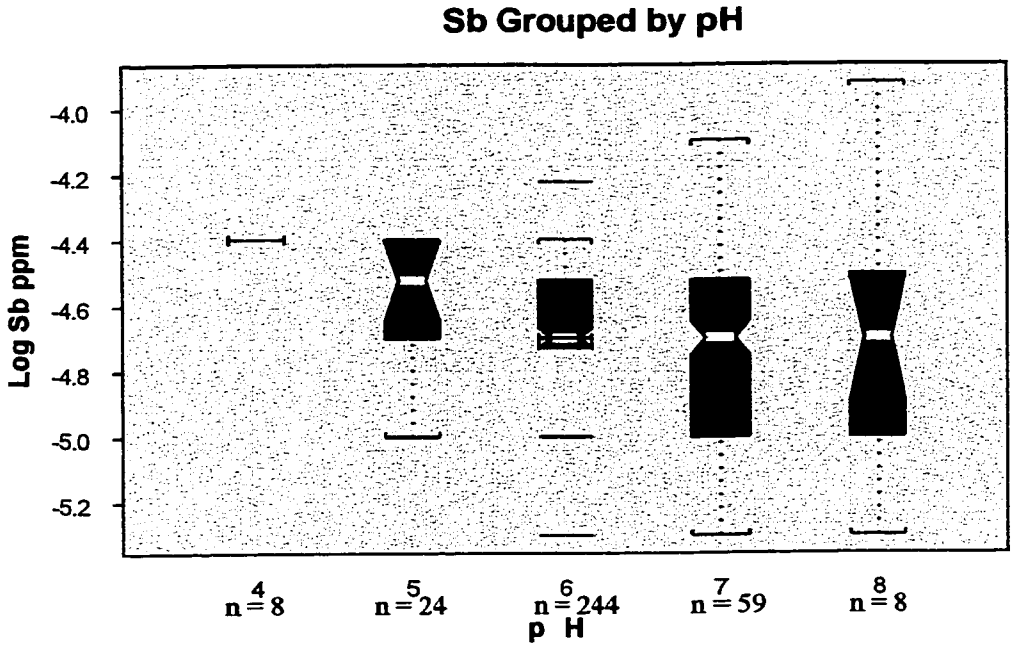

Figure 3.4 Box plot, showing Sb ppm grouped by pH, demonstrating trend 3, no significant relationship with pH. Sb shows some increase at pH < 5, indicating a tendency to follow trend 2 under strongly acid conditions.

Box plots also show that the underlying bedrock geology has a direct effect on the concentration of the metallic elements in stream water. Box plots grouped by the reclassified geology show that the dissolved concentrations of these elements can be divided into 3 trends. Elements Sr, Mg and Mo are found in the first trend. The distinguishing characteristic of this trend is that the concentrations of these elements are significantly higher for the Windsor Group, as indicated by the notch in the box plots, than for the other three other groups (Figure 3.5 and figures in Appendix E). In addition, these elements have approximately the same distribution for the other three groups. As previously discussed, the Windsor Group is comprised predominantly of carbonates, and this appears to be a major controlling factor on the concentration of Mg, Sr and Mo in the stream water. As well since pH is high over the Windsor Group these results are entirely consistent with the pH – metal relationship discussed previously. Mg and Sr are found in high concentrations in carbonates because of their ability to exchange for Ca; as well Mg is a main element in dolomite. In this study area Mo has been associated with the carbonate hosted sulphide occurrences which are found in the Windsor Group, which may explain this association (Kirkham, 1985). The box plots show that the concentrations of these three elements are preserved in the stream water geochemistry during the weathering of the carbonates.

The second trend of elements includes Fe, Mn, Pb, Cr, and Cu. Distinctively this group of elements has significantly lower concentrations over basement rocks and a similar distribution pattern for the Carboniferous clastics and the Windsor Group (Figure 3.6 and figures in Appendix E). Common in the Carboniferous clastics and the Windsor group are

red siltstone and sandstone beds. These red siltstone and sandstone beds are terrestrial sediments deposited in an oxidizing environment. The elements in this trend typically have higher concentrations in this type of environment and are reflected in stream water geochemistry.

The third trend of elements includes, Al, As, Co, Ti, and Zn. In this group the Carboniferous clastic sediments and the Horton Group contains the highest concentrations (Figure 3.7 and in figures in Appendix E). These two units are significantly different than the Basement Group, and the Windsor Group overlaps the two. This pattern cannot be entirely explained at this point.

Common to all three groupings of elements is that the basement rock always has the lowest concentration levels. This demonstrates that these older rocks are weathered less easily than the other three rock groups. Most of the units in this group are Precambrian or older and most are metamorphosed to various degrees. These characteristics result in lower weathering rates, so dissolution is more difficult and thus the concentration of elements in the stream water with these units as the dominant lithology is much lower than in waters overlying the other rock groups.

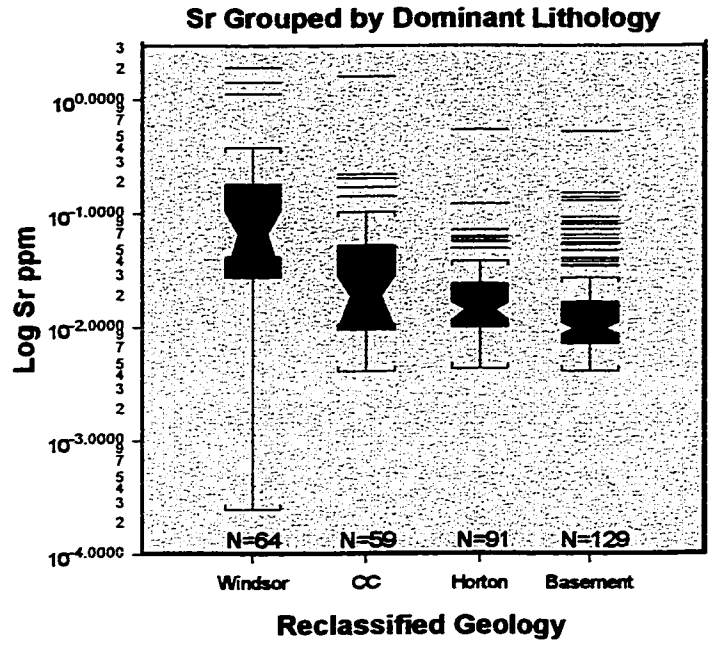

Figure 3.5 Box plot, showing Sr ppm grouped by dominant lithology, demonstrating trend 1.

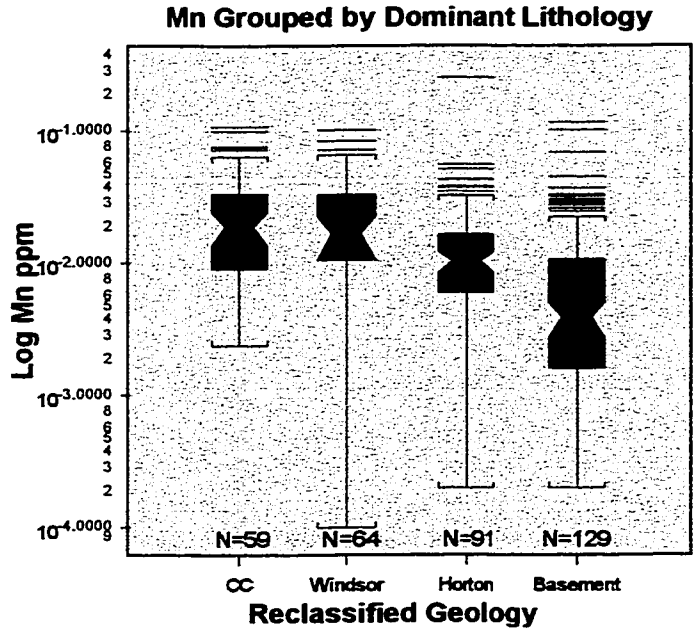

Figure 3.6 Box plot, showing Mn ppm grouped by dominant lithology demonstrating trend 2.

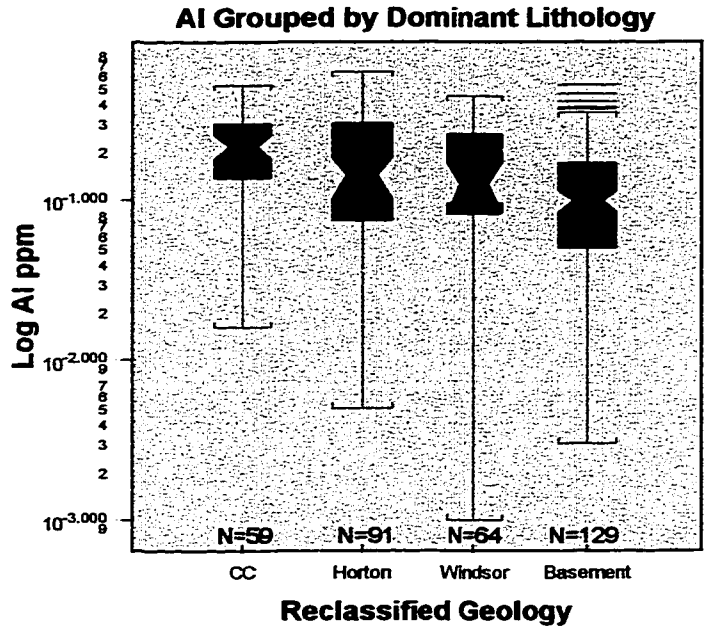

Figure 3.7 Box plot, showing Al ppm grouped by dominant lithology, demonstrating trend 3.

3.3 Multiple Linear Regression

Multiple linear regression analysis was used to show the variability in the stream water geochemistry caused by differences in lithology, changes in the pH, and effects of Fe and Mn oxides and hydroxides. This method is also used to estimate background geochemical values, remove the background effects, and highlight areas of anomalous element concentrations. High residual element concentrations can be associated with mineralization or other sources such as anthropogenic influences. Multiple linear regression has been used by Bonham-Carter and Goodfellow (1986) in the Yukon and North West Territories and by Bonham-Carter, et al. (1987) in the Cobequid Highlands, Nova Scotia to examine the association between mapped geology and surficial geochemistry. However to this point, this approach does not appear to have been used with water data.

The multiple linear regression approach uses the basic regression model to predict background element concentrations (Equation 3.1).

The data corrected for the factors affecting variation in the i^{th} basin are simply the residuals ($Y_i - \hat{Y}_i$), which may be positive or negative. The amount of total variation in a response variable explained by the model can be evaluated by the value of R^2, the ratio of the sum of the squares calculated using regression divided by the total sum of the squares (Davis, 1986). In this study the value of R^2 is represented as a percentage, and is used as a measure to explain the amount of variation of a response variable. The response variable in each case is the logarithm (base10) of the element content. The method assumes that the response variable has a normal distribution. Geochemical elements often have a distribution that is

positively skewed which can be corrected for by taking logarithms. This produces a more symmetrical distribution, the mean of the logarithms becomes a better estimate of central tendency, and the variance is stabilized. The presence of outliers may also cause a problem with regression results. A test was carried out on a few regressions in S-Plus to evaluate the effect of outliers. This test evaluates the scaled difference in fit of the i-th sample with and without the i-th observation. The tests showed that the effect of outliers was not significant.

In this study four sets of regression experiments were used to evaluate the variation of element concentrations in the stream water survey (Table 3.1). The response variable was always the $\log_{10}$ of element concentration. The explanatory variable used in the first experiment was the unclassified dominant lithology, expressed in binary presence/absence form, within each catchment basin. The second experiment examines the variation caused by changes in pH and Fe and Mn. The third evaluates the variation caused by pH alone, a test to determine whether the variation from experiment two is independent of the presence of Fe and Mn oxides and hydroxides. The fourth is a combination of the first two experiments to check the total variation of all the above mentioned factors.

3.3.2 Results and Discussion

Experiment 1: Variation of geochemical concentrations explained by changes in the dominant lithology within each catchment basin. Explanatory variables: the presence/absence of each of the unclassified map units ($m = 24$).

$$\hat{Y}_i = b_o + \sum_{j=1}^{m} b_j X_{ij}$$

Where:

$\hat{Y}_i$ = estimate of element concentration of the response variable at stream catchment i.

X_{ij} = value of explanatory variable j at stream catchment i.

b_j = regression coefficient for explanatory variable j, j = 1, 2, 3, ..., m.

b_o = constant coefficient.

The coefficients are determined by the method of least squares, by minimizing the quantity:

$$\sum_{j=1}^{m} (\hat{Y}_i - Y_i)^2$$

where the summation is over the i = 1, 2, 3, ..., m basins, and Y_i is the observed element content. The statistical package S-plus was used for the calculations.

Equation 3.1. Equation of regression model used to predict background element concentrations.

	Experiment			
Variables	1	2	3 **	4
X1	Carboniferous Clastics *			Carboniferous Clastics *
X2	Windsor Group *			Windsor Group *
X3	Horton Group *			Horton Group *
X4	Basement *			Basement *
X5		pH	pH	pH
X6		log Fe		log Fe
X7		log Mn		log Mn
* = Variables are binary for presence/absence of dominant unit within catchment				
** = Linear regression, whereas other experiments are multiple linear regression				

Table 3.1. Regression experiments with explanatory variables ranging from X1 to X7 and the response variable is the $\log_{10}$ of element concentration.

The results from this experiment are presented in Table 3.2 and represented by solid diamonds in Figure 3.8. The variance explained by the dominant lithology within each catchment in the geochemistry of the metallic elements of the water samples ranges from 18 - 43%. The most substantial variation explained by different lithologic units was found in the elements Fe, Cr, Sr, and Mn, suggesting that geologic differences may have a stronger control on the distribution of these elements than other elements.

Experiment 2: Variation of geochemical content explained by the combined effects of Fe, Mn and pH in the stream water geochemistry. Explanatory variables: $\log_{10}$(Fe), $\log_{10}$(Mn) and pH.

Fe was excluded from the explanatory variable list when Fe was the response variable, and Mn was excluded when Mn was the response variable. The variance explained by changes in Fe, Mn and pH is shown in Table 3.2 and represented by solid squares in Figure 3.8. The amount of variance explained by these factors was high with values ranging from 33% to 78% with the majority greater than 50%. The elements showing the highest amount of variance are Al, Fe, Mn, Pb, Co, Ti, Zn and Mg. The precipitation of Fe and Mn oxides and hydroxides are dependent on the pH of the stream water. Elements Al, Pb, Co, Ti, Zn, and Mg can be preferentially sorbed to these compounds and are likely controlled by a combination of both factors (Drever, 1997).

Experiment 3: Variation of geochemical content explained by changes in the pH in the stream water geochemistry. Used as a test to determine the extent of the variation caused by pH alone in experiment 2. Explanatory variable: pH only.

The results from this experiment are shown in Table 3.2 and the variance is represented by green squares in Figure 3.8. The amount of variance explained by pH alone compared to the combination of pH, Fe, and Mn is dependent on the element chosen as the response variable. pH accounts for a larger percentage (31% – 50%) of the variation in elements Mg, Al and Zn and to a lesser degree for Fe, Sr, Mn, Co and Pb (15% - 28%). For elements such as Cr, Cu, Ti, Sb, Mo and As, pH explains little (.0009% - 12%) of the variation in their concentrations. The ratio of the variance explained by pH over the variance explained by pH + Mn + Fe (Table 3-2) shows the relative importance of pH in the combination of pH + Fe + Mn. The ratio ranges from 0 to 1, where 0 implies that pH accounts for little variance in the pH + Fe + Mn combination and 1 implies that all the variance explained by pH + Fe + Mn can be accounted for by pH. The results suggest that for elements Mg and Mo almost all the variance explained by pH + Fe + Mn is caused by pH. For elements Sr, Zn, Pb, Al, Co, U, Fe, Mn, Ti and Cr the ratio ranges from 0.191 to 0.628 suggesting that pH is an important factor in accounting for the variance in the pH + Fe + Mn combination but also the concentrations of Fe and Mn in the stream water are important factors in accounting for the variance. The ratio for elements As, Cu and Sb range from 0.000495 to .0498 suggesting that the concentration of Fe and Mn control almost all of the variance in the pH + Fe + Mn combination.

Experiment 4: Variation of geochemical concentration explained by the combination of dominant lithology, Fe, Mn and pH in the stream water geochemistry. Explanatory variables: presence/absence of unclassified map units, $\log_{10}$(Fe), $\log_{10}$(Mn) and pH.

The results from this experiment are shown in Table 3.2 and are represented by solid circles in Figure 3.8. Between 26% (Mo) and 83% (Al) of the total variance of the elements in Table 3.2 can be accounted for by the combined effects of these variables. This experiment shows how much of the lithologic variability alone is already accounted for by adding lithology to the Fe + Mn + pH combination, i.e. a check to see how much of the variability in the Fe + Mn + pH combination is dependent on lithology. A measure of the additional variability explained by lithology is shown by the ratio of the variance explained by lithology + Fe + Mn + pH minus the variability explained by Fe + Mn + pH divided by the amount of variance explained by lithology. Results from Table 3-2 show the ratio ranges from 0.112 (Mn) to 1.219 (Mo). Elements U and Mo have the highest ratio demonstrating that the lithology alone adds substantially to the variability of these elements. The ratio for elements such as Mn, Al, and Fe is low suggesting that the variability of these elements is predominantly controlled by the effects of Fe + Mn + pH.

In this study it is demonstrated that Fe, Mn and pH are the most important factors affecting the variance of the metallic elements in the stream water geochemistry, with the exception of Sr, U, As, and Mo.

Residual Analysis

By subtracting the predicted values (using Experiment 4) from the observed values, maps of the residuals show the distribution of metallic elements after removing the combined effects of lithologic, pH, Fe and Mn effects on the geochemistry. The resulting anomalous areas are zones where the metallic concentrations cannot be explained by these "primary" factors. Secondary factors that may account for large residuals include the presence of mineralization, changes in lithology not reflected in the mapping and others such as pollution, and glacial transport. Figure 9-3a, b show catchment basins maps for observed Cu (a) and modeled Cu (b) and Figure 9-4 shows Cu residuals within catchments.

In order to see whether residual values are spatially related to known mineral occurrences, a test was made to compare the observed and residual values for catchments containing known mineralization. Within the catchments there are four Zn and sixteen Cu mineral occurrences (NSDR, 1996). Comparison of the map of residuals with these known Zn occurrences (Figure 3.9) indicates that three of the four occurrences, including the Lime Hill zinc deposit are found in the 98th and 99th percentile of the residuals. Similarly, eleven of the fourteen Cu occurrences located within catchments (Figure 3.10) are found in the 50th percentile or greater of the residuals. These results indicate that the use of linear regression to remove the background effects on the geochemistry of stream water may be a useful tool for locating mineral occurrences in this study area. In addition, the concurrence between the high residuals and the known occurrences suggests that stream water is a suitable sample media for locating potential mineralization in this type of study. The technique of weights of

evidence (Chapter 5) compares Cu in catchments to the residuals and directly supports this result. Figure 3-11 and 3-12 illustrates the difference between Cu within catchments, predicted Cu and Cu residuals within catchments.

Element	Experiment					
	(1) Lithology	(2) Fe + Mn + pH	(3) pH	(4) Lith + Fe + Mn + pH	3/2	(4-2)/1
Fe	42.06	68.99*	22.81	75.49*	0.331	0.150
Cr	37.25	46.06	8.801	61.23	0.191	0.407
Sr	33.96	33.21	20.86	52.93	0.628	0.580
Mn	34.3	66.16**	15.78	70**	0.239	0.112
Co	28.87	59.69	24.99	65.66	0.419	0.207
Pb	29.5	54.84	27.62	61.23	0.504	0.217
Cu	29.07	45.11	2.247	55.21	0.0498	0.347
Ti	28.73	54.63	12.05	63.77	0.221	0.318
Al	28.23	78.37	35.61	82.58	0.454	0.149
Mg	20.82	51.82	50.17	60.5	0.968	0.417
Sb	25.76	33.54	0.753	40.23	0.0225	0.260
Zn	23.28	53.37	31.24	60.41	0.585	0.302
U	20.94	13.6	4.953	32.42	0.364	0.900
As	19.16	17.71	0.00877	28.09	.000495	0.542
Mo	12.17	11.28	10.5	26.06	0.931	1.219

- * = Fe is not included as an explanatory variable
- ** = Mn is not included as an explanatory variable

3/2 = R^2 for experiment 3 divided by R^2 for experiment 2

(4-2)/1 = (R^2 for experiment 4 - R^2 for experiment 2) divided by R^2 for experiment 1

Table 3-2. Regression results expressed as goodness-of-fit R^2, as percentage.

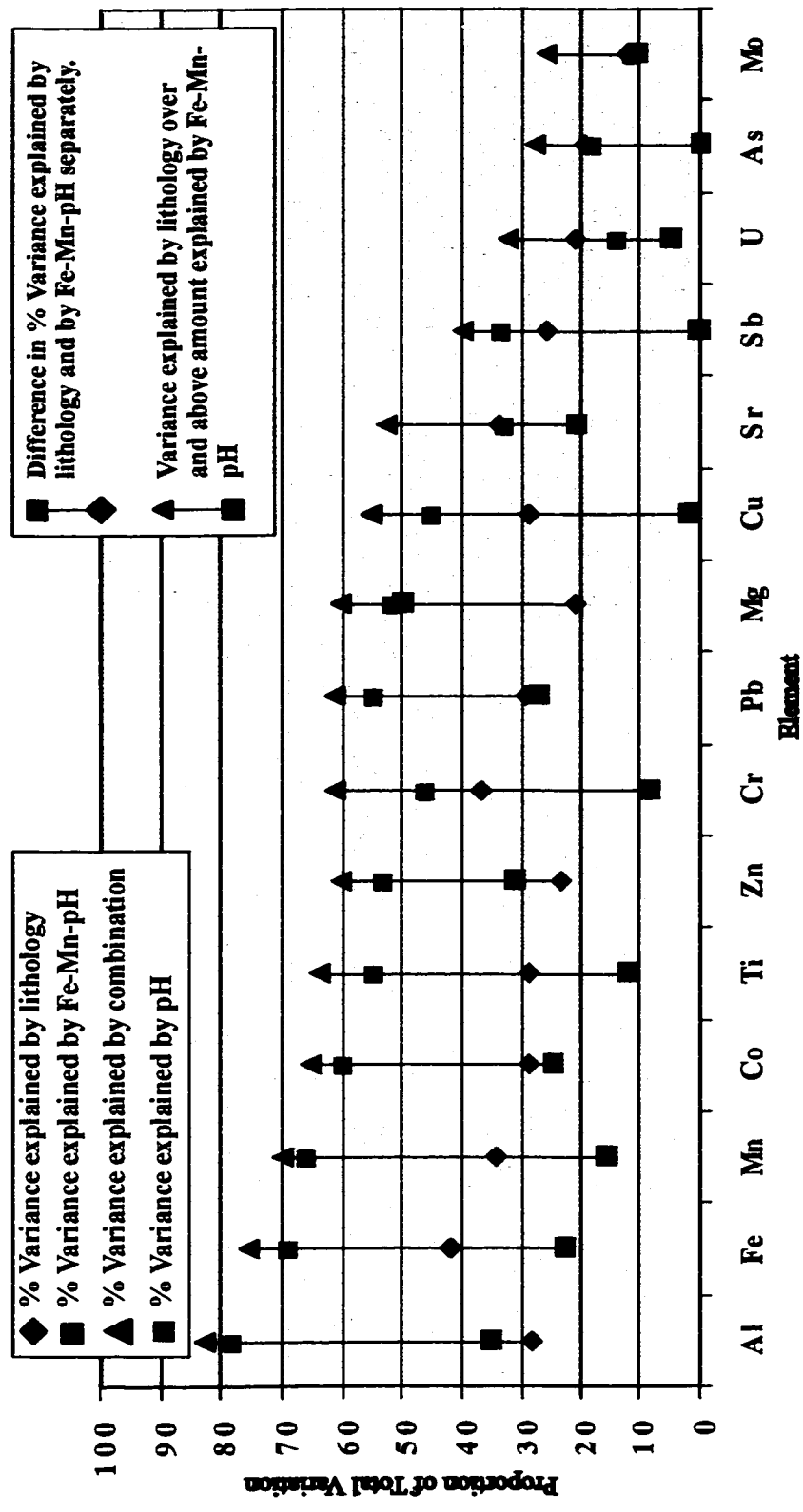

Figure 3.8. Variance diagram showing relative contributions of lithology and (Mn, Fe, pH) to total geochemical variation.

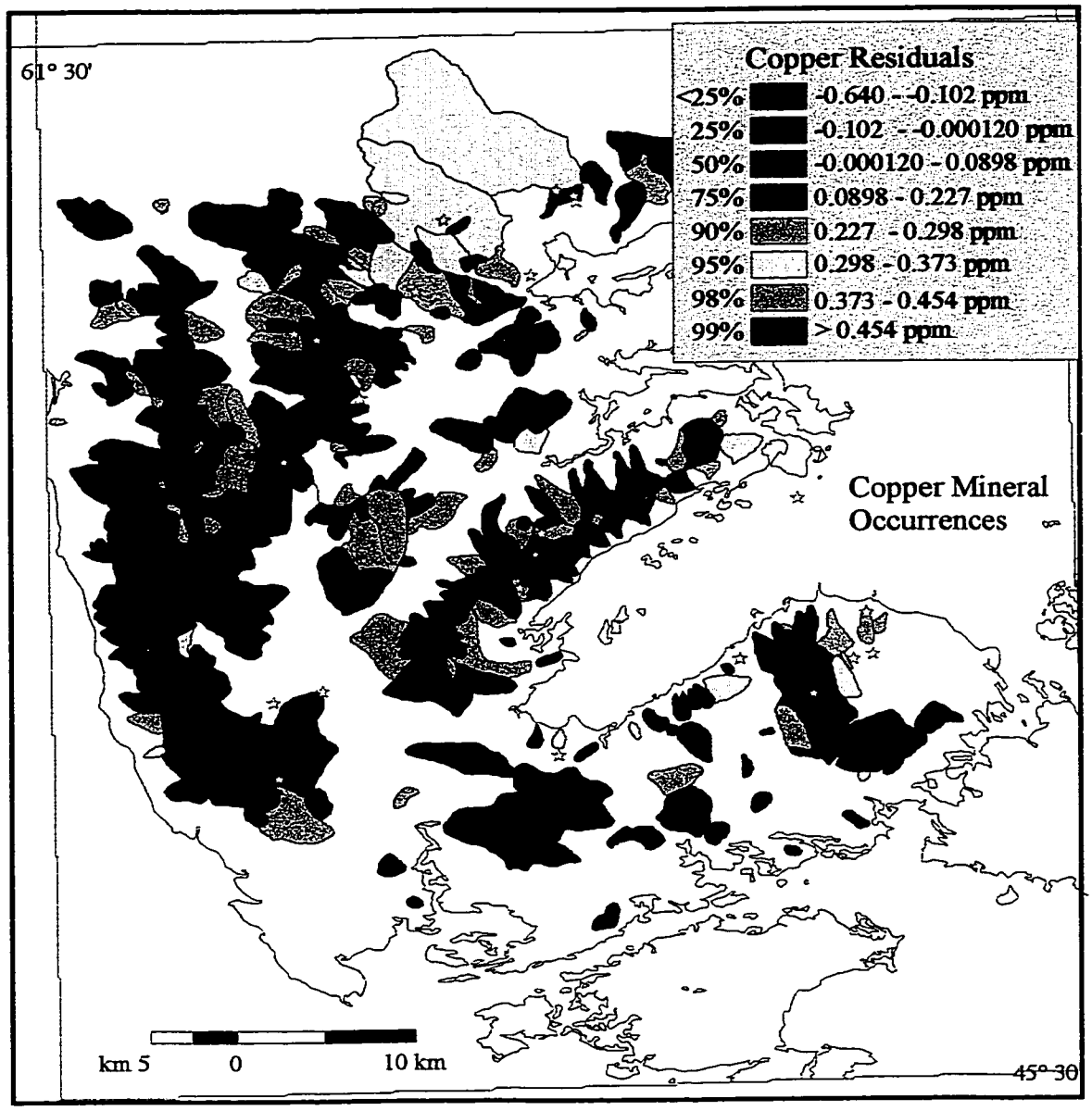

Figure 3.9. Copper residual map with Cu mineral occurrences .

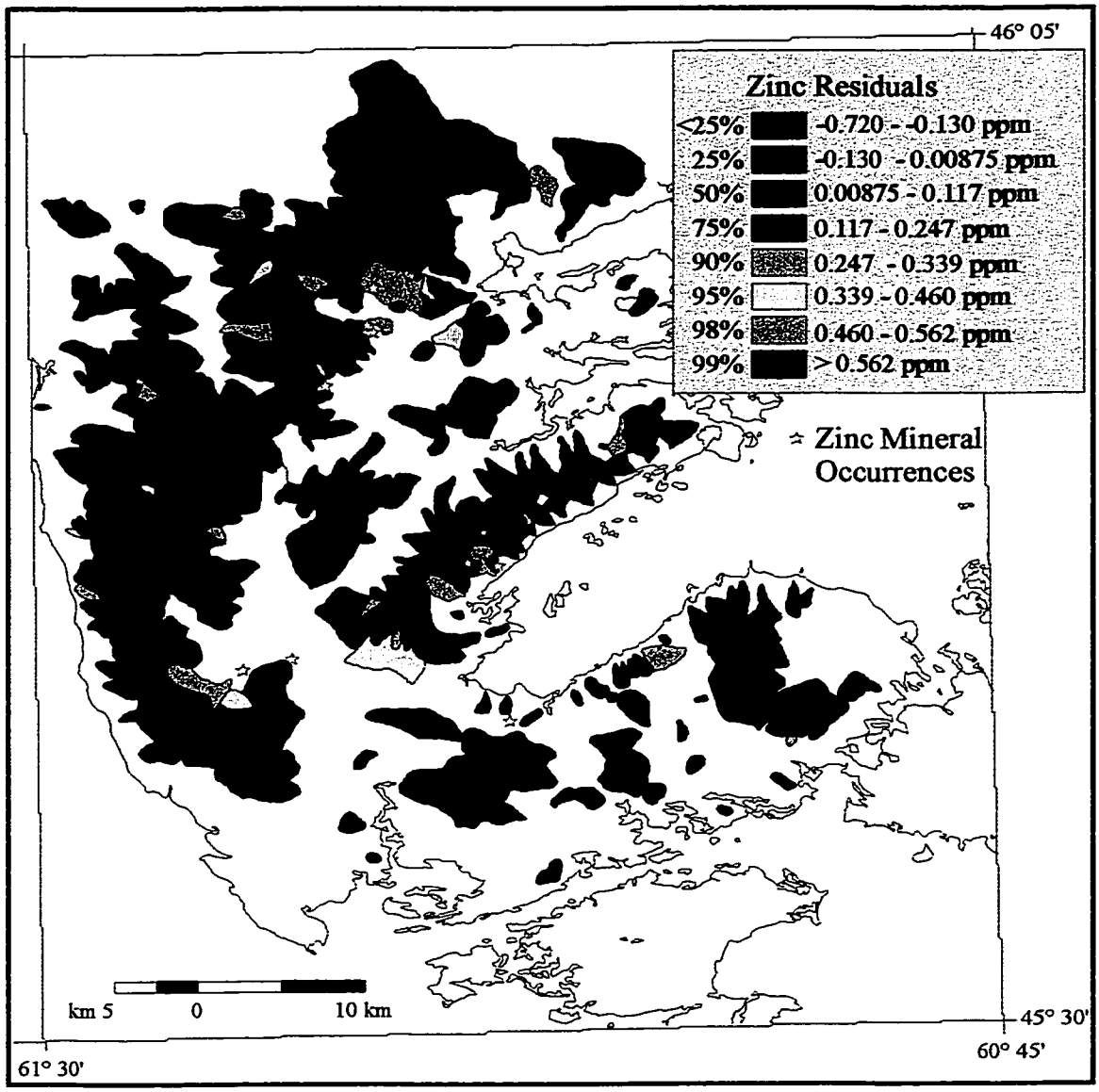

Figure 3.10. Zinc residual map with Zn mineral occurrences .

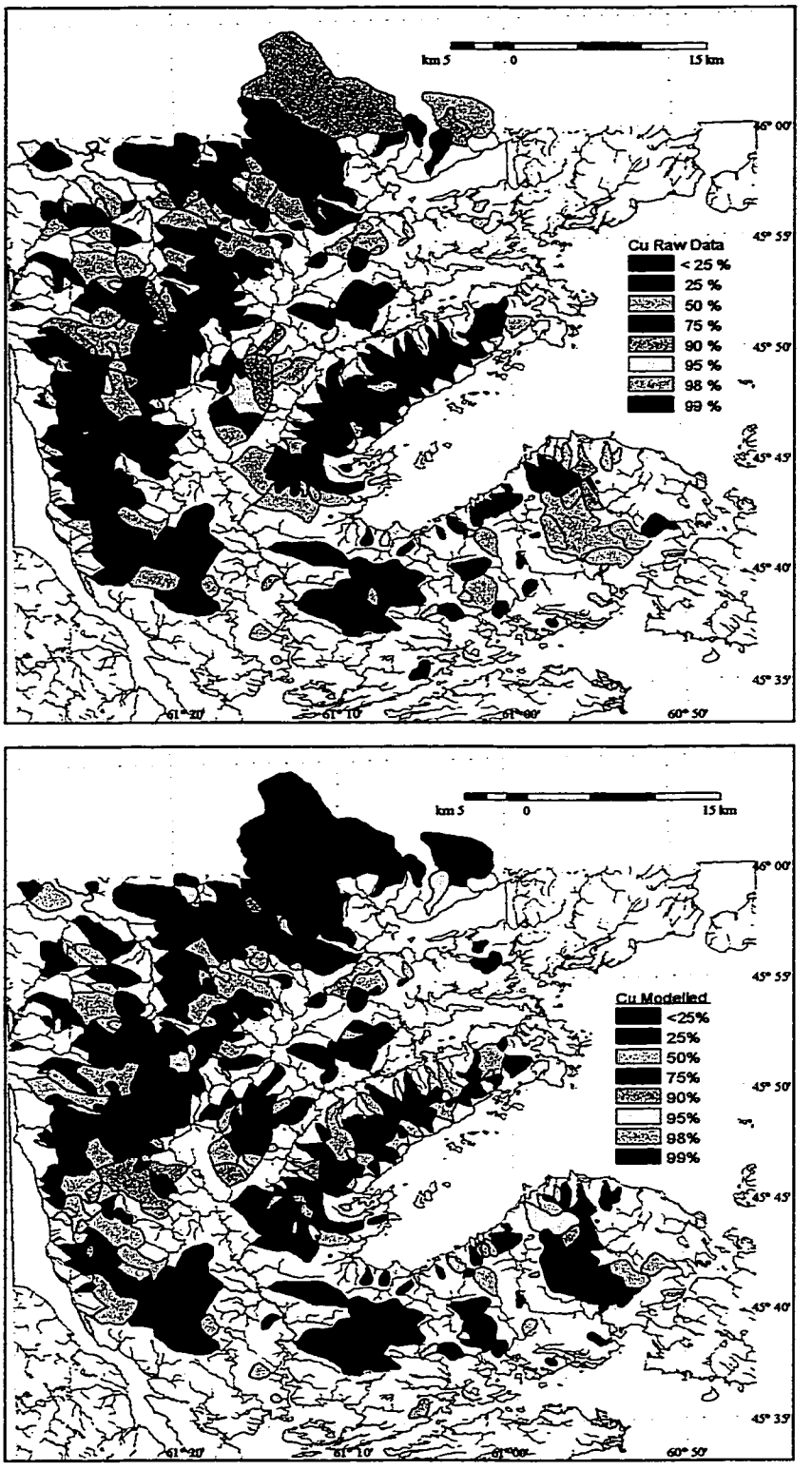

Figure 3-11. Copper within catchments A) raw data, B) predicted values.

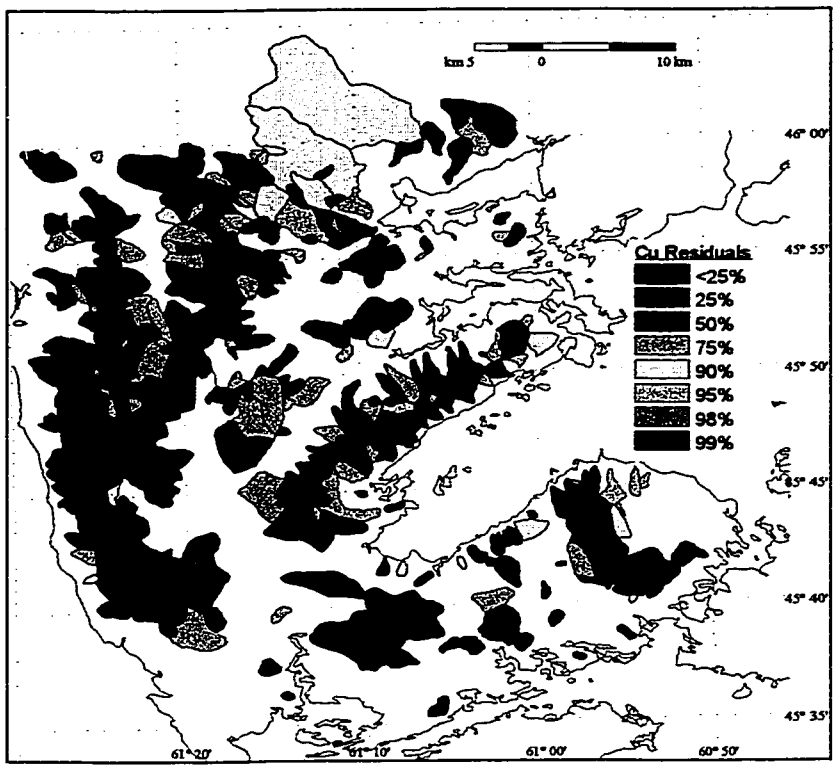

Figure 3-12. Residual copper within catchments.

4 Comparison of the Stream Water and the Balsam Fir Twig Surveys

4.1 Introduction

It has been shown in the previous section that bedrock geology, the pH of the water and Fe and Mn oxides and hydroxides play a significant role in controlling the geochemistry of stream water and that data from stream water can be helpful to locate mineral anomalies. Like stream water surveys, vegetation surveys can be an effective tool used in mineral exploration (Dunn et al., 1991). During sample collection balsam fir twig samples were collected in conjunction with the stream water sampling for the purpose of comparing the two techniques. In this section GIS and spatial statistics are used to compare these two sample media to determine if they reflect similar areas of anomalously high concentrations which may suggest mineralization. It is possible to simply use X-Y plots to compare the points, but because not all stream water and balsam fir twig sample points spatially coincide the GIS method is better suited for this study.

In order to be able to compare the two data sets the point sample locations must be converted to surface representations. Two different approaches were used to represent the data as a gridded surface. The first method involves the interpolation from observation points to grid points using an inverse distance weighting technique (contouring) with a circular zone of influence of constant radius in both the surveys. In the second approach the stream water is represented using catchment basins (as in Chapter 3) and the twig samples

using an inverse distance weighting technique in an attempt to more accurately represent the zone of influence of both data sets.

4.2 Methodology

Various approaches for comparing two geochemical data sets were considered. Scatter plots and correlation coefficients calculated between the two sets of gridded values (such as Zn – water and Zn – twigs) showed little apparent correlation. It seemed reasonable, however, that there might be spatial correlations present where the maps from both media were anomalously high. Therefore the continuous gridded values were converted to binary form (anomalous versus background) for each map, and the two binary maps were compared.

The metallic elements of the stream water and the balsam fir twig geochemical surveys were compared using Yule's coefficient (Equation 4-1), a technique described by Bonham-Carter (1994, Ch. 8). Yule's coefficient is used to compare binary (or indicator) variables, in this case binary map patterns referred to as class 1 and class 2. The coefficient is similar to a product-moment correlation coefficient, in that it has values ranging from -1 to 1, with –1 meaning complete inverse correlation, 0 meaning no correlation, and 1 showing complete correlation. This coefficient is more useful than a Pearson's correlation coefficient (or rank coefficient) in comparing mineral exploration data because it focuses on the comparison of high or anomalous values as opposed to the whole range of variation in each variable. Two problems must be dealt with first: (1) interpolation to a continuous surface for each variable, and (2) selection of a threshold for creating indicator (binary) variables.

Instead of picking a single threshold value, a range of thresholds were used to compare the two sample sets.

In the first attempt to compare the two surveys the point data sets were converted to a surface using an inverse distance weighting technique. When the surfaces were created a radius of 2 km was chosen as the zone of influence for each point (Figures 4-1a and 4-1b). The surfaces were then contoured using a 7-class percentile scheme (<25th, 25th – 50th, 50th – 75th, 75th – 90th, 90th – 95th, 95th – 98th, 98th – 99th and 99th). In the GIS, an area cross-

$$\textbf{Yule's Coefficient} = \frac{\sqrt{T_{11}/T_{21}} - \sqrt{T_{12}/T_{22}}}{\sqrt{T_{11}/T_{21}} + \sqrt{T_{12}/T_{22}}}$$

Where:
T_{11}= Area where map A= class 1 and map B= class 1.
T_{12}= Area where map A= class 1 and map B= class 2.
T_{21}= Area where map A= class 2 and map B= class 1.
T_{22}= Area where map A= class 2 and map B= class 2.

Equation 4-1. Equation for Yule's coefficient.

tabulation between the two maps (each with 7 classes) was created, summarizing the areas of overlap for each of the percentiles (Figure 4-2). The resulting areas from the unique conditions map were then used in the formula for Yule's coefficient. The highest coefficient above the 75th percentile was then used as the point where the two maps were most similar and this value was used as a cutoff point to produce binary maps. In the binary maps, class 1 is equal to the area above the cutoff and class 0 is equal to area less than the cutoff. These two maps were then overlain to show the areas of overlap between the two data sets, as

demonstrated in Figure 4-3. The final cutoff point or the threshold is the point where the two maps are most similar. Above this point, at higher percentile, the coefficient decreases demonstrating that the area of overlap is reduced.

In the second experiment a more representative zone of influence was used for the water data in an attempt to reduce the error caused by interpolation process. In this experiment the catchment basin for each of the sample points was used as the zone of influence. The surface for the balsam fir twig survey was again interpolated using inverse distance weighting, however, this time the zone of influence was decreased to 1 km. As in the first experiment these surfaces were classified according to a percentile scheme and a unique conditions map was created for the overlay of the two geochemical surveys. Yule's coefficient was then calculated for these areas and a map showing the similarities was created.

4.3 Results and Discussion

In the first attempt to compare the two surveys the Yule's coefficient generally demonstrated that the two surveys were comparable for 9 of the 15 elements. Elements such as Al, Ba, Co, Cr, Fe, Mn, Pb, Sr and Zn had comparable higher percentile areas in both surveys indicated by Yule's coefficient that ranged from 0.48 for Sr to 0.92 for Zn (Table 4.1, Appendix F). The highest Yule's coefficient above the 75th percentile for both of the surveys was chosen as the cutoff point, the point where the two surveys were most similar, and these areas were used in the binary map comparison (Table 4.1). Figure 4.1 illustrates how these

area maps can be converted using the percentile cutoff point and overlain to show the overlap between the two surveys. The resulting map shows four areas; 1) areas where neither of the map patterns are present, 2) areas where map 1 is present and map 2 is absent, 3) areas where map 1 is absent and map 2 is present and 4) areas where both map patterns overlap.

In the case of zinc the highest Yule's coefficient above the 75th percentile was at the 99th percentile for both the stream water map and the balsam fir map. Figure 4.1 illustrates the two surface maps and the resulting map of the overlays. The resulting map of overlap produced one small area, located in the central portion of the map on the shores of Bras d'Or lake. Of significance, the Lime Hill zinc deposit is found within this area of overlap.

		Percentiles From the Stream Water Geochemical Survey						
		< 25th%	25th%	50th%	75th%	90th%	95th%	98th%
Percentiles from the Balsam Fir Twig Survey	<25th%	-0.2384	-0.1587	-0.1289	-0.0277	0.9584	0.941	0.8495
	25th%	-0.2629	-0.1929	-0.0978	0.2145	0.9748	0.964	0.9063
	50th%	-0.1477	-0.1629	-0.0383	0.2325	0.4547	0.3712	0.6447
	75th%	-0.0493	-0.1124	-0.0084	0.2568	0.5154	0.4388	0.7585
	90th%	0.1064	-0.0613	0.0577	0.374	0.5756	0.6682	0.8893
	95th%	0.2181	-0.022	0.0954	0.4334	0.6165	0.7043	0.9172
	98th%	0.2838	0.0107	0.1252	0.4621	0.6395	0.7238	**0.9224**

Table 4-1. Yule's coefficient for Zn calculated from percentiles for the stream water and balsam fir twig surveys. Zn is representative of elements that were comparable in both datasets.

The Yule's coefficient for elements As, Mg, Sb and Cu show that these elements are poorly to negatively correlated (Appendix E). Table 4.2 demonstrates that the Yule's coefficient for Mg is an example of the elements that do not compare between the two surveys. The values for Yule's coefficient range from 0 for Cu to –0.8 for As. The poor correlation of the surveys for elements As and Sb is may be due to the fact that these elements are non-essential in plant life (Dunn and Balma, 1997). In particular, As can be toxic to the plants (Dunn and Balma, 1997) and therefore may not be absorbed by the plant or transported to the twigs. Comparison of the geochemistry and pH of the stream demonstrates that the highest concentrations of Mg and Cu are found in the more basic stream water whereas for the balsam fir twigs the highest concentrations are found in more acidic areas. This inverse relationship suggests that the distribution of these elements may be due to a pH dependent control on the ability of the balsam fir to uptake these elements.

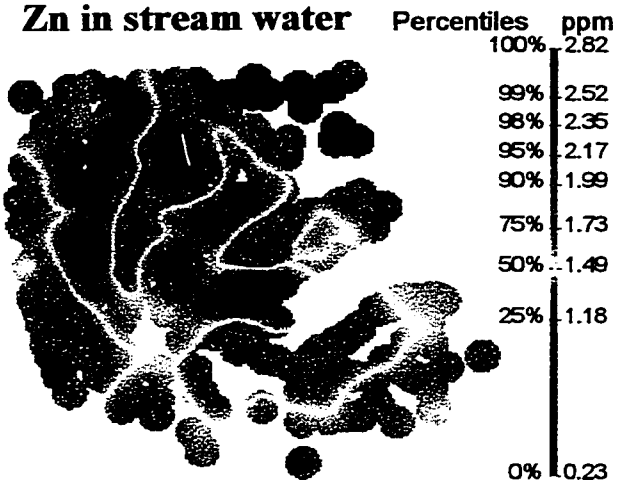

A)

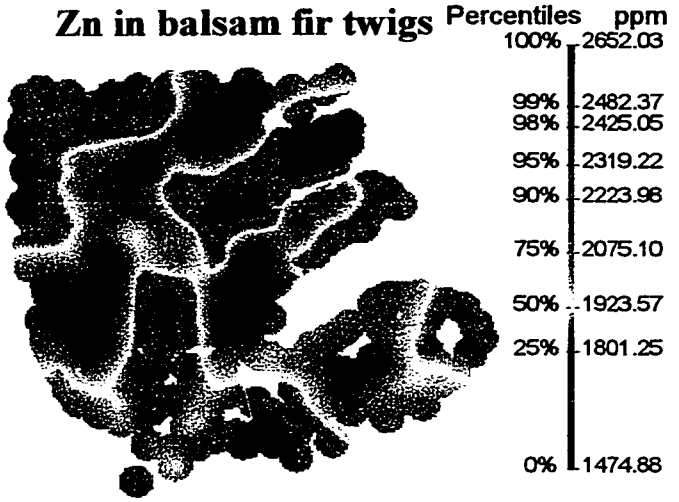

B)

Figure 4-1. A) Interpolated surface for Zn in the stream water geochemical survey. B) Interpolated surface for Zn in the balsam fir twig survey. Area overlap for the 99th percentiles from the stream water and balsam fir twig surveys.

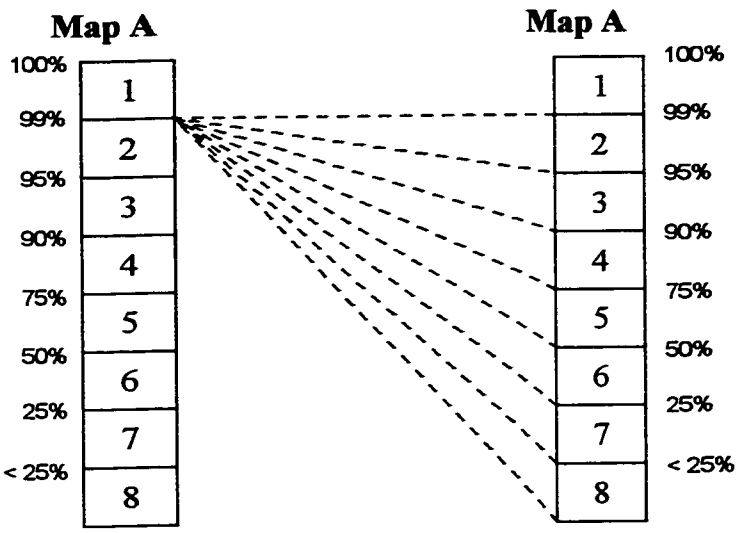

Figure 4-2. Diagram to show scheme for calculating Yule's coefficient for binary maps. The 99th percentile from Map A was first selected as a binary threshold in both maps, and Yule's coefficient calculated from the overlay areas. Then the 99th for Map A with 98th for Map B, 99th for map A with 95th for Map B, ... etc. Then the process was repeated for the 98th, 95th, 90th, 75th, 50th, 25th and less than the 25th. The results are then summarized as a table, e.g. Table 4.1.

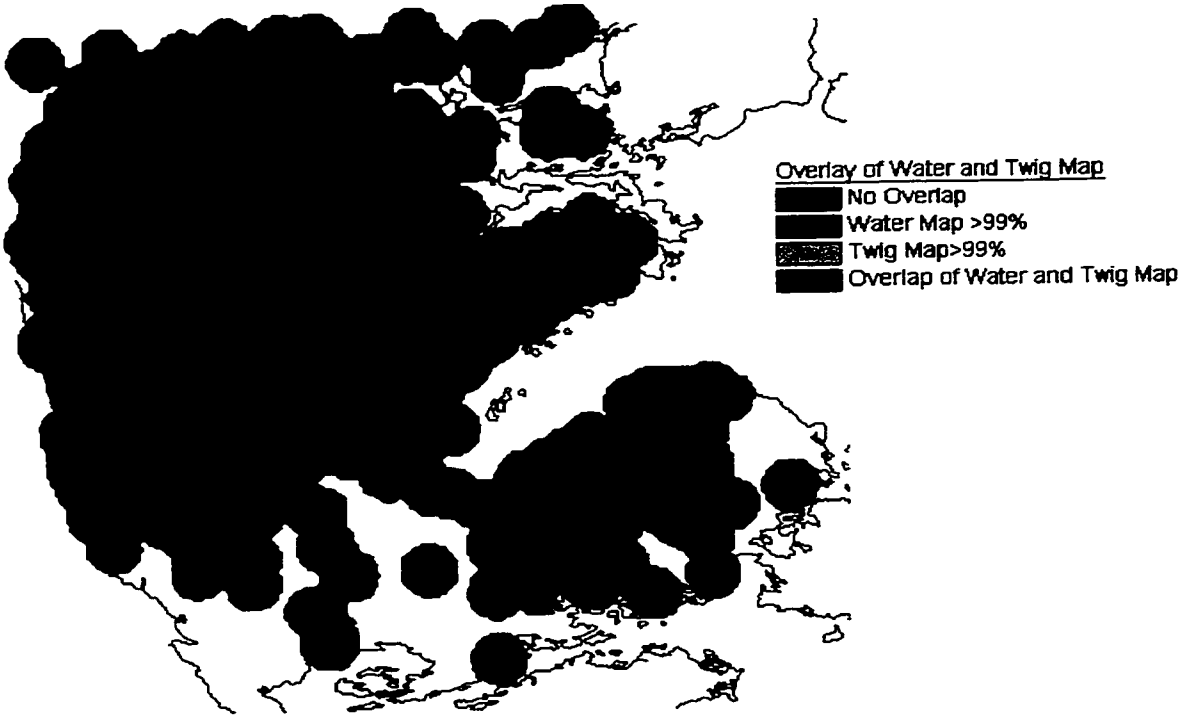

Figure 4-3. Area overlap for the 99th percentiles from the stream water and the balsam fir twig surveys.

		Percentiles From the Stream Water Geochemical Survey						
		<25th%	25th%	50th%	75th%	90th%	95th%	98th%
Percentiles from the Balsam Fir Twig Survey	<25th%	0.0283	0.1694	0.1592	0.0629	0.0152	-0.003	0.0013
	25th%	0.0244	0.1054	0.1084	0.0444	0.0203	0.0044	0.002
	50th%	-0.0627	-0.0098	-0.0698	-0.1979	-0.1041	-0.0772	-0.0611
	75th%	-0.1389	-0.1545	-0.2165	-0.1285	-0.0493	-0.0236	-0.0097
	90th%	-0.0885	-0.2825	-0.1834	-0.1691	-0.0604	-0.036	-0.0229
	95th%	-0.101	-0.3074	-0.1458	-0.0649	0.0508	0.0748	0.0877
	98th%	-0.0972	-0.3141	-0.1884				

Table 4-2. Yule's coefficient for Mg calculated from percentiles for the stream water and balsam fir twig surveys.

In the second attempt to show similarities between the two data sets catchment basins were used to represent the zone of influence for the stream water and a smaller radius was used to interpolate the grid for the balsam fir twig survey. This was done in an attempt to more closely represent the zone of influence for both sample sets. The results from this test are tabulated in Appendix E. Yule's coefficients calculated for this test show that for all elements, except for Fe, Mn and Al, the two surveys are poorly correlated. An example, using Zn, of the Yule's coefficients determined using this method are shown in Table 4.3. In general, Yule's coefficients for Zn are negative or close to 0 indicating that the area containing higher percentile Zn concentrations are not similar in the two surveys.

		Percentiles From the Stream Water Geochemical Survey						
		< 25th%	25th%	50th%	75th%	90th%	95th%	98th%
Percentiles from the Balsam Fir Twig Survey	<25th%	-0.2366	-0.1326	-0.0371	-0.0158	-0.142	-0.0508	0.1313
	25th%	-0.1373	-0.0675	-0.0023	-0.0381	-0.1308	-0.1168	-0.106
	50th%	0.0844	-0.0137	0.1016	0.0989	0.0204	0.0268	0.018
	75th%	0.2929	0.0514	0.112	-0.0357	-0.4697	-0.6651	-0.6085
	90th%	0.4395	-0.0107	-0.1315	-0.4668	-0.5265	-0.4289	-0.3485
	95th%	0.705	0.0768	-0.0306	-0.3481	-0.4095	-0.2989	-0.2104
	98th%			0.1829	-0.3572	-0.1657	-0.0407	0.0539

Table 4-3. Yule's coefficient for Zn calculated from percentiles for the stream water and balsam fir twig surveys, where the zone of influence for the stream water is the catchment basins and is smaller than the first attempt for the balsam fir twigs.

Results for elements Fe, Mn and Al can be seen in Tables 4.4, 4.5 and 4.6 respectively. The Yule's coefficient for these elements range from 0.5972 for Fe to 0.361 for Al. As discussed previously, linear regression demonstrated that the variance explained by pH was higher for these elements than all other elements (Section 3.3.2). Fe, Mn and Al quickly form oxides and hydroxides when they are dissolved in water and are therefore quickly removed from solution (Drever, 1997) thus the deposition of these molecules is close to the source of input. Other metallic elements analyzed in this study are not as unstable as Fe, Mn and Al and can remain in solution for longer periods of time and therefore can be transported further away from their source of input. The soils in which the balsam fir twigs obtain their nutrients are comprised of these oxides and hydroxides and because of this they are not transported far from their source. Elements Fe, Mn and Al in the balsam fir twigs

therefore more closely represent the nearby influence of the underlying bedrock geology. The geochemistry of the stream water samples also reflects the dominant lithology (input) within catchment basins. For these reasons the upper percentiles of Fe, Mn and Al for the catchment basins and the smaller zone of influence for the balsam fir twig surveys are correlated. With weathering of the soils the elements which are more stable in solution are transported further from their source and their concentrations are not reflected in the balsam fir survey with the smaller zone of influence. These elements therefore show a poor correlation between the stream water and the balsam fir twig surveys.

		Percentiles From the Stream Water Geochemical Survey						
		<25th%	25th%	50th%	75th%	90th%	95th%	98th%
Percentiles from the Balsam Fir Twig Survey	<25th%	0.5109	0.5368	0.4105	0.5327	0.4359	0.9283	0.9277
	25th%	0.3418	0.2997	0.2755	0.35	0.4378	0.7456	0.7434
	50th%	0.1789	0.1538	0.1999	0.3036	0.2573	0.3143	0.3063
	75th%	0.2851	0.1924	0.3342	0.35	0.2027	0.3056	0.3118
	90th%	0.3263	0.2924	0.4838	0.4752	-0.1716	-0.0849	-0.08
	95th%		0.5958	0.5814	0.4795			
	98th%			0.7015	0.5972			

Table 4-4. Yule's coefficient for Fe calculated from percentiles for the stream water and balsam fir twig surveys, where the zone of influence for the stream water is the catchment basins and is much smaller for the balsam fir twigs.

		Percentiles From the Stream Water Geochemical Survey						
		<25th%	25th%	50th%	75th%	90th%	95th%	98th%
Percentiles from the Balsam Fir Twig Survey	<25th%	0.1063	0.1166	0.0874	0.0497	-0.0784	-0.067	-0.067
	25th%	0.1279	0.1237	0.1282	0.0335	-0.1292	-0.1295	-0.1295
	50th%	0.1389	0.1506	0.1784	0.1198	-0.0063	-0.0111	-0.0111
	75th%	0.1682	0.2058	0.0875	0.1138	-0.0882	-0.0897	-0.0897
	90th%	0.3869	0.3568	0.1385	0.1727	0.0486	0.0546	0.0546
	95th%		0.6123	0.5436	0.4762	0.3028	0.3083	0.3083
	98th%		0.4448	0.5985	0.6928			

Table 4-5. Yule's coefficient for Mn calculated from percentiles for the stream water and balsam fir twig surveys, where the zone of influence for the stream water is the catchment basins and is much smaller for the balsam fir twigs.

		Percentiles From the Stream Water Geochemical Survey						
		<25th%	25th%	50th%	75th%	90th%	95th%	98th%
Percentiles from the Balsam Fir Twig Survey	< 25th%	0.3765	0.1911	0.1816	0.1812	0.0766	-9.9999	-9.9999
	25th%	0.2247	0.1193	0.033	0.0522	-0.0618	0.4763	0.3905
	50th%	0.0893	0.1453	0.0943	-0.0405	0.0293	0.5634	0.4675
	75th%	0.6182	0.3207	0.2488	0.0658	0.3228	0.7364	0.667
	90th%	0.5298	0.3622	0.2786	-0.0839	0.3085	0.6585	0.7361
	95th%	0.4468	0.2559	0.1796	-0.2752	0.1047	0.458	0.5302

Table 4-6. Yule's coefficient for Al calculated from percentiles for the stream water and balsam fir twig surveys, where the zone of influence for the stream water is the catchment basins and is much smaller for the balsam fir twigs.

The fact that the results of these two tests are very different show that the zone of influence for each sample in each of the surveys is important as to whether the surveys can be compared. The first attempt demonstrated that the two surveys were similar and that physical processes affecting the availability of some elements controlled the similarities between the two surveys. In the second attempt a smaller zone of influence was chosen to represent the balsam fir twig survey. In this test the results show the two surveys are not similar except for elements Fe, Mn and Al. This suggests that most of the elements are being removed from the area from which the balsam fir twigs obtain their nutrients and therefore do not reflect the geochemistry of the bedrock geology closest to the sample sites. Another possible source of error in the calculation of Yule's coefficient in the second test may lie in the fact that the areas of comparison from the two surveys are not similar. The catchment basin, used for the stream water geochemistry is the upstream portion and the zone of influence for the balsam fir twig survey is a circle radiating from the sample point. This would produce more areas where the two surveys do not overlap and thus alter the value of Yule's coefficient. In conclusion these results show the method of using Yule's coefficient to compare the geochemistry of balsam fir twigs to geochemistry of stream water is highly dependent on the element analyzed and the zone of influence chosen to represent the sample.

5 Mineral Potential Mapping

5.1 Introduction

Linear regression from the section 3.3 was used to remove factors such as lithology, pH, and Fe and Mn oxides to isolate catchment basins with anomalous Zn and Cu concentrations. These results were then used to produce maps of residuals showing the catchment basins with anomalous values that are potentially due to mineralization. While regression was useful in determining the sources of variation of Zn and Cu in stream water, a weights of evidence technique (with the GIS) in ArcView is used in this section to examine the location of the mineral deposits in relation to the geology and the geochemical maps. In addition, the maps of residuals determined using linear regression were incorporated into the weights of evidence approach to evaluate whether the removal of background effects improves the probability of locating mineral occurrences.

The weights of evidence technique requires a set of points representing mineral occurrences in order to calculate the probabilities of occurrence. Copper was chosen as the element to produce a mineral potential map, as there are over 30 Cu occurrences in the study area, 11 of which are found within the catchment basins. In weights of evidence, the spatial association of an explanatory variable (also known as "evidential themes") in binary form can be measured by using the "contrast", C (to be introduced in the next section). The contrast can be used to test whether the copper in the water map (observed values) is a better or worse predictor of the known Cu occurrences than the copper in the residual map. The map of residuals represents the anomalous copper concentrations that may be due to mineralization

and may have a higher probability of a mineral occurrence than the map of catchments for copper percentiles based on the "raw" data and may be used as an evidential theme to predict mineral potential. Other evidential themes used to model mineral potential are the underlying bedrock geology and proximity of occurrences to faults in the study area.

5.2 Weights of Evidence

Weights of evidence is a quantitative method to combine spatial data in order to describe and analyze interactions between the data, and to make predictive models (Raines et al., 1999). Originally developed for non-spatial medical diagnosis, the method was adapted into a spatial technique for mineral potential mapping (Bonham-Carter, et al., 1988). Weights of evidence evaluates the spatial distribution of known mineral deposits, the response variable, with respect to multi- or binary-class maps, the explanatory variables. For each explanatory variable, a set of weights is calculated (one for each "class" value on the map). By assuming conditional independence, several explanatory variables maybe combined to calculate a favourability map (Bonham-Carter et al., 1989). The explanatory variables, in this case the bedrock geology, the stream water geochemistry, and proximity to faults are combined using a log linear form of Bayes rule in a multi-map overlay. The prior probability, probability of an occurrence given no information, is updated by the addition of explanatory variables and their weights to produce a posterior probability map of occurrence, which is used as a mineral potential map (Bonham-Carter et al., 1989). A conceptual model is used to guide the selection of suitable explanatory variables. The conceptual model in

mineral potential mapping is an exploration model, often embodying deposit model characteristics, where they can be observed on regional data sets.

An important assumption made in weights of evidence modeling is that each of the explanatory variables are conditionally independent of one another with respect to the mineral deposit data (Bonham-Carter, 1994). In practice, conditional independence is violated to some degree in most situations (Bonham-Carter, 1991). Because of the assumption of conditional independence the model does not perfectly fit the data, but provides a simplification. The conditional independence can be checked statistically to determine which layers violate this assumption and may be removed or modified before being used in the final version of the model.

5.3 Methodology

The weights of evidence method can be divided into two main steps, the preparation of the data and the implementation of the modeling. The first step involves the calculation of the weights of spatial association between the response variable (location of selected mineral occurrences) and the explanatory variables, multi-class maps representing geological phenomena such as bedrock geology or stream water geochemistry. The explanatory maps are often generated by reclassification of the multi-class maps to binary form using the weights as a guide. The second step uses the loglinear form of Bayes rule to integrate these explanatory variables in a multi-class overlay to produce a map of mineral potential.

The generation of the weights in the first step involves a combination of GIS analysis and Bayesian statistics. In order to calculate the weights for each class in each of the maps the GIS determines the total area of each class and the number of mineral occurrences within each class. The results from this analysis characterize the spatial attributes of the response and explanatory variables and are used to determine a pair of weights for each predictor map class. The value of the weights is approximately equal to the natural logarithm of the "normalized" density, or the proportion of the total number of deposits on the class divided by the proportion of the total study area occupied by the map class which represents the ratio of areal proportions of each map class to the total map area (Bonham-Carter, 1991). In these calculations each map class in the multi-class maps is treated as a binary pattern and the mineral deposits are considered to be in binary form, either present or absent. Each deposit is assumed to occupy a small (arbitrary) unit area (unit cell), and all area measurements are expressed in unit cells. The combination of the binary predictor maps (B) and the binary deposit map (D) produces four possible spatial overlap relationships (Figure 5.1). From the four possible spatial overlap relationships four conditional probabilities can be estimated using area ratios (Equation 5.1). Using these conditional probabilities the weights for each of the classes can be calculated as log ratios, as in Equation 5.2. A positive value of a weight indicates that more deposits occur within a map class than would be expected by chance, whereas a negative weight indicates the opposite situation. The difference between the weights (for binary maps) produces a coefficient of contrast (C), which is a measure of the strength of the spatial association between the deposits and map classes. Bayes' rule is used

in the second step to combine the weights from 2 or more explanatory variables to produce a map of mineral potential. By adding more explanatory information the probability of a mineral occurrence is modified by increasing or decreasing the posterior probability according to the information added. The explanatory variable (binary) is either present, at which case W+ is added, or absent where W- is added, and if there is no data W = 0. If the presence of a predictor variable is positive the posterior probability is greater than the prior probability. These calculations are made for each unit cell on the map producing a map of posterior probability. In the weights of evidence formulation probabilities are expressed in terms of logits, the natural logarithms of odds, Equation 5.4.

The effectiveness of the posterior probability map is dependent on the conditional independence of each of the predictor variables to one another with respect to the response variable and whether the explanatory variables are adequate sources of evidence to predict occurrences. Conditional independence is always violated to some degree, but the degree of violation must be determined (Bonham-Carter, 1994). To calculate the degree of independence a pairwise test of independence is used. This method determines the conditional independence of all possible pairings of binary patterns using the chi–squared statistic and compares this value to tabled values having one degree of freedom (Bonham-Carter, 1994, ch. 9).

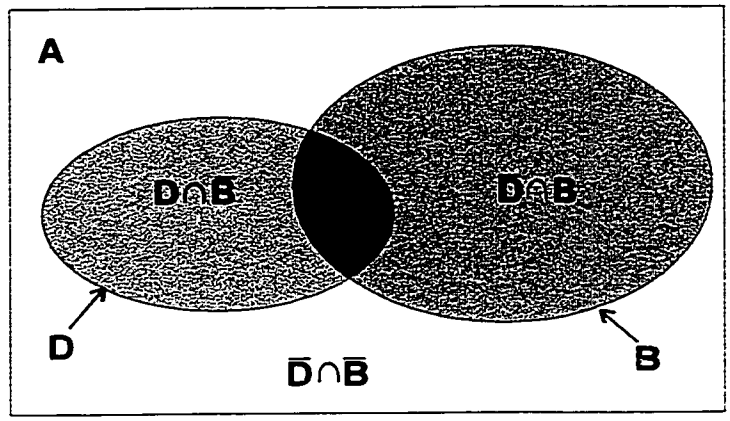

A = Map area
D = Mineral deposit distribution
B = Mineral predictor pattern (explanatory variable)

1) Both patterns are present $D \cap B$
2) The deposit pattern is present and the predictor pattern is absent $D \cap \bar{B}$
3) The deposit pattern is absent and the predictor pattern is present $\bar{D} \cap B$
4) Both patterns are absent. $\bar{D} \cap \bar{B}$

Figure 5.1. Venn diagram showing the four possible spatial overlap relationships used to calculate the weights.

$$P(D|B) = \frac{N(B \cap D)}{N(B)} \qquad P(D|\bar{B}) = \frac{N(\bar{B} \cap D)}{N(\bar{B})}$$

$$P(\bar{D}|B) = \frac{N(B \cap \bar{D})}{N(\bar{B})} \qquad P(\bar{D}|\bar{B}) = \frac{N(\bar{B} \cap \bar{D})}{N(\bar{B})}$$

Equation 5.1. Conditional probability equations from the four mutually exclusive overlap relationships. N ( ) denotes areas as a count of unit cells.

$$W^+ = \ln \frac{P(B|D)}{P(B|\bar{D})} \qquad W^- = \ln \frac{P(\bar{B}|D)}{P(\bar{B}|\bar{D})}$$

Equation 5.2. W^+ and W^- equations for binary explanatory variable. W^+ refers to the presence of B, W^- refers to the absence of B. A weight of zero is used if B is unknown.

The chi-squared statistic is calculated by comparing the observed and expected number of deposits occurring within each overlap combination of the two binary maps. The observed and expected values can be shown in a two-by-two contingency table (Table 5.1). The observed number of deposits is the number of deposits with the overlap area of B1 and B2. The expected number of deposits is the number of deposit in B1 multiplied by the number in B2 divided by the total. The cutoff point for conditional independence assuming a 98% level of confidence (with one degree of freedom) is equal to 5.4 (Bonham-Carter, 1994, ch. 9). Values less than 5.4 indicate that the pairwise conditional dependence is unlikely.

Probability of deposit (D) given evidence (B)

$$P(D|B) = P(D)\frac{P(B|D)}{P(B)} \qquad \textbf{5.3a}$$

Where P(D) = the prior probability, assumed to be the average density of known deposits in the map area.

For two explanatory variables (evidence):
Probability of deposit (D) given evidence (B1) and (B2)

$$P(D|B1\cap B2) = \frac{P(B1\cap B2|D)\,P(D)}{P(B1\cap B2|D)\,P(D)\;\; P(B1\cap B2|\bar{D})\,P(\bar{D})} \qquad \textbf{5.3b}$$

Assuming condtional independence between B1 and B2 this can be rewritten as:

$$P(D|B1\cap B2) = P(D)\;\frac{P(B1|D)}{P(B1)}\;\frac{P(B2|D)}{P(B2)} \qquad \textbf{5.3c}$$

Equation 5.3. Posterior probability formulas.

$$\ln O(D|B1^{k(1)}\,B2^{k(2)}\,\ldots.\,B2^{k(2)}) = \ln O(D) \sum_{j=1}^{n} W_j^{k(j)}$$

Where:
O = the odds and is equal P/(1-P), where P = probability
D = the number of mineral deposits
j = 1, 2, 3, ...,n is the number of explanatory variables.
B_j= the area of the j-th explanatory variable
W_j = the weight of variable j
k(j) = the class of the j-th variable.

Equation 5.4. Posterior probability formula expressed in logits. Posterior logits can be converted to probablity for final mapping.

	B1 Present	B1 Absent	Totals
B2 Present	$N(B_1 \cap B_2 \cap D)$	$N(\overline{B}_1 \cap B_2 \cap D)$	$N(B_2 \cap D)$
B2 Absent	$N(B_1 \cap \overline{B}_2 \cap D)$	$N(\overline{B}_1 \cap \overline{B}_2 \cap D)$	$N(\overline{B}_2 \cap D)$
Totals	$N(B_1 \cap D)$	$N(\overline{B}_1 \cap D)$	$N(D)$

$N(B_1 \cap B_2 \cap D)$ = the observed number of deposits occurring in the overlap region between binary pattern 1 and 2. The predicted number is $\frac{N(B_2 \cap D) * N(B_1 \cap D)}{N(D)}$

Table 5.1. Contingency table for testing conditional independence, based on cells containing a deposit only. B is the presence or absence of a binary pattern, subscripts denote pattern 1 and 2. D is the presence of mineral deposits. The four values within the table are either expected values assuming conditional independence, calculated from marginal totals, or the observed values measured from maps (Bonham-Carter, 1994).

$$\chi^2 = \sum_{i=1}^{n} \frac{(\text{Observed}_i - \text{Expected}_i)^2}{(\text{Expected}_i)}$$

Equation 5.5. Equation to calculate the chi-squared statistic. In this case n = 4, and the number of degrees of freedom equal to (number of rows - 1) * (number of columns -1) = (2 - 1) * (2 - 1) = 1.

5.4 Results

5.4.1 Geochemistry

The map of Cu concentrations within the catchment basins is used to represent the spatial distribution of Cu in stream water. This map was classified to convert from ppm Cu to a smaller number of intervals using a percentile scheme. Weights and contrast values for Cu catchment basins associated with Cu occurrences were computed and are reported in Table 5.2. No mineral occurrences were found in the 90th percentile or above for Cu in stream water. Qualitatively this suggests that there is a poor relationship between Cu occurrences and high dissolved concentrations of Cu in stream water represented by catchment basins. This is further supported by the maximum value for the contrast (C), which is –0.5043 at the 75th percentile and only 0.0156 at the 50th percentile. Using the residual Cu in stream water calculated using linear regression (see pg. 37), the weight and contrast values are reported in Table 5.3. In this case, 4 of the 14 occurrences are found in the 90th and greater percentile and all 14 occurrences are found in the 50th or greater percentile. This suggests that there may be a spatial association between the Cu occurrences and the higher Cu residuals. The maximum value for C is 1.7795, occurring at the 95th percentile. This indicates that the strongest correlation with occurrences for the residual map is in catchments where the residual is greater than and including the 95th percentile.

In section 3.3.2 the residual maps for Cu and Zn were used to demonstrate that the use of linear regression to remove the background effects on the geochemistry of stream water can be an effective tool for locating mineral occurrences. The use of linear regression to

remove the background effects can be further evaluated by comparing the C values for Cu in stream water and for Cu residuals. The results show that the highest C value from Cu in stream water is 0.0156 for the 50th percentile while the highest C value for the residuals of Cu is 1.7795 for the 95th percentile. In addition, the probabilities of finding an occurrence within higher percentile Cu concentrations in catchment basins are much higher for the residuals than in the stream water (Figure 5.2). Results from the weights of evidence provides additional support that the use of linear regression to remove the background effects is an important element in using stream water geochemistry to locate mineral occurrences.

Based on the maximum C values determined using the Cu residuals the 95th percentile was used as the cutoff point to reclassify this map to binary form. At this point the resulting W^+ and W^- were 1.5834 and –0.1962 respectively giving a contrast of 1.7795. The residual map was converted to binary form where the values greater than or equal to the 95th percentile were equal to class 2 and values less than were classified as class 1.

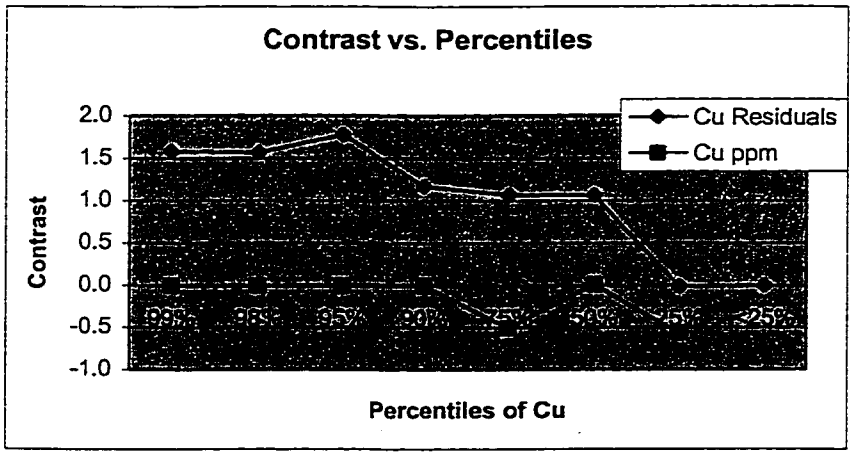

Figure 5-2. Comparison of contrast values calculated for various percentile cutoffs for Cu in catchments, and the residuals for Cu in catchments.

CLASS	Cumulative AREA Km²	Cumulative Number of Occurrences	W+	Std. (W+)	W-	Std. (W-)	C	STUD_C
99% >.00160 ppm	6.3	0						
98% .00135464 - .0016072 ppm	14.9	0						
95% .001058 .0013564 ppm	29.1	0						
90% .000916 - .001058 ppm	60.7	0						
75% .00067 - .001058 ppm	240.8	3	-0.3728	.5810	0.1315	.3046	-0.5043	-0.7688
50% .00046 - .00067 ppm	441.9	8	0.0067	.3568	-0.0089	.4119	0.0156	0.0287
25% .00046 - .00067 ppm	710.3	12	-0.0637	.2911	0.5020	.7177	-0.5658	-0.7304
<25% < .00046 ppm	778.4	14						
Missing	2009.9	31						

Table 5-2. Weights and contrasts for Cu (observed values) in stream water geochemistry at successive cutoffs from the 99th% downwards.

5.4.2 Regional Geology

As demonstrated earlier, bedrock geology can play a role in controlling the distribution of element values in the stream water, particularly of certain elements in the study area. It is also indicated that copper occurrences are more frequent in specific lithologic units than others. For these reasons the bedrock geology is considered an important evidential theme in predicting mineral potential.

The reclassified geology map was represented as a multi-class grid. Table 5.4 shows the weights calculated for the four reclassified bedrock units. In this table, the rows are not cumulative, as they are for the geochemical themes. The highest contrast value is 1.654 for the reclassified basement unit suggesting that this unit is correlated with the Cu occurrences. This result directly supports the mineral deposit models discussed in section 1.5. It is known from previous studies that the basement rocks host strata-bound sulphide deposits. It should be noted that the contrast for the Carboniferous Clastics and the Horton Group is negative, suggesting that these units have fewer Cu mineral occurrences than would be expected by chance. The Windsor Group has a contrast value of 0.3883 indicating that this unit contains slightly more Cu mineral occurrences than expected due to chance.

5.4.3 Proximity to Faults

Mineral occurrences in the study area may be spatially associated with structural faults and thus fault proximity was used as an evidential theme. The faults are represented as linear features on the map throughout the study area. To be analyzed as an evidential theme the faults were converted to a theme showing proximity to the nearest fault. To do this they were buffered at 250 m spacings out to 5 km from the fault, producing a multi-class theme. Table 5.5 shows the weights and contrasts of each cumulative buffer distance. It can be seen that the largest contrast is equal to 0.6439 at 750 m, signifying that this distance has the strongest correlation to Cu occurrences and is therefore used as the cutoff point for this evidential theme.

CLASS	Cumulative AREA Km²	Cumulative Number of Occurrences	W+	Std (W+)	W-	Std (W-)	CONTRAST	STUD_C
99% (.453884 - .55)	12.9	1	1.5240	1.0412	-0.0584	.2797	1.5824	1.4677
98% (.3732 - .453884)	13.1	1	1.5095	1.0406	-0.0582	.2797	1.5677	1.4549
95% (.298336 - .3732)	36.6	3	1.5834	.6026	-0.1962	.3038	1.7795	2.6372
90% (.22743 - .298336)	88.4	4	0.9509	.5117	-0.2195	.3185	1.1704	1.9418
75% (.089765 - .22743)	202.2	7	0.6722	.3847	-0.3984	.3803	1.0706	1.9793
50% (-.00012 - .089765)	438.0	11	0.3411	.3054	-0.7226	.5799	1.0636	1.6229
25% (-.1049 – -.00012)	613.5	11	-0.0031	.3043	0.0113	.5827	-0.0143	-0.0218
<25% (-0.64 – -.10149)	778.4	14						
Missing	2009.9	17						

Table 5-3. Weights and contrasts for Cu residuals in stream water geochemistry at successive cutoffs from the 99th % downward.

CLASS	AREA Km²	Number of Occurrences	W+	Std. (W+)	W-	Std. (W-)	Contrast	STUD_CNT
Basement	432.3	18	1.0201	.2408	-0.6341	.2785	1.6543	4.4935
Carboniferous Clastics	540.9	1	-2.1351	1.0009	0.2858	.1845	-2.4209	-2.3786
Horton Group	512.2	2	-1.3853	.7085	0.2315	.1875	-1.6167	-2.2060
Intrusions	31.5	0						
Windsor Group	493.1	10	0.2787	.3195	-0.1096	.2197	0.3883	1.0015

Table 5-4. Weights and contrasts for bedrock geology.

CLASS	Cumulative AREA Km^2	Cumulative Occurrences	W+	W-	Contrast	STUD_CNT
250	76.1	2	0.5436	-0.0285	0.5722	0.7726
500	151.9	3	0.2517	-0.0236	0.2753	0.4488
750	227.5	6	0.5476	-0.0964	0.6439	1.3994
1000	304.1	6	0.2506	-0.0518	0.3024	0.6589
1250	380.4	6	0.0228	-0.0054	0.0281	0.0614
1500	456.6	9	0.2498	-0.0866	0.3363	0.8423
1750	530.0	9	0.0977	-0.0374	0.1351	0.3387
2000	602.5	9	-0.0326	0.0136	-0.0462	-0.1158
2250	675.8	9	-0.1489	0.0679	-0.2168	-0.5439
2500	750.4	10	-0.1483	0.0792	-0.2274	-0.5877
2750	824.5	11	-0.1471	0.0912	-0.2382	-0.6300
3000	897.7	12	-0.1451	0.1038	-0.2489	-0.6701
3250	969.5	14	-0.0669	0.0586	-0.1255	-0.3451
3500	1039.9	16	-0.0025	0.0027	-0.0051	-0.0142
3750	1110.5	19	0.1055	-0.1471	0.2526	0.6801
4000	1180.1	21	0.1454	-0.2502	0.3956	1.0224
4250	1246.2	21	0.0900	-0.1662	0.2562	0.6619
4500	1310.6	22	0.0861	-0.1836	0.2697	0.6768
4750	1372.7	22	0.0390	-0.0894	0.1284	0.3221
5000	1433.9	22	-0.0053	0.0131	-0.0184	-0.0462
Missing	2009.9	31				

Table 5-5. Weights and contrasts for fault buffers.

5.5 Conditional Independence

Tests for pairwise conditional independence were carried out to ensure none of the maps violated the conditional independence assumption. The results summarized in Table 5.6 show that the chi-squared statistic calculated for all map pairs is less than 5.4, meaning

that for a probability level of 98% there is no reason to reject the hypothesis that conditional independence exists for any of the pairs of maps. As a result all map layers were used to produce the posterior probability map.

Chi-squared Statistic	Reclass of Residual_cu	GEOLOGY
Reclass of Buffers	1.05	0.37
Reclass of Residual_cu		0.94

Table 5-6. Chi-squared statistic for pairwise comparison for the evidential themes in the mineral potential model. These values are for 1 degree of freedom, and indicate that a hypothesis of conditional independence can be accepted.

5.6 Posterior Probability Map (Favourability) for Cu

A map showing the posterior probabilities was generated using the optimum weights from the residuals of the stream water geochemistry in catchment basins, the structural faults and underlying bedrock geology (Figure 5.1). The posterior probability ranged from 0.011 – 0.141. Figure 5.1 illustrates the areas of higher potential for Cu occurrences. On this map there are four small areas with the highest probability range (0.079 – 0.141) which are the areas of highest probability of finding a Cu occurrence in the field area. The second highest range of posterior probability was from 0.033 – 0.079. This group of probabilities appear to be located along the boundary between the Aspy and Bras d'Or terranes signifying this tectonic boundary may be a control on the deposition of Cu occurrences in this area.

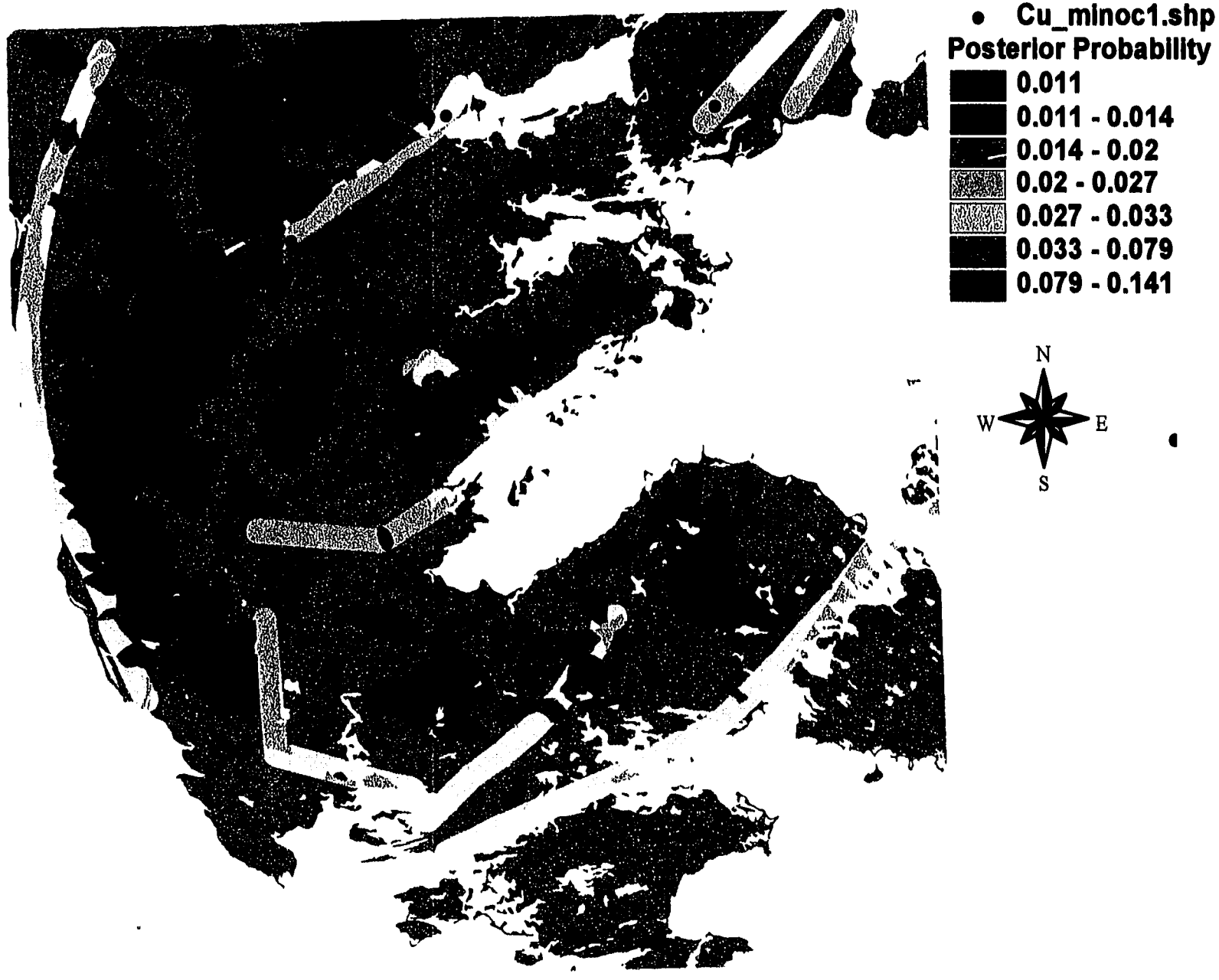

Figure 5-3. Copper mineral potential map with Cu mineral occurrences.

6 Summary and Conclusions

In this study five digital geoscience databases, from southwestern Cape Breton Island, Nova Scotia, were compiled and co-registered in a GIS format in Spans. These were stream water geochemistry, represented by catchments, a balsam fir twig geochemical survey, bedrock geology, surficial geology, and mineral occurrence data.

Summary statistics and box plots were used to characterize the stream water geochemistry and to identify physical and chemical controls on the geochemistry of fifteen metallic elements in the stream water. The box plots showed that bedrock geology and the pH of the water are important controls on the concentration of the metallic elements in the stream water.

Box plots show that the pH of the stream water has substantial control on the distribution of the fifteen metallic elements analyzed with the exception of As, Mo and Sb. Concentrations of elements such as Mg, Sr and U were found to increase with increasing pH. These elements are associated with the dissolution of carbonate rich rocks, which subsequently increases the pH of the stream water. The concentration of elements Fe, Mn decreases with increasing pH. These elements form oxides and hydroxide molecules, which have surfaces which Al, Pb, Zn, Cr, Ti and Cu can sorb to thus reducing their concentration in the stream water.

The influence of the underlying bedrock geology on the composition of the stream water was found to follow three major trends. The lowest concentrations for all of the

elements were found in catchment basins dominated by the basement rock group suggesting that rocks of this type found in the study area may be less susceptible to weathering than the other groups. As commonly seen in stream water geochemistry, elements such as Mg and Sr have highest concentrations over units containing carbonate rich rock, the Windsor Group. The box plots also show that elements, such as Fe and Pb, associated with terrestrial rocks are found in higher concentrations in the lithologic groups containing these types of rocks (red sandstones and siltstone).

Linear regression analysis was used to calculate the variability of the stream water geochemistry explained by variance in lithology, pH, and Fe and Mn oxides and hydroxides. The results indicate that the pH, Fe and Mn oxides and hydroxides exhibit the strongest control on the variation of the metallic elements, Fe, Mn, Al, Cu, Zn, Cr, Co, Pb, Ti, Al and Mg, concentration in stream water. The underlying bedrock geology explained a small amount of variance for these elements. The deposition of the Fe and Mn oxides and hydroxides is controlled by the pH of the water. As these oxides and hydroxides form, other elements such as Al, Cu, Zn, Cr, Co, Pb and Mg, are sorbed to their surfaces and are removed from solution. This suggests that the concentrations of these elements are affected by the pH of the stream water. In contrast the underlying bedrock geology was the dominant factor in controlling the variation in element concentration in stream water for elements Sr, U, As and Mo. As well, these elements are not sorbed to Fe and Mn oxides and hydroxides and therefore changes in pH and the presence of Fe and Mn oxides and hydroxides do not affect

their concentrations. Although the use of catchment basins and regression analysis has been used for stream sediment this is the first known use with stream water geochemistry and shows good results.

Linear regression was also effectively used to remove the effects of these variables on the concentrations Zn and Cu in stream water in order to highlight catchments with anomalously high residuals. Comparison of the map residuals with known Zn and Cu mineral occurrences indicate that the use of linear regression to remove background effects caused by these factors is an important tool for locating mineral occurrences. In addition, these results provide evidence that stream water is a useful sample media type for identifying areas of potential mineralization.

The effectiveness of Yule's coefficient as a tool to compare the stream water and the balsam fir twig surveys was highly dependent on the zone of influence chosen to represent the sample points and on the element compared. Two attempts were made to represent the zone of influence for each sample point in both surveys. The first used a large zone of influence and the results illustrated that for most elements analyzed the higher percentile areas were comparable. In the second attempt catchment basins were used to represent the zone of influence for the stream water sample points and a smaller zone of influence was used to represent the balsam fir twig sample points. In this attempt only elements Fe, Mn and Al were comparable at higher percentiles. These elements are known to be unstable in solution and may be quickly deposited in the form of oxides and hydroxides near their input

source. This suggests that for these elements the balsam fir twigs represent the surrounding environment, the zone of influence, similar to the stream water samples. All other elements, elements which are more stable in solution, are transported further from their input source and are therefore not accurately represented in the balsam fir twigs. These results indicate that this method is not a viable way to compare the two sample sets. Perhaps geostatistical methods that include spatial neighborhood effects may be more useful for comparison of these data sets.

Comparison of the weights and contrasts determined using weights of evidence show that the probability of finding a mineral occurrence increases when the Cu residuals determined using linear regression are used in the catchment basin as opposed to the Cu concentration in the stream water. In addition, weights of evidence provided additional support that the use of linear regression to remove the background effects is an important element in using stream water geochemistry to locate mineral occurrences. Response variables such as bedrock geology, Cu residuals and proximity to faults were found to be conditionally independent using weights of evidence. All three-map patterns representing factors favorable for Cu mineralization were then combined to locate areas of potential Cu occurrences.

In conclusion it has been shown that a GIS system in association with other statistical packages was very useful in the integration of multi-media data sets to improve the

understanding of the geochemical distribution of stream water and balsam fir twigs in southwestern Cape Breton Island. A mineral potential map for Cu produced, as a part of this study will aid in improving the constraints on future mineral exploration in the region.

References

Barr, S.M., 1993. Geochemistry and tectonic setting of late Precambrian volcanic and plutonic rocks in southeastern Cape Breton Island, Nova Scotia. Canadian Journal of Earth Science, 30: 1147-1154.

Barr, S.M. and Raeside, R.P., 1989. Tectono-Stratigraphic terranes in Cape Breton Island, Nova Scotia: Implications for the configuration of the northern Appalachian orogen. Geology, 17: 822-825.

Barr, S.M., Raeside, R.P. and White, C.E., 1998. Geological correlations between Cape Breton Island and Newfoundland, northern Appalachian orogen. Canadian Journal of Earth Sciences, 35: 1252-1270.

Barr, S.M., White, C.E. and Macdonald, A.S., 1996. Stratigraphy, tectonic setting, and geological history of Late Precambrian volcanic-sedimentary-plutonic belts in southeastern Cape Breton Island, Nova Scotia. Geological Survey of Canada, Bulletin, 468. Geological Survey of Canada, Ottawa.

Bevier, M.L., Barr, S.M., White, C.E. and Macdonald, A.S., 1993. U-Pb geocrhonologic constraints on the volcanic evolution of the Mira (Avalon) terrane, southeastern Cape Breton Island, Nova Scotia. Canadian Journal of Earth Science, 30: 1-10.

Bonham-Carter, G.F., 1991. Integration of geoscientific data using GIS. In: D.J. Maguire, M.F. Goodchild and D.W. Rhind (Editors), Geographical Information Systems. Pergamon Press/Elsevier Science Publications, Tarrytown, New York.

Bonham-Carter, G.F., 1994. Geographic Information Systems For Geoscientists: Modelling with GIS. Pergamon, Oxford, 398 pp.

Bonham-Carter, G.F., Agterberg, F.P. and Wright, D.F., 1988. Integration of geological data sets for gold exploration in Nova Scotia. Photogrammetric Engineering and Remote Sensing, 54(11): 1585-1592.

Bonham-Carter, G.F., Agterberg, F.P. and Wright, D.F., 1989. Weights of evidence modelling; A new approach to mapping mineral potential. In: F.P. Agterberg, and Bonham-Carter, G.F. (Editor), Statistical Applications in Earth Science. Geological Survey of Canada, pp. 171-183.

Bonham-Carter, G.F. and Goodfellow, W.D., 1986. Background corrections to stream geochemical data using digitized drainage and geological maps: Application to Selwyn Basin, Yukon and Northwest Territories. Journal of Geochemical Exploration, 25: 139-155.

Bonham-Carter, G.F., Rogers, P.J. and Ellwood, D.J., 1987. Catchment basin analysis applied to surficial geochemical data, Cobequid Highlands, Nova Scotia. Journal of Geochemical Exploration, 29: 259-278.

Davenport, P., 1990. A comparison of regional geochemical data from lakes and stream in northern Labrador; implications for mixed-media geochemical mapping. Journal of Geochemical Exploration, 39: 117-151.

Davis, J.C., 1986. Statistics and Data Analysis in Geology. John Wiley and Sons Inc., New York.

Drever, J.L., 1997. The Geochemistry of Natural Waters; Surface and Groundwater Environments. Prentice-Hall, Inc., New Jersery.

Dunn, C.E. and Balma, R.G., 1997. Reconnaissance Biogeochemical Survey of Southwestern Cape Breton Island, Nova Scotia, Using Balsam Fir Twigs. Open File 3344. Geological Survey of Canada, Ottawa, 35 pp.

Dunn, C.E., Coker, W.B. and Rogers, P.J., 1991. Reconnaissance and detailed geochemical surveys for gold in eastern Nova Scotia using plants, lake sediment, soil and till. Journal of Geochemical Exploration, 40: 143-163.

Dunning, G.R., Barr, S.M., Raeside, R.P. and Jamieson, R.A., 1990. U-Pb zircon, titanite and monazite ages in the Bras d'Or and Aspy terranes of Cape Breton Island, Nova Scotia. Implications for magmatic and metamorphic history. Geological Society of America Bulletin, 102: 322-330.

ESRI Incorporated, 1999. ArcView GIS.

Finch, C., Hall, G. and McConnell, J. 1992. The development and application of geochemical analyses of water. In: Current research. Newfoundland. Geological Survey Branch. Pages 297-307.

Friske, P.W.P. and Hornbrook, E.H.W., 1991. Canada's National Geochemical Reconnaissance Program. Transactions of the Institute of Mining and Metallurgy, Section B, 100: 47-56.

Garrett, R.G., 1991. The Management, Analysis and Display of Exploration Geochemical Data, Paper 9, Exploration Geochemistry Workshop, Prospectors and Developers Association of Canada, Toronto.

Tydac Inc., 1997. SPANS, Ottawa.

Tydac Inc., 1995. Tydig, Ottawa.

Jamieson, R.A., van Breeman, O., Sullivan, R.W. and Currie, K., L., 1986. The age of igneous and metamorphic events in the western Cape Breton Highlands, Nova Scotia. Canadian Journal of Earth Science, 23: 1891-1901.

Justino, M.F. and Sangster, A.L., 1987. Geology in the vicinity of the Lime Hill zinc occurrence, south-western Cape Breton Island, Nova Scotia, Current Research Part A. Geological Survey of Canada, pp. 2325-2341.

Keppie, J.D., 1993. Geology of the eastern Creignish Hills, central Cape Breton Highlands: implications for gold mineralization. Nova Scotia Department of Natural Resources, Mines and Energy Branch, Report 93-2.

Kirkham, R.V., 1985. Base metals in Upper Windsor (Cordroy) Group oolitic and stromatolitic limestones in the Atlantic provinces. Current Research Part A, Geological Survey of Canada, 85-1A: 573-585.

Lynch, G., Barr, S.M., Houlahan, T. and Giles, P., 1995. Geological compilation, Cape Breton Island, Nova Scotia. 3159, Geological Survey of Canada, Ottawa.

Macdonald, A.S. and Barr, S.M., 1985. Geology and age of polymetallic occurrences in volcanic and granitoid rocks, St. Anne's area, Cape Breton Island, Nova Scotia. Current Research, Part B., Geological Survey of Canada, 85-1B: 117-124.

Macdonald, A.S. and Barr, S.M., 1993. Geological setting and depostional environment of the Stirling Group of southeastern Cape Breton Island, Nova Scotia. Atlantic Geology, 29: 137-147.

Mapinfo Cooperation, 1996. MapInfo.

Northwood Geosciences Ltd., 1998. Vertical Mapper, Ottawa.

NSDNR 1996. Nova Scotia Mineral Occurrence Database, Halifax, Nova Scotia.

Raeside, R.P. and Barr, S.M., 1990. Geology and tectonic development of the Bras d'Or suspect terrane, Cape Breton Island, Nova Scotia. Canadian Journal of Earth Science, 27: 1371-1381.

Raines, G.L., Bonham-Carter, G.F. and Kemp, L., 1999. Weights of Evidence - An Arcview Extension for Predictive and Probabilistic Modeling. Arcuser(In press).
Rose, A.W., Dahlberg, E.C. and Keith, M.L., 1970. A Multiple Regression Technique for Adjusting Background Values In Stream Sediment Geochemistry. Economic Geology, 65: 156-165.

Sangster, A.L., Justino, M.F. and Thorpe, R.I., 1990a. Metallogeny of Proterozoic marble-hosted zinc occurrences at Lime Hill and Meat Cove, Cape Breton Island, Nova Scotia. In: A.L. Sangster (Editor), Mineral Deposit Studies in Nova Scotia. Geological Survey of Canada.

Sangster, A.L., Thorpe, R.I. and Chatterjee, A.K., 1990b. A reconnaissance lead isotopic study of mineral occurrences in pre-Carboniferous basement rocks of northern and central Cape Breton Island, Nova Scotia. In: A.L. Sangster (Editor), Mineral Deposit Studies in Nova Scotia. Geological Survey of Canada.

Simpson, P.R., Edmunds, W.M., Breward, N., Cook, J.M., Flight, D., Hall, G.E.M. and Lister, T.R. 1993. Geochemical mapping of stream water for environmental studies and mineral exploration studies in the UK. Journal of Geochemical Exploration, 49: 63-88.

Swinden, S.H. and Dunsworth, S.W., 1995. Metallogeny, Ch. 9. In: H. Willams (Editor), Geology of the Appalachian-Caledonian Orogen in Canada and Greenland. Geological Survey of Canada, Ottawa.

Thompson, M., and Howarth, R.J., 1978. A new approach to the estimation of analytical precision . Journal of Geochemical Exploration, 9: 23-30.

Tukey, J.W., 1977. Explanatory Data Analysis. Addison – Wesley, Reading Massachusetts.

Wright, D.F., 1996. Evaluating Volcanic -Hosted Massive Sulphide Favourability using GIS-Based spatial data integration models, Snow Lake area, Manitoba. Ph.D. Thesis, University of Ottawa, Ottawa, 338 pp.

Wright, D.F. and Bonham-Cater, G.F., 1996. VHMS favourability mapping with GIS-based integration models, Chisel Lake-Anderson Lake area. In: G.F. Bonham-Cater, A.G. Galley and G.E.M. Hall (Editors), EXTECH 1: A Multidisciplinary Approach to Massive Sulphide Research in the Rusty Lake-Snow Lake Greenstone Belts, Manitoba. Geological Survey of Canada, Ottawa, pp. 339-376.

Appendix A

Summary statistics of stream water geochemistry.

Units and Method of determination shown as suffixes to the element name.

[illegible]	[illegible]					
[illegible]	[illegible]					
[illegible]	50.0	210.0	4644.0	1425.9	1340.0	1266.0
[illegible]	5.0	5.0	1113.0	160.9	123.0	24.0
[illegible]	50.0	348.0	9126.0	1158.6	820.0	533.0
[illegible]	0.1	1.9	325.0	6.4	3.6	3.2
[illegible]	0.1	0.1	3.2	0.3	0.2	0.1
[illegible]	0.1	0.4	355.0	11.2	3.8	1.7
[illegible]	4.0	4.0	72.0	13.3	11.0	7.0
[illegible]	0.1	0.2	255.4	15.2	7.9	3.0
[illegible]	2.0	3.0	626.0	162.4	129.0	39.0
[illegible]	1.0	4.0	1964.0	54.3	13.0	7.0
[illegible]	1.0	1.0	65.0	11.2	8.0	4.0
[illegible]	5.0	9.0	2926.0	420.2	313.0	172.0
[illegible]	5.0	5.0	135.0	24.2	20.0	14.0
[illegible]	0.5	0.5	7.7	1.7	1.5	0.8
[illegible]	0.1	0.1	2.2	0.3	0.2	0.1
[illegible]	0.1	0.1	1.1	0.3	0.3	0.1
[illegible]	50.0	50.0	570.0	121.7	90.0	70.0
[illegible]	0.1	0.1	2.3	0.5	0.5	0.4
[illegible]	0.5	0.5	11.0	1.7	1.3	0.8
[illegible]	0.1	0.1	3.3	0.4	0.3	0.2
[illegible]	0.5	4.1	1943.7	53.7	13.5	7.2
[illegible]	10.0	10.0	1020.0	220.6	190.0	140.0
[illegible]	0.1	0.1	1.6	0.2	0.1	0.1
[illegible]	10.0	10.0	120.0	23.4	20.0	20.0
[illegible]	0.2	0.6	56.1	10.9	8.4	3.5
[illegible]	0.0	0.0	0.8	0.2	0.1	0.1
[illegible]	0.0	0.0	1.3	0.3	0.2	0.2
[illegible]	5.0	5.0	200.0	49.4	41.0	19.0
[illegible]	5.0	9.0	745.0	210.3	173.0	121.0
[illegible]	5.0	5.0	196.0	48.9	40.0	34.0
[illegible]	5.0	5.0	47.0	12.0	10.0	7.0
[illegible]	5.0	5.0	195.0	48.6	44.0	18.0
[illegible]	5.0	5.0	27.0	9.8	9.0	6.0
[illegible]	5.0	6.0	164.0	41.4	36.0	29.0
[illegible]	5.0	5.0	39.0	10.2	9.0	6.0
[illegible]	5.0	5.0	122.0	23.7	19.0	19.0
[illegible]	5.0	5.0	109.0	21.9	18.5	11.0
[illegible]	0.1	0.1	1.5	0.3	0.2	0.1
[illegible]	5.0	5.0	808.0	68.1	43.0	32.0
[illegible]	0.1	0.9	793.0	16.6	3.0	3.0
[illegible]	0.1	1.6	526.0	10.1	5.2	5.8
[illegible]		3.1	140.0	16.9	10.2	#N/A
[illegible]	0.0	2.1	8.3	6.6	6.7	7.0

[redacted]							
[redacted]	1047.0	1340.0	1657.0	2199.4	2507.5	2793.6	3132.9
[redacted]	45.0	123.0	219.0	353.6	425.2	593.5	688.0
[redacted]	617.5	820.0	1265.0	2101.0	2886.2	4526.5	5914.5
[redacted]	3.1	3.6	5.0	7.7	14.1	25.8	41.5
[redacted]	0.2	0.2	0.3	0.4	0.5	0.6	0.9
[redacted]	2.2	3.8	7.9	17.2	27.9	69.2	184.0
[redacted]	7.0	11.0	16.0	23.1	33.0	45.2	52.1
[redacted]	3.0	7.9	16.6	33.6	59.5	83.5	101.5
[redacted]	69.3	129.0	233.5	340.5	414.8	461.2	514.3
[redacted]	8.5	13.0	27.0	84.8	162.0	439.2	1130.9
[redacted]	4.0	8.0	15.0	23.0	30.0	41.0	48.2
[redacted]	203.5	313.0	487.5	788.4	1065.4	1384.6	1864.1
[redacted]	12.0	20.0	31.0	41.6	50.6	83.8	103.8
[redacted]	1.0	1.5	2.1	3.1	3.5	4.4	4.9
[redacted]	0.2	0.2	0.4	0.5	0.7	0.9	1.1
[redacted]	0.2	0.3	0.4	0.5	0.7	0.9	1.0
[redacted]	70.0	90.0	140.0	226.0	306.0	411.6	507.2
[redacted]	0.3	0.5	0.7	0.9	1.1	1.4	1.6
[redacted]	0.9	1.3	2.4	3.2	3.6	4.8	5.1
[redacted]	0.2	0.3	0.4	0.6	0.7	1.1	1.3
[redacted]	8.4	13.5	27.6	87.3	176.5	415.6	900.7
[redacted]	122.5	190.0	290.0	389.0	490.0	610.0	641.8
[redacted]	0.1	0.1	0.2	0.5	0.7	0.9	1.0
[redacted]	20.0	20.0	30.0	30.0	40.0	40.0	60.0
[redacted]	4.4	8.4	14.7	22.2	27.1	37.3	44.0
[redacted]	0.1	0.1	0.2	0.3	0.4	0.5	0.6
[redacted]	0.1	0.2	0.4	0.6	0.8	1.0	1.1
[redacted]	26.0	41.0	65.0	94.8	112.0	142.1	153.4
[redacted]	113.0	173.0	277.0	408.0	485.0	608.7	663.6
[redacted]	26.0	40.0	66.0	93.4	115.0	140.5	160.3
[redacted]	7.0	10.0	14.0	20.0	25.0	32.2	34.8
[redacted]	23.0	44.0	63.0	91.7	115.7	139.0	153.7
[redacted]	7.0	9.0	12.0	15.8	18.4	23.2	24.0
[redacted]	22.0	36.0	54.0	77.8	95.4	109.8	117.7
[redacted]	6.0	9.0	12.0	17.0	18.9	23.7	25.0
[redacted]	13.0	19.0	30.0	43.0	49.0	59.2	78.9
[redacted]	12.0	18.5	28.0	40.0	46.2	58.0	75.8
[redacted]	0.2	0.2	0.3	0.6	0.7	0.9	1.2
[redacted]	25.0	43.0	78.0	123.0	185.4	304.3	466.2
[redacted]	2.3	3.0	4.5	16.1	42.7	136.6	403.3
[redacted]	4.1	5.2	7.3	11.0	19.8	45.3	129.2
[redacted]	6.0	10.2	20.4	35.1	56.0	75.8	97.6
[redacted]	6.5	6.7	6.9	7.2	7.5	8.0	8.1

Appendix B

Thompson-Howarth plots showing precision of the analyses of the metallic elements in the stream water geochemical survey.

Results based of field duplicates, so the precision refers to the combined field and analytical variability. For each plot, units are log ppm for both axes.

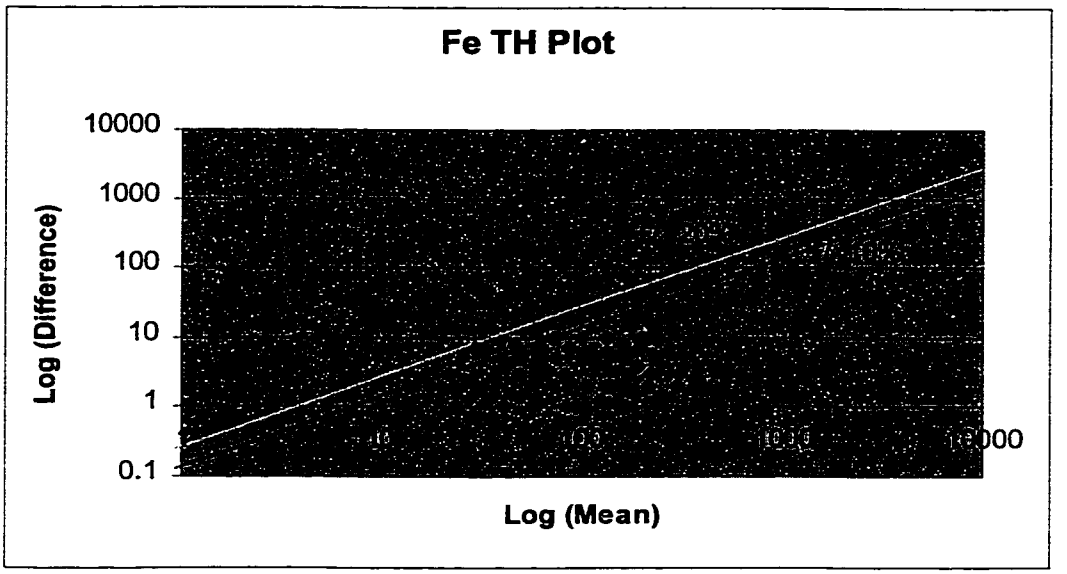
Fe TH Plot
10000
1000
100
10
1
0.1
Log (Difference)
Log (Mean)

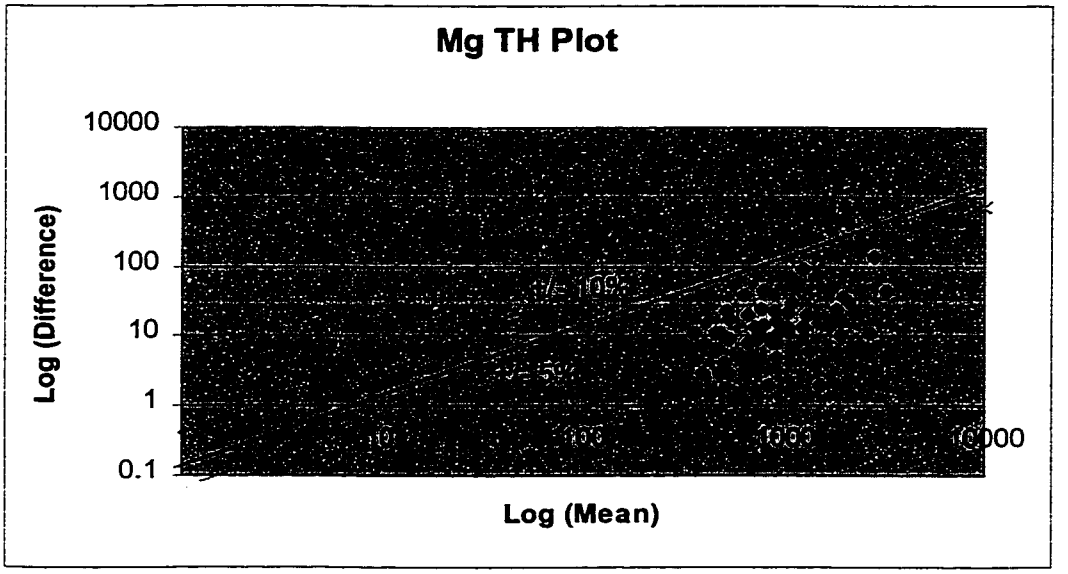
Mg TH Plot
10000
1000
100
10
1
0.1
Log (Difference)
Log (Mean)

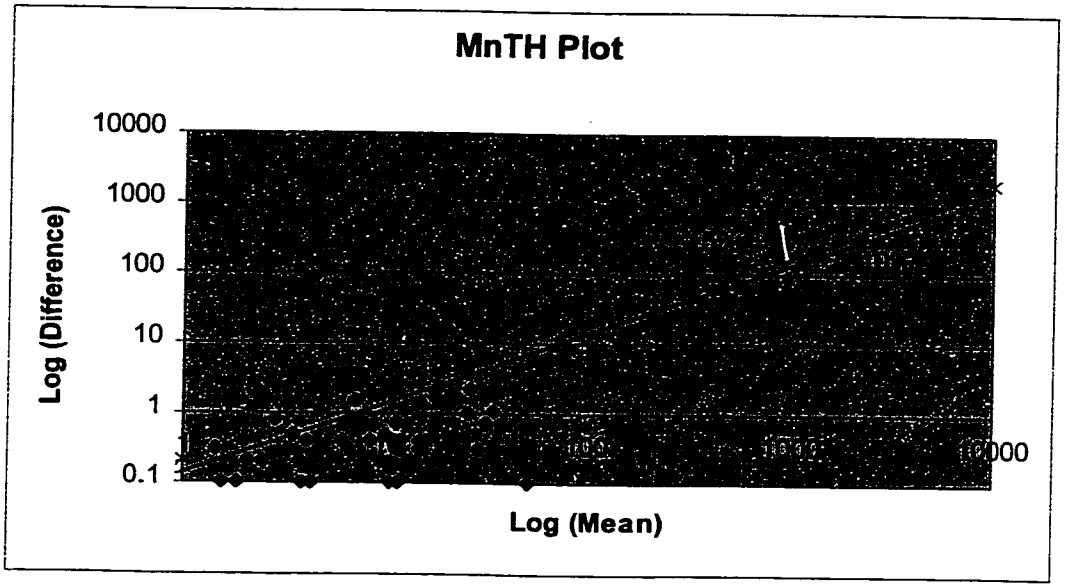
MnTH Plot
10000
1000
100
10
1
0.1
Log (Difference)
Log (Mean)

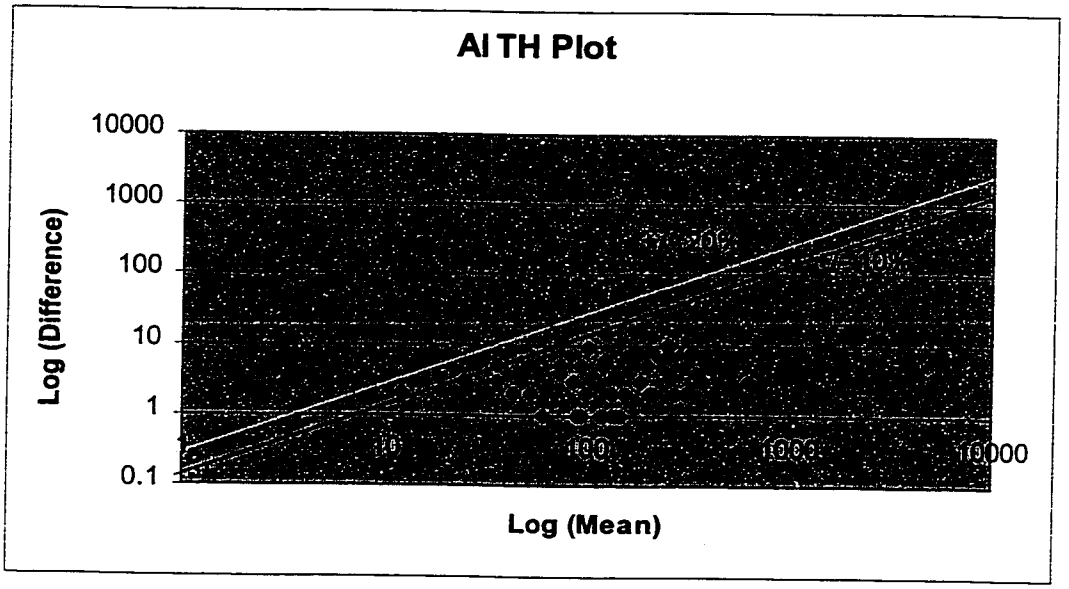
Al TH Plot
10000
1000
100
10
1
0.1
Log (Difference)
Log (Mean)

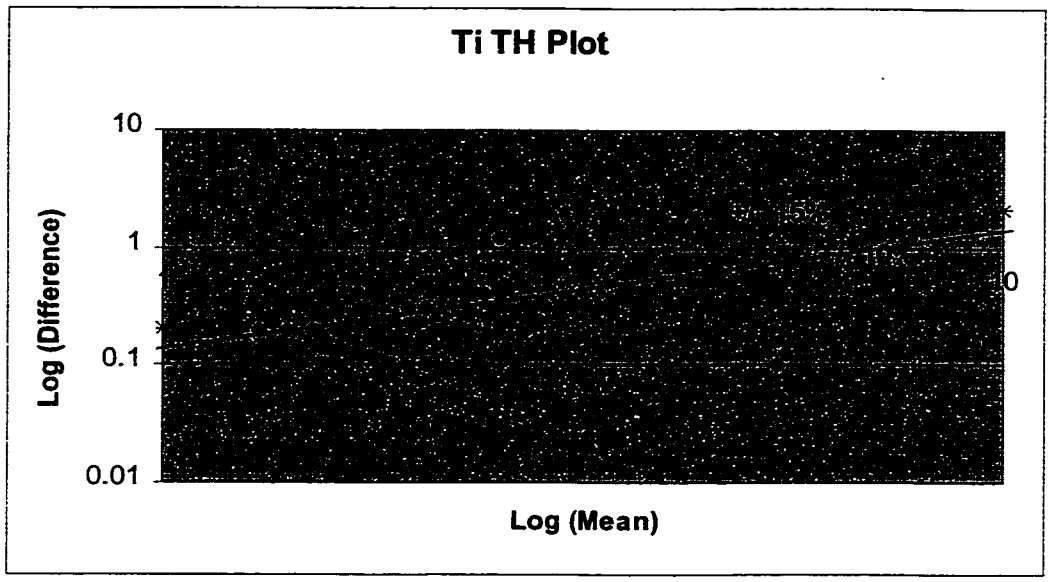
Ti TH Plot
10
1
0.1
0.01
Log (Difference)
Log (Mean)

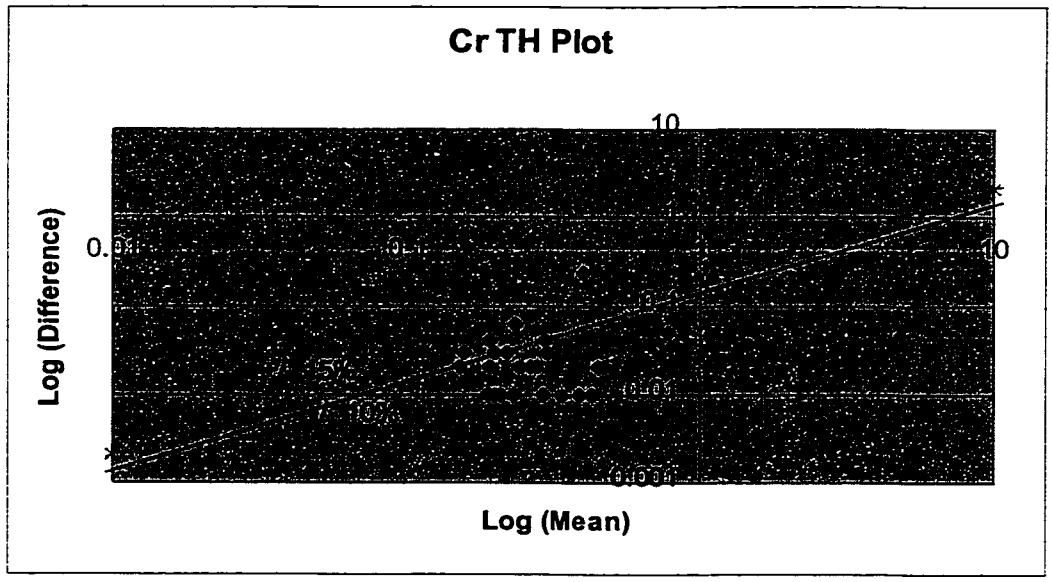
Cr TH Plot
10
Log (Difference)
Log (Mean)

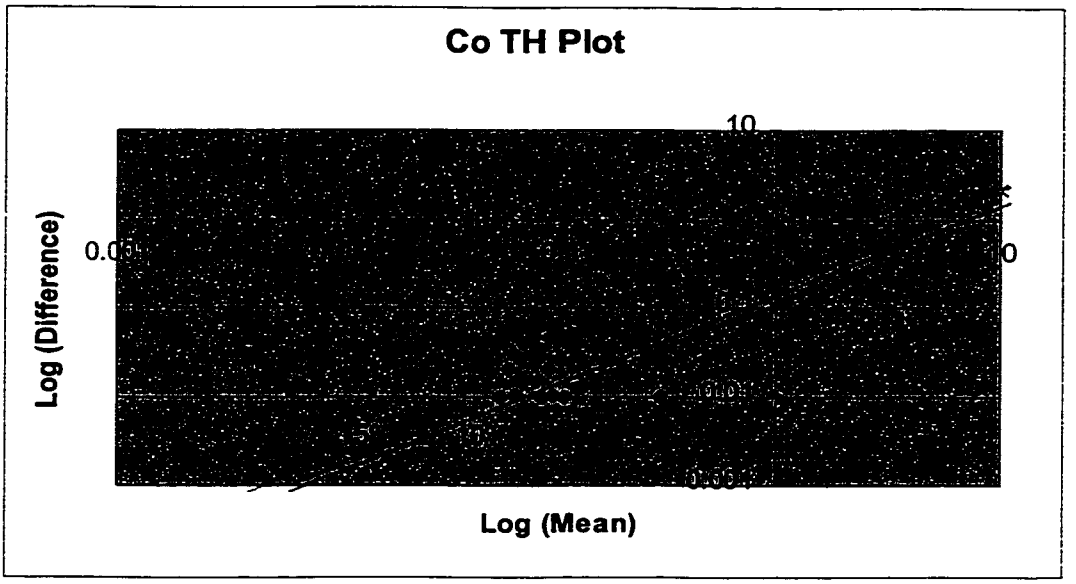
Co TH Plot
10
Log (Difference)
Log (Mean)

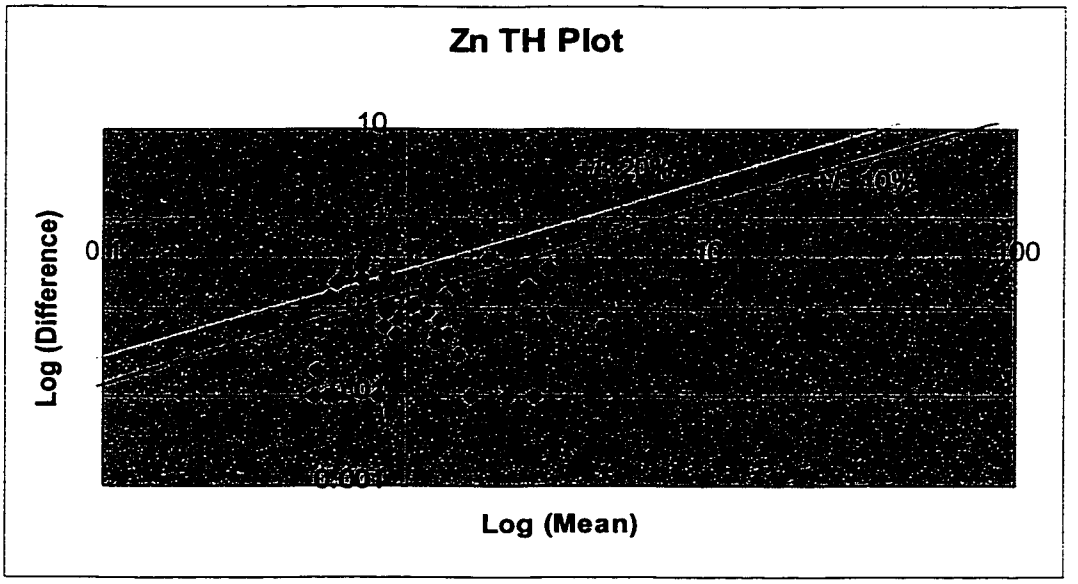
Zn TH Plot
10
Log (Difference)
Log (Mean)

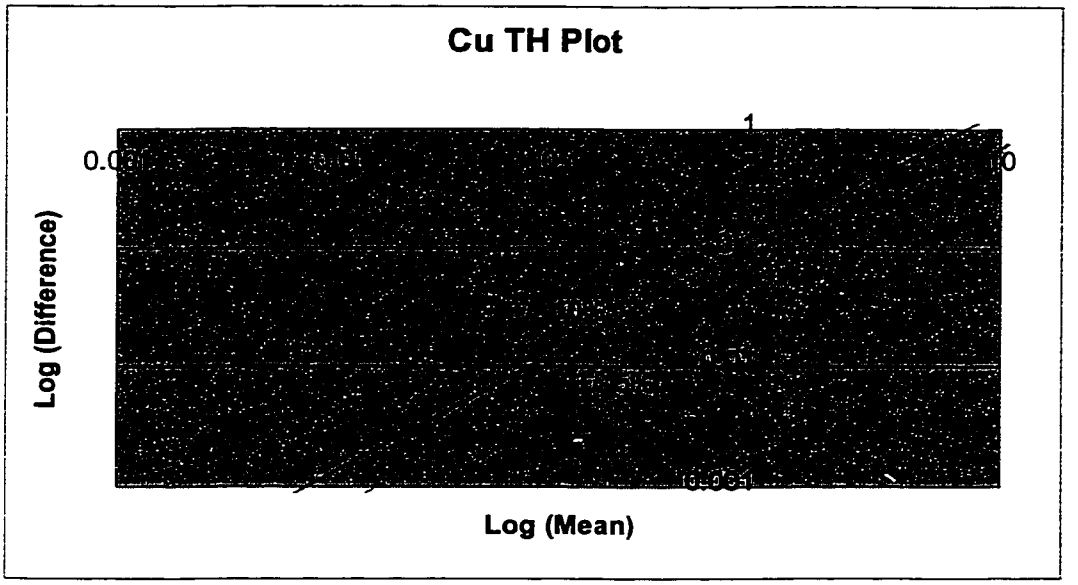
Cu TH Plot
Log (Difference)
Log (Mean)

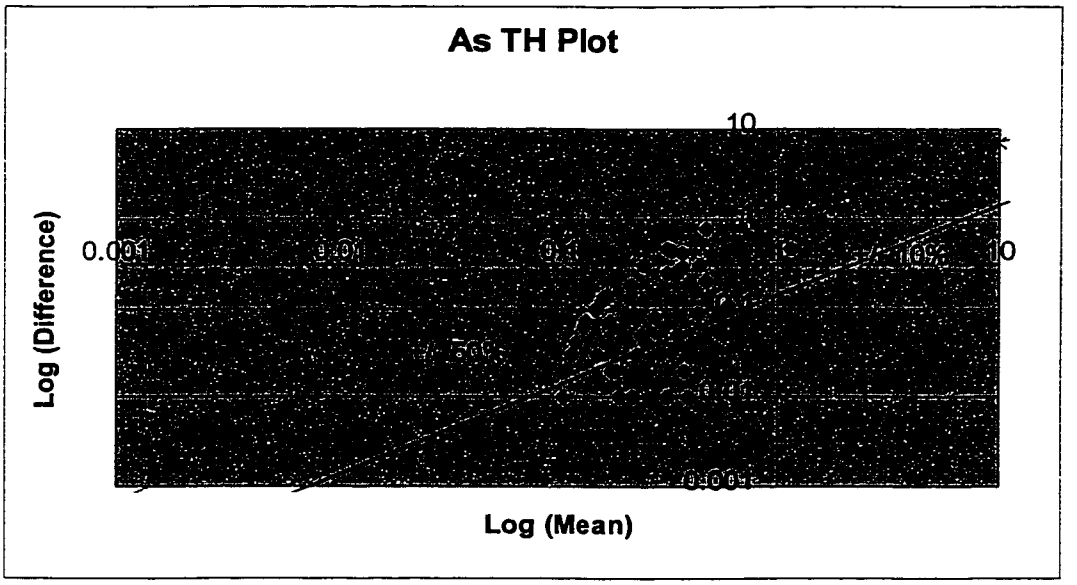
As TH Plot
Log (Difference)
Log (Mean)

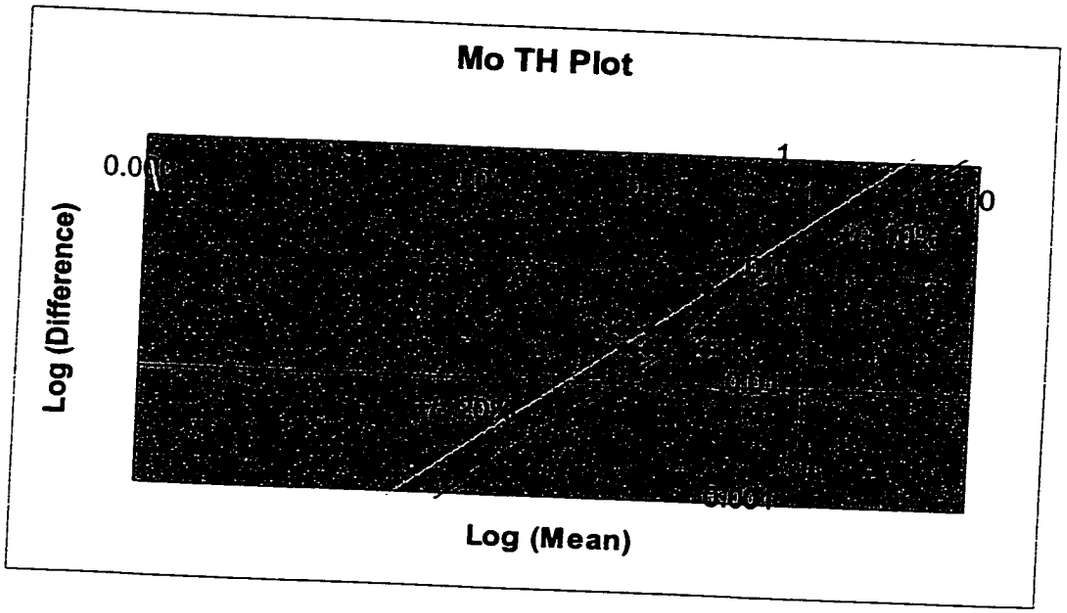
Mo TH Plot
Log (Difference)
Log (Mean)

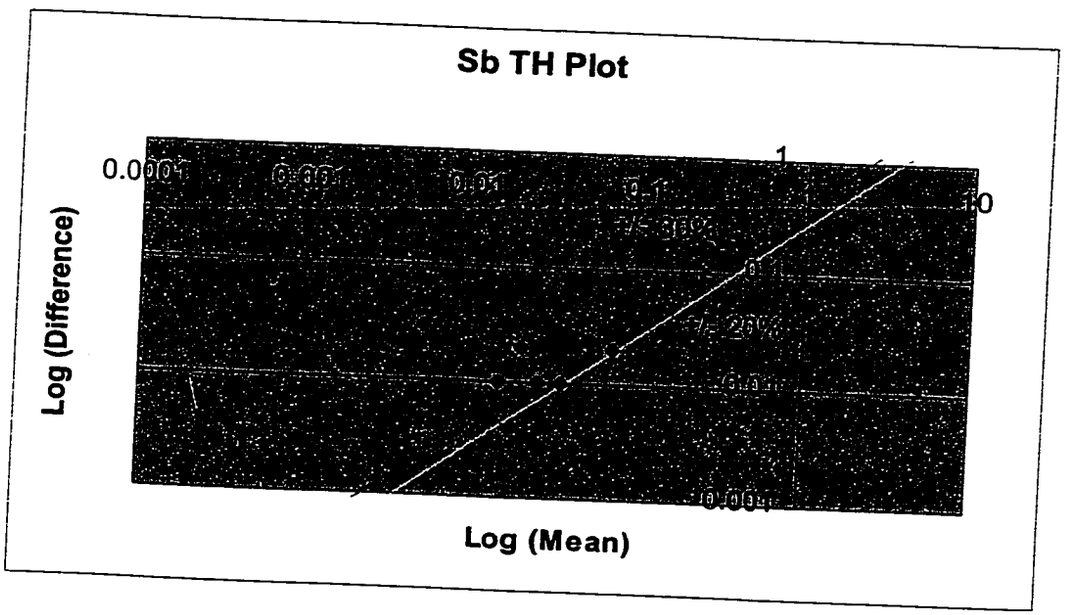
Sb TH Plot
Log (Difference)
Log (Mean)

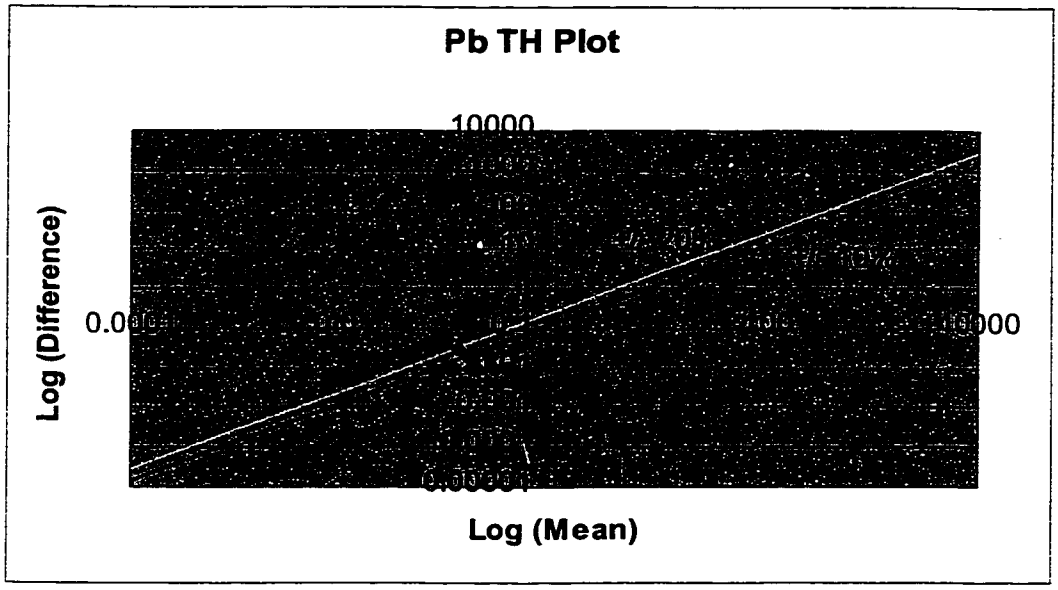
Pb TH Plot
10000
0.0
Log (Difference)
Log (Mean)

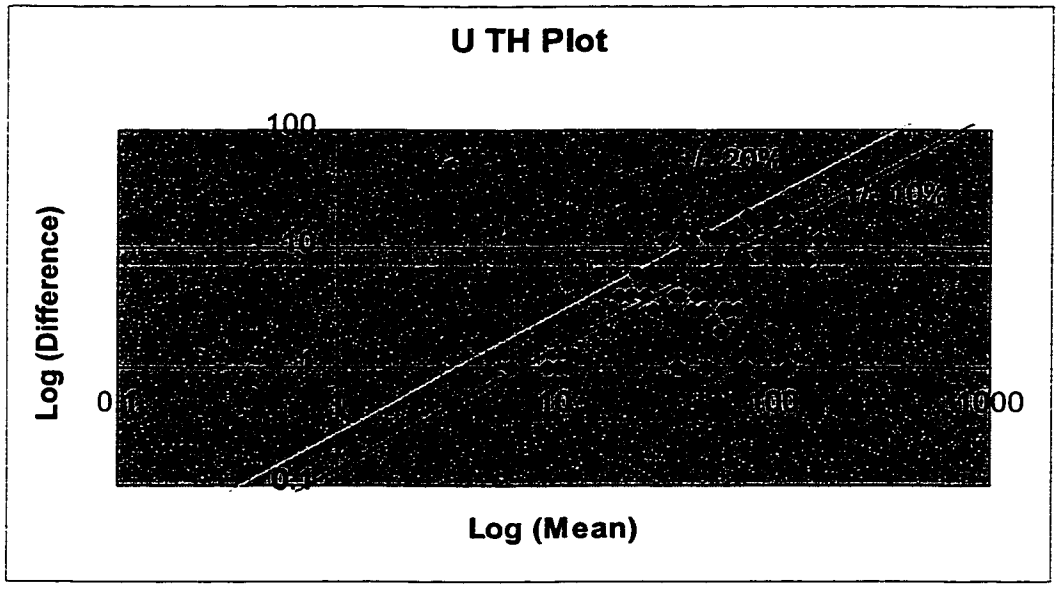
U TH Plot
100
0
Log (Difference)
Log (Mean)

Appendix C

Summary statistics of balsam fir twig geochemistry.

[illegible]						
[illegible]		1.5	3.3	2.3	2.2	0.27
[illegible]	5	5	78	13.2	12.0	11.89
[illegible]	0.5	0.5	6	1.8	1.8	1.04
[illegible]	10	370	6600	2137.9	2000.0	1156.41
[illegible]	1	13	190	36.8	30.0	19.66
[illegible]	2000	91000	279000	169747.9	169000.0	33793.34
[illegible]	3	3	50	5.7	5.0	6.39
[illegible]	1	1	15	4.7	4.0	2.20
[illegible]	1	1	100	25.2	18.0	20.00
[illegible]	0.5	0.5	11	1.2	1.0	1.77
[illegible]	0.01	0.04	1.02	0.05	0.02	0.13
[illegible]	500	500	14400	3060.5	2400	1960.11
[illegible]	0.5	0.5	5.3	0.5	0.6	1.01
[illegible]	5000	134000	348000	234509.6	234000	40422.80
[illegible]	0.1	0.8	25	3.6	2.6	2.57
[illegible]	10	651	9050	2749.3	2460	1292.29
[illegible]	5	32	940	185.8	160	107.10
[illegible]	0.1	-0.1	1.9	0.4	0.4	0.15
[illegible]	0.1	0.2	5.3	0.9	0.7	0.69
[illegible]	0.1	0.1	4.6	0.5	0.4	0.45
[illegible]	300	300	5800	803.2	780	631.30
[illegible]	0.1	0.1	4.7	0.5	0.3	0.59
[illegible]	0.05	0.05	2.28	0.3	0.22	0.28
[illegible]	20	960	4200	1963.4	1900	502.32
[illegible]	1000	0	14300	5336.4	5200	2126.06
[illegible]	2	142	445	269.6	262.5	60.65
[illegible]	0.2	1.7	52.5	10.1	8.65	6.80
[illegible]	1	99	244	150.4	148	33.44
[illegible]	2	2	15	1.1	2	2.92
[illegible]	1	1	48400	25495.3	26000	6397.23
[illegible]	1	1407	84622	22911.2	20759	11728.34
[illegible]	1	7	142	33.2	29	19.89
[illegible]	1000	1000	45450	22742.0	22290	7008.40
[illegible]	3	14	124	51.2	48	20.91
[illegible]	1	1	125	10.1	8	5.14

	2.04	2.22	2.4	2.7	2.8	3.0	3.1
	8	12	17.0	26.0	32.0	42.7	60.5
	1.3	1.8	2.3	3.0	3.8	4.5	5.0
	1300	2000	2700.0	3600.0	4100.0	5172.0	5600.0
	24	30	40.0	57.6	87.6	110.0	133.6
	143000	169000	195000.0	216000.0	228400.0	245440.0	253800.0
	3	5	8.0	12.6	18.0	25.0	32.7
	3	4	6.0	7.6	9.0	12.0	13.0
	13	18	27.0	59.0	69.8	78.0	90.4
	0.6	1	1.5	2.7	4.4	7.4	9.2
	-0.03	-0.02	0.0	0.2	0.3	0.5	0.7
	1600	2400	3600.0	5700.0	7180.0	10144.0	11652.0	
	-0.5	0.6	1.1	1.9	2.5	3.3	3.7
	206000	234000	261000.0	290000.0	306000.0	323160.0	328720.0
	1.8	2.6	4.2	6.6	9.2	13.7	17.0
	1800	2460	3240.0	4428.0	5588.0	7056.0	7823.2
	110	160	230.0	320.0	388.0	530.0	658.8
	0.3	0.4	0.5	0.6	0.6	0.8	0.9
	0.4	0.7	1.0	1.9	2.5	3.5	4.1
	0.2	0.4	0.6	1.0	1.4	2.2	3.0
	600	780	1000.0	1300.0	1400.0	2000.0	2636.0
	-0.1	0.3	0.7	1.2	1.7	2.7	3.1
	-0.05	0.22	0.4	0.6	0.8	1.3	1.6
	1600	1900	2200.0	2600.0	2900.0	3172.0	3236.0
	3700	5200	6600.0	8260.0	9480.0	10816.0	11300.0
	240	262.5	294.0	329.3	352.1	388.9	396.4
	6	8.65	13.0	16.9	21.0	28.4	35.6
	131	148	167.0	185.0	195.3	209.0	224.4
	-2	2	3.0	5.0	6.1	9.0	9.4
	21600	26000	29200.0	32860.0	34680.0	36472.0	38136.0
	13561	20759	29848.0	39277.3	44665.4	55099.7	62675.2
	20	29	41.0	58.0	71.0	79.9	95.2
	18350	22290	26270.0	32212.0	35748.0	39767.2	41587.2
	37	48	62.0	76.3	88.3	101.0	114.0
	6	8	12.0	17.0	21.0	26.7	41.7

Appendix D

Mineral occurrence data

(NSDNR, 1996)

Occurrence	Northing	Easting	COMMODITIES	STATUS	Stratigraphic Unit	Minerals
[illegible]	5042280	657370	Cu	occurrence	Horton Group	chalcopyrite, malachite, pyrite
[illegible]	5059350	694430	Au, Cu, Fe, Zn	occurrence	Fourchu Group	chalcopyrite, gold, pyrite, sphalerite
[illegible]	5062170	673380	Fe, Cu	occurrence	Horton Group	pyrite, hematite, magnetite, chalcopyrite, siderite
[illegible]	5059000	669430	Fe	occurrence	Horton Group	magnetite, specularite
[illegible]	5068450	678730	Fe, Mn, Cu, Co, Ni	prospect	Horton Group	chalcopyrite, hematite, limonite, magnetite, manganese oxide, pyrite, pyrrhotite
[illegible]	5041680	657000	Pb, Cu, Ag	prospect	Windsor Group	galena, pyrite, chalcopyrite
[illegible]	5057200	666210	Cu, Pb, Zn	occurrence	Windsor Group	chalcopyrite, galena, marcasite, pyrite, sphalerite
[illegible]	5066550	663160	Cu, Mo	occurrence	Fourchu Group	bornite, chalcopyrite, covellite, hematite, native copper, pyrite, molybdenite, graphite
[illegible]	5066340	662230	Cu, Fe, Zn	occurrence	Fourchu Group	bornite, chalcopyrite, magnetite, pyrite, specularite, sphalerite
[illegible]	5062950	692550	Cu, Fe	occurrence	Bourinot Group	bornite, chalcopyrite, pyrite
[illegible]	5062340	694300	Cu, Fe	boulder	Bourinot Group	chalcopyrite, siderite
[illegible]	5066230	662120	Cu	occurrence	Fourchu Group	pyrite, chalcopyrite, malachite
[illegible]	5064080	659900	Cu	occurrence	Sporting Mountain Pluton	pyrite, chalcopyrite
[illegible]	5066290	655750	Cu, Ag, Au	occurrence	Sporting Mountain Pluton	chalcocite, bornite, tetrahedrite
[illegible]	5061460	693360	Fe	boulder	Fourchu Group	pyrite
[illegible]	5064380	632110	Ba, Zn, Pb, Cu, Ag, Sr, Fe	occurrence	Horton Group	barite, hematite, pyrite, sphalerite, galena, chalcopyrite, malachite, bornite, fluorite
[illegible]	5065560	653570	Fe	prospect	Pringle Mountain Group	hematite, ochre
[illegible]	5060450	645600	Sr, Cu, Pb, Zn, Ba	occurrence	Windsor Group	barite, celestite, chalcopyrite, galena, pyrite, sphalerite
[illegible]	5054910	623270	Fe, Cu, Au	occurrence		chalcopyrite, native copper, pyrite, native gold
[illegible]	5058860	617320	Pb, Zn, Ba, Fe	prospect	Horton Group	galena, sphalerite, barite, ankerite, pyrite
[illegible]	5059030	629640	Cu	occurrence	Canso Group	pyrite, chalcopyrite
[illegible]	5063760	629380	Cu, Pb, Zn	occurrence	Horton Group	chalcopyrite, pyrite, malachite, galena
[illegible]	5082450	634210	Pb, Zn, Cu, Fe	occurrence	Macumber Formation	galena, sphalerite, chalcopyrite, pyrite
[illegible]	5093310	638850	Cu	occurrence	George River Group	azurite, chalcopyrite, chrysocolla, malachite, pyrite
[illegible]	5094480	646600	Cu, W, Mo, Fe	prospect	George River Group	chalcopyrite, magnetite, molybdenite, pyrite, scheelite, wolframite, pyrrhotite
[illegible]	5074080	618150	Au	placer	Recent Sediments	gold
[illegible]	5094800	646430	As, Au, Cu	occurrence	George River Group	pyrite, hematite, chalcopyrite, arsenopyrite, malachite
[illegible]	5089920	643980	Fe, Cu	occurrence	George River Group	magnetite, pyrite, hematite, chalcopyrite
[illegible]	5086400	630560	Fe, Cu	deposit	George River Group	magnetite, pyrite, chalcopyrite, specularite
[illegible]	5087690	641070	Pb	boulder	Windsor Group	galena
[illegible]	5070780	643200	Zn, Cu, W, Fe, wollastonite	deposit	Lime Hill Gneissic Complex	skarn, wollastonite
[illegible]	5086020	631840	Cu, Fe, W	occurrence	George River Group	chalcopyrite, pyrite, pyrrhotite, wolframite
[illegible]	5080150	654510	Pb	occurrence	Windsor Group	galena
[illegible]	5080500	633370	Au, Fe	occurrence	George River Group	gold, pyrite, pyrrhotite
[illegible]	5074820	642160	Pb	boulder	Windsor Group	galena
[illegible]	5076790	628620	Au, As, Pb, Cu	prospect	George River Group	pyrite, arsenopyrite, galena, chalcopyrite, hematite, sphalerite
[illegible]	5078430	630000	C, Fe, Cu	prospect	George River Group	graphite, pyrite, chalcopyrite
[illegible]	5082920	633730	Fe	occurrence	George River Group	magnetite
[illegible]	5080820	630650	As, Au	occurrence	George River Group	arsenopyrite, pyrite
[illegible]	5074040	644470	As, Fe, Sb, Cu, Ag, Au, Co	occurrence	George River Group	pyrite, arsenopyrite, stibnite, chalcopyrite
[illegible]	5082890	632520	Fe, As, Au	occurrence	George River Group	arsenopyrite, limonite, pyrite, hematite
[illegible]	5088930	637230	Pb, Zn, Cu	occurrence	George River Group	pyrite, galena, sphalerite, chalcopyrite
[illegible]	5095140	645470	Cu, Mo, As, Fe	occurrence	George River Group	magnetite, pyrite, pyrrhotite, chalcopyrite, arsenopyrite
[illegible]	5068610	626040	As, Fe, Mo	occurrence	Craignish Hills Pluton	arsenopyrite, hematite, molybdenite, pyrite
[illegible]	5085870	637180	Pb, Zn	occurrence	George River Group	pyrite, galena, sphalerite
[illegible]	5086340	636840	Zn, C, Fe, Mo	occurrence	George River Group	sphalerite, graphite, pyrite, molybdenite
[illegible]	5078660	647980	As	boulder	George River Group	arsenopyrite, pyrite
[illegible]	5081210	654700	Fe, As	boulder	Undefined	pyrite, arsenopyrite
[illegible]	5075800	643340	As	boulder	George River Group	pyrite, arsenopyrite
[illegible]	5083918	649329	Mg	occurrence	Windsor Group	magnesite, chalcopyrite
[illegible]	5070640	645100	Zn, Fe	occurrence	Lime Hill Gneissic Complex	sphalerite, pyrite
[illegible]	5072880	644050	Zn, Cu	boulder	Lime Hill Gneissic Complex	pyrrhotite, sphalerite, chalcopyrite
[illegible]	5076000	677100	Cu	occurrence	Windsor Group	chalcopyrite

Occurrence	Northing	Easting	COMMODITIES	STATUS	Lithostratigraphic Unit	Minerals
[illegible]	5048920	682970	Cu	occurrence	Horton Group	chalcopyrite, malachite, pyrite
[illegible]	5074730	690410	Fe, Mn, Pb, Zn	prospect	Loch Lomond Formation	hausmannite, hematite, limonite, manganite, pyrolusite, rhodochrosite
[illegible]	5074640	677570	Ba, Fe	occurrence	Fourchu Group	barite, hematite
[illegible]	5092380	686040	Fe	prospect	Bourinot Group	hematite
[illegible]	5094140	659190	Zn, Pb, Cu, Ba	deposit	Horton Group	sphalerite, galena, chalcopyrite, barite, pyrite, marcasite, malachite
[illegible]	5075700	693860	Mn	deposit	Loch Lomond Formation	hausmannite, manganite, pyrolusite
[illegible]	5081540	691460	Mn	occurrence		braunite, pyrolusite
[illegible]	5080350	689970	Fe, Pb, Zn	prospect	Silvermine Formation	galena, pyrite, sphalerite
[illegible]	5093030	661250	Zn, Pb	occurrence	Windsor Group	sphalerite, marcasite, pyrite, galena
[illegible]	5091980	660450	Cu, Fe	occurrence	Windsor Group	chalcopyrite, pyrite
[illegible]	5090510	660960	Cu, Pb, Zn	boulder	Windsor Group	chalcopyrite, galena, pyrite, marcasite, sphalerite
[illegible]	5090810	668130	Pb	occurrence	Windsor Group	galena
[illegible]	5071080	689920	Cu, Pb, Zn	occurrence	Loch Lomond Plutonic Suite	chalcopyrite, galena, malachite, sphalerite
[illegible]	5075200	687000	Ba, Pb, Zn, Cu	occurrence	Windsor Group	barite, pyrite, galena, chalcopyrite, bornite
[illegible]	5072990	690110	Fe	occurrence	Windsor Group	hematite
[illegible]	5073980	687250	Pb	occurrence	Silvermine Formation	galena
[illegible]	5074440	690250	Pb, Zn, Sr, Ba	occurrence	Windsor Group	galena, sphalerite, celestite, barite, hematite, hydrozincite
[illegible]	5075280	690990	Sr, Pb, Zn, Cu	occurrence	Windsor Group	celestite, galena, sphalerite, chalcopyrite, malachite
[illegible]	5073300	684550	Ba, Cu, Pb, Zn	occurrence	Windsor Group	barite, chalcopyrite, galena, sphalerite
[illegible]	5089660	692940	Fe	prospect	Windsor Group	hematite
[illegible]	5095950	693180	Cu, Pb, Zn, Fe, Ag, Cd, Ni, Au	occurrence	Bras D'or Gneiss	pyrite, sphalerite, chalcopyrite, galena, graphite, pyrrhotite, magnetite
[illegible]	5095780	668820	Au, Ag, Cu	occurrence		pyrite, chalcopyrite
[illegible]	5071950	682270	Cu	occurrence		chalcopyrite
[illegible]	5074270	690330	Au	occurrence	Uist Formation	gold

Appendix E

Box plots of metallic element grouped by pH and lithology.

Lithology is reported by major groupings; CC = Carboniferous Clastics, Horton = Horton Group, Windsor = Windsor Group, Basement = Basement rock.

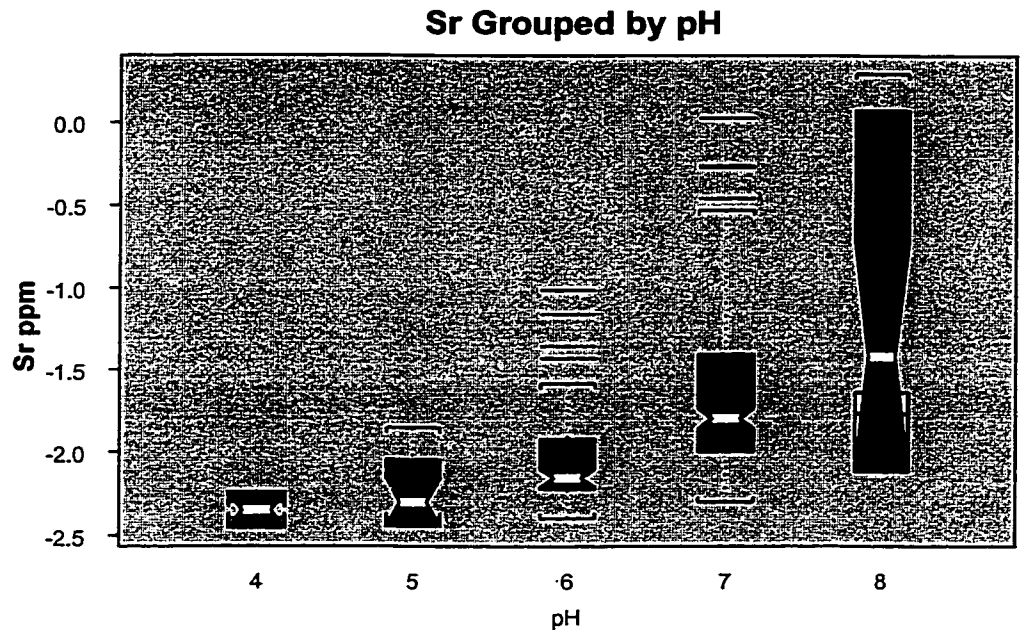
Sr Grouped by pH
Sr ppm
0.0
-0.5
-1.0
-1.5
-2.0
-2.5
4
5
6
7
8
pH

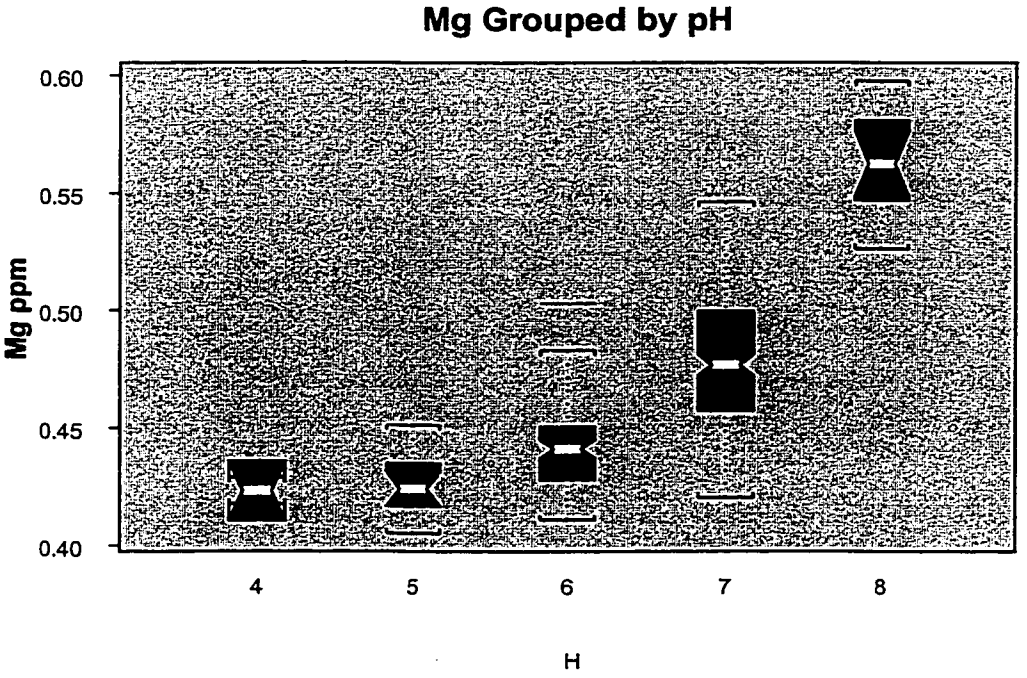
Mg Grouped by pH
Mg ppm
0.60
0.55
0.50
0.45
0.40
4
5
6
7
8
H

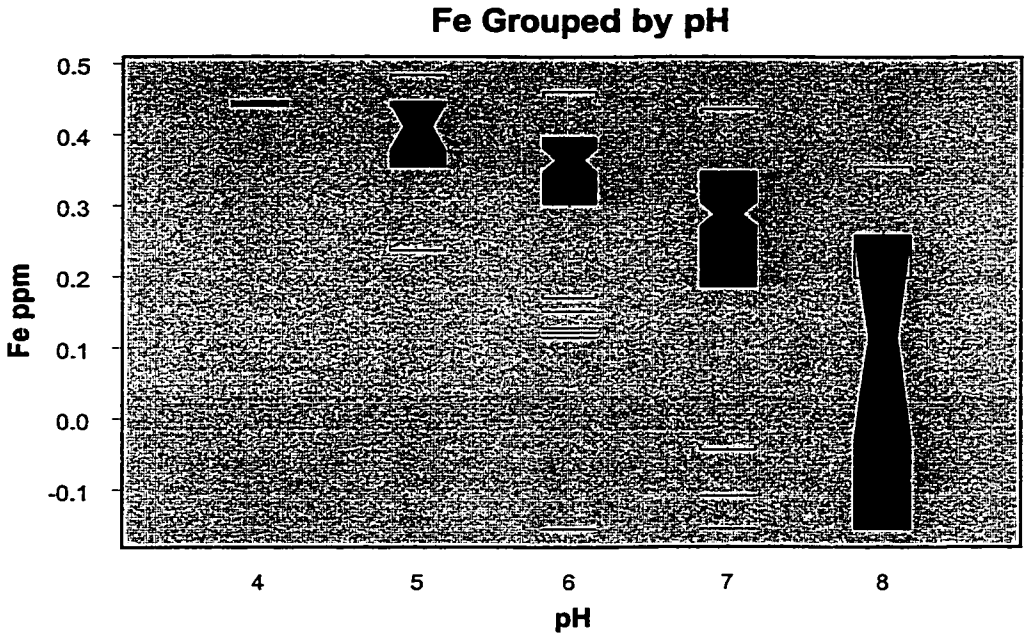
Fe Grouped by pH
0.5
0.4
0.3
0.2
0.1
0.0
-0.1
Fe ppm
4
5
6
7
8
pH

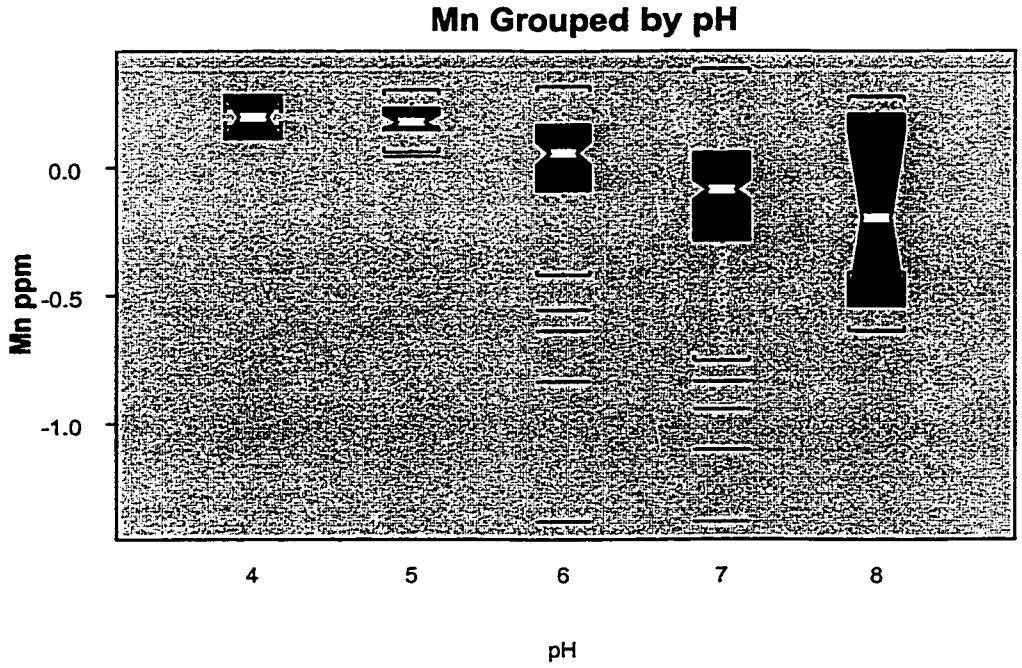
Mn Grouped by pH
0.0
-0.5
-1.0
Mn ppm
4
5
6
7
8
pH

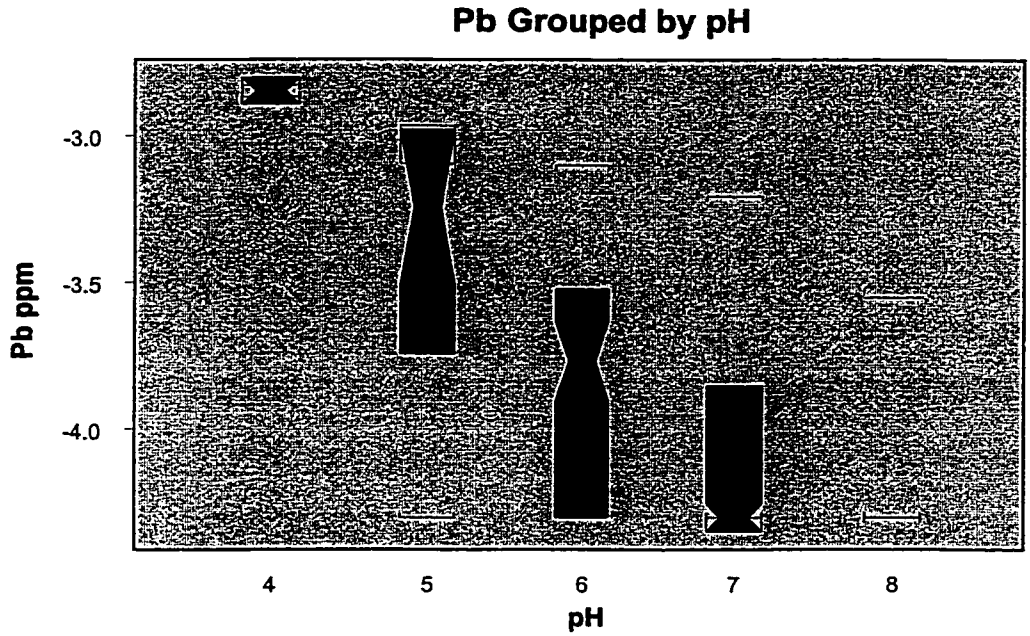
Pb Grouped by pH
Pb ppm
-3.0
-3.5
-4.0
4
5
6
7
8
pH

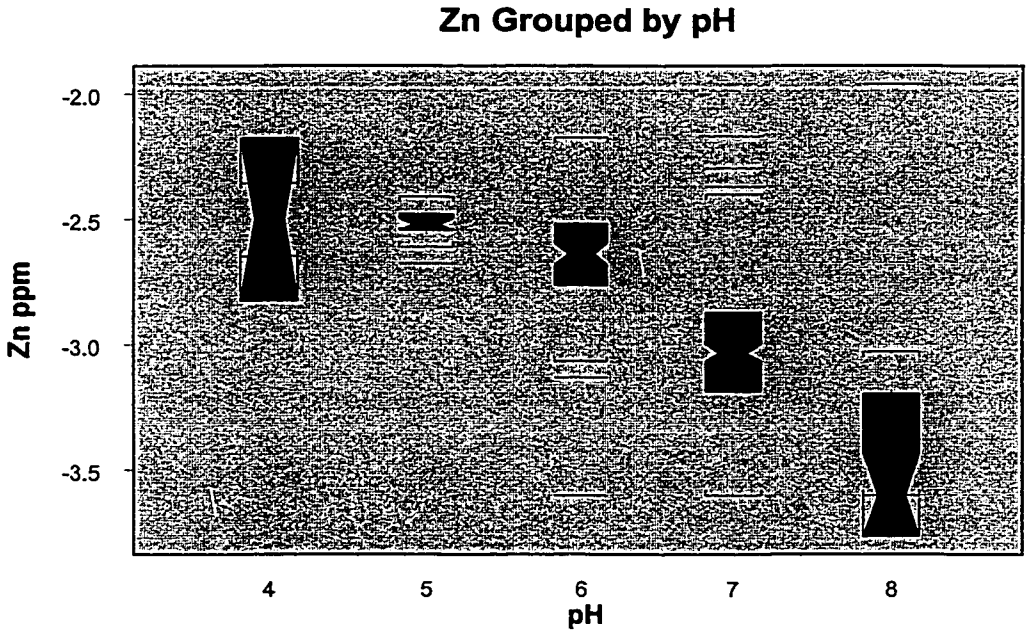
Zn Grouped by pH
Zn ppm
-2.0
-2.5
-3.0
-3.5
4
5
6
7
8
pH

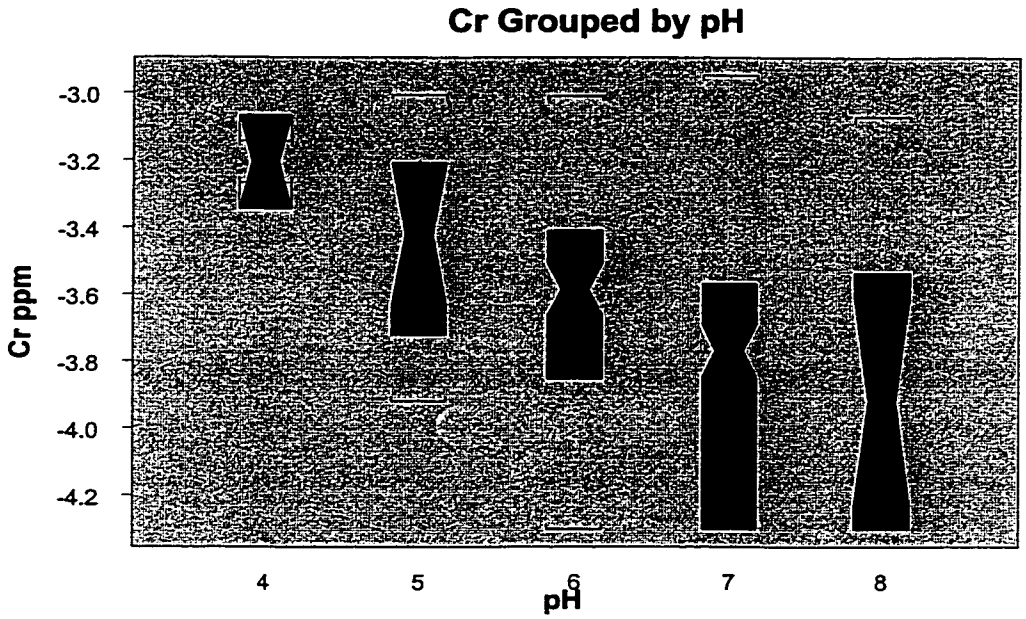
Cr Grouped by pH
-3.0
-3.2
-3.4
-3.6
-3.8
-4.0
-4.2
Cr ppm
4
5
6
7
8
pH

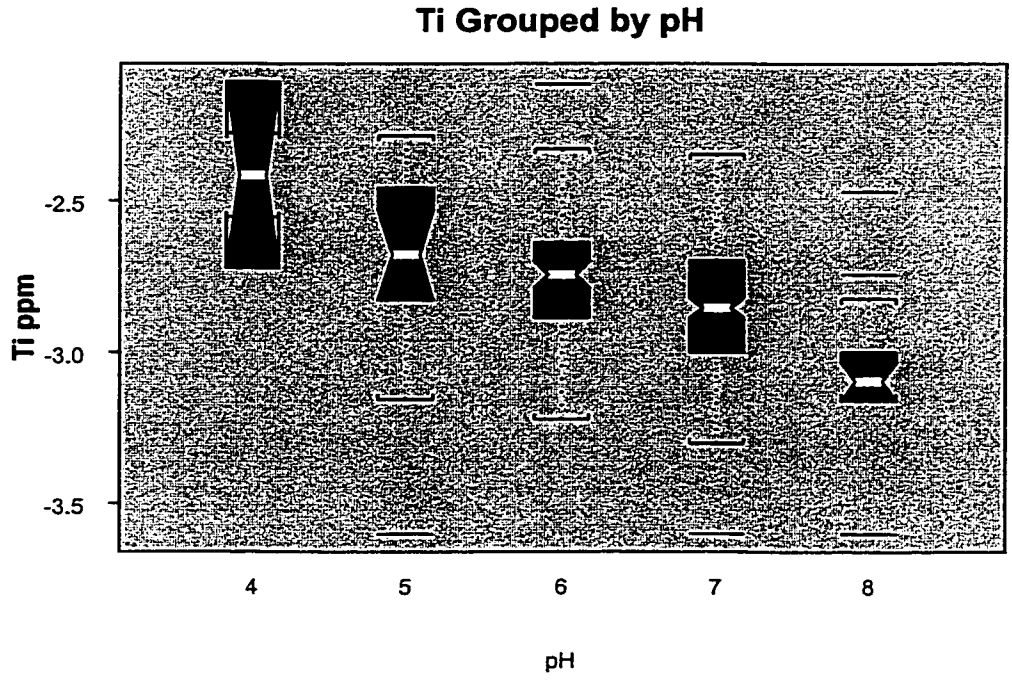
Ti Grouped by pH
-2.5
-3.0
-3.5
Ti ppm
4
5
6
7
8
pH

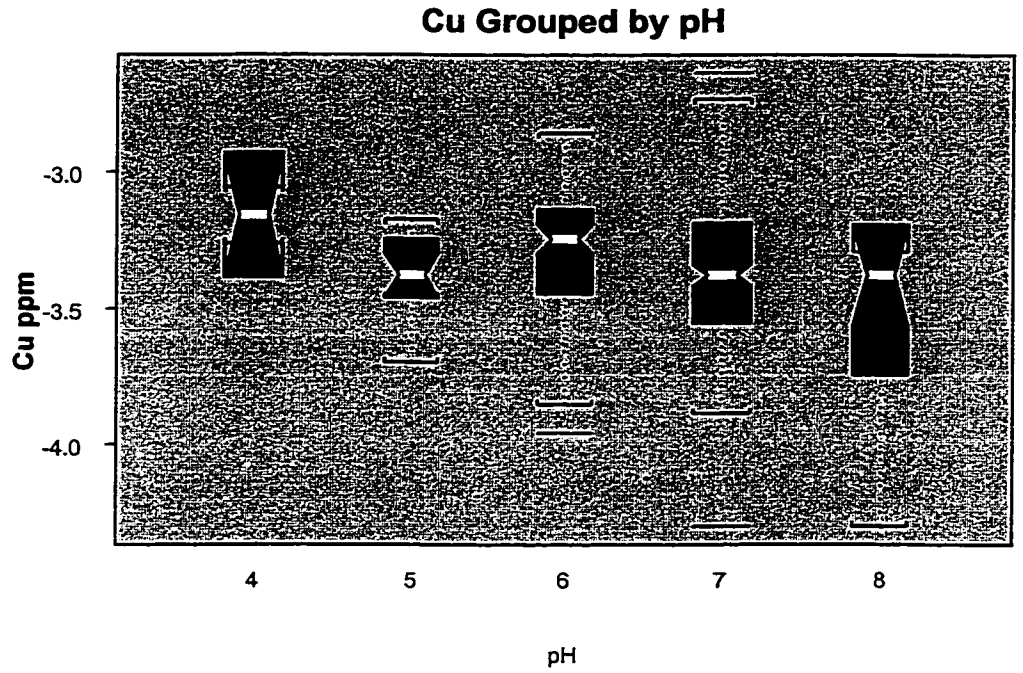
Cu Grouped by pH
Cu ppm
-3.0
-3.5
-4.0
4
5
6
7
8
pH

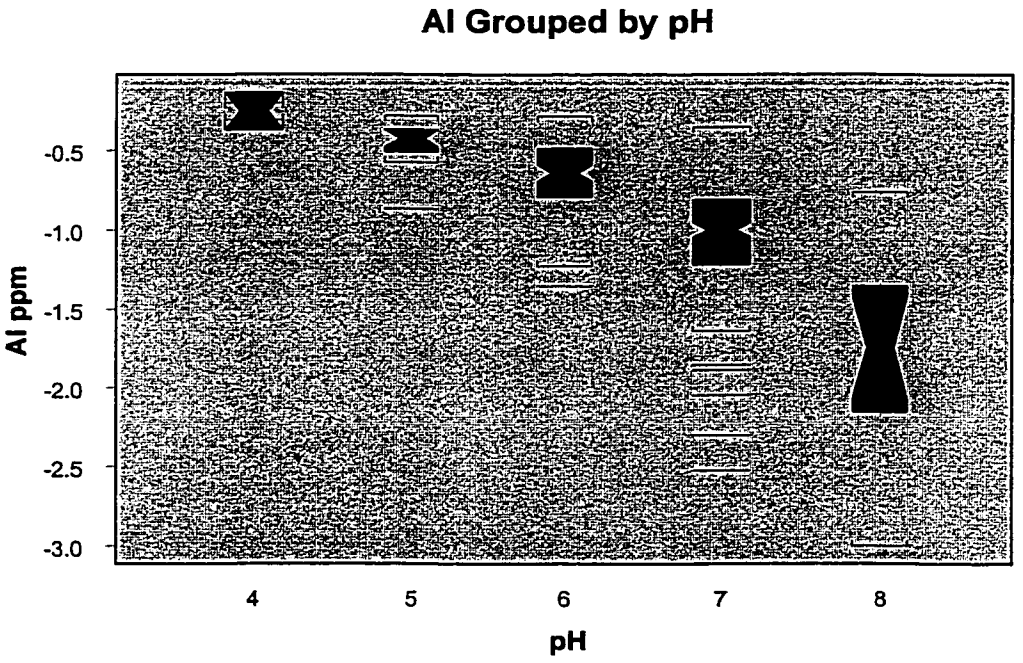
Al Grouped by pH
Al ppm
-0.5
-1.0
-1.5
-2.0
-2.5
-3.0
4
5
6
7
8
pH

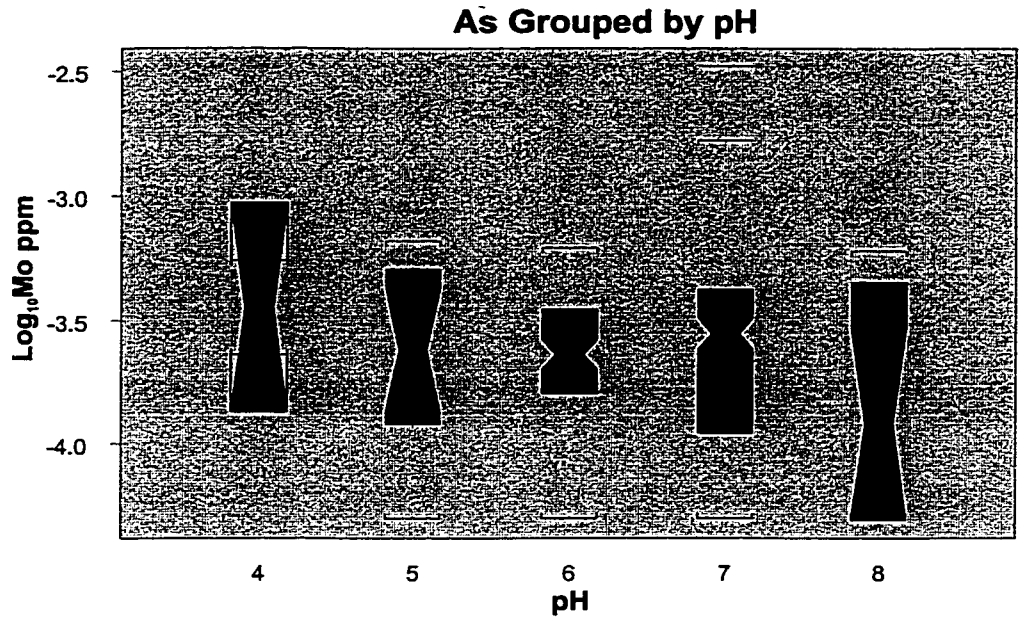
As Grouped by pH
-2.5
-3.0
-3.5
-4.0
Log10Mo ppm
4
5
6
7
8
pH

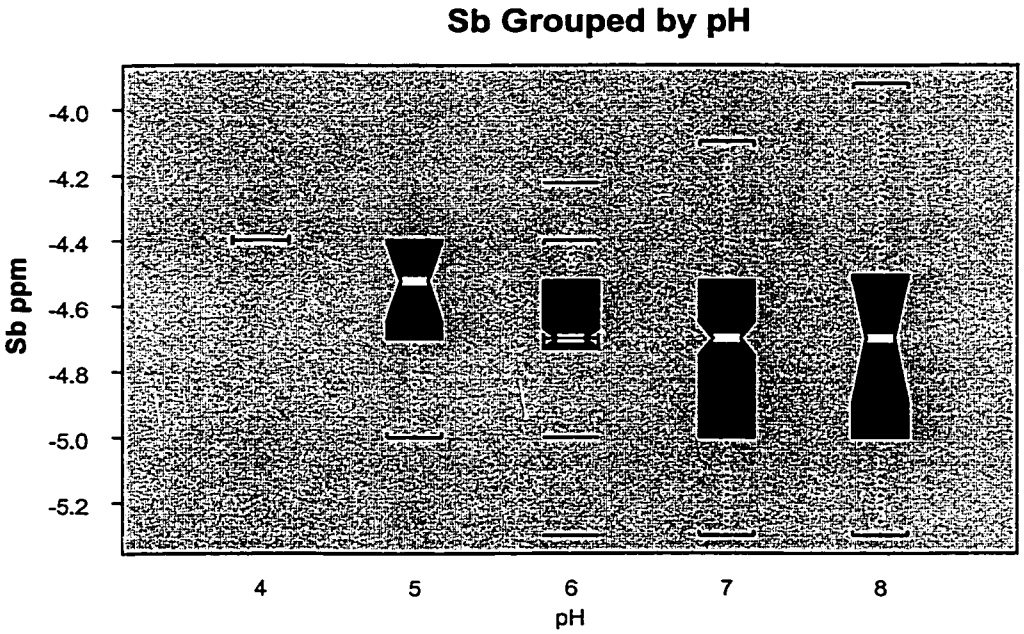
Sb Grouped by pH
-4.0
-4.2
-4.4
-4.6
-4.8
-5.0
-5.2
Sb ppm
4
5
6
7
8
pH

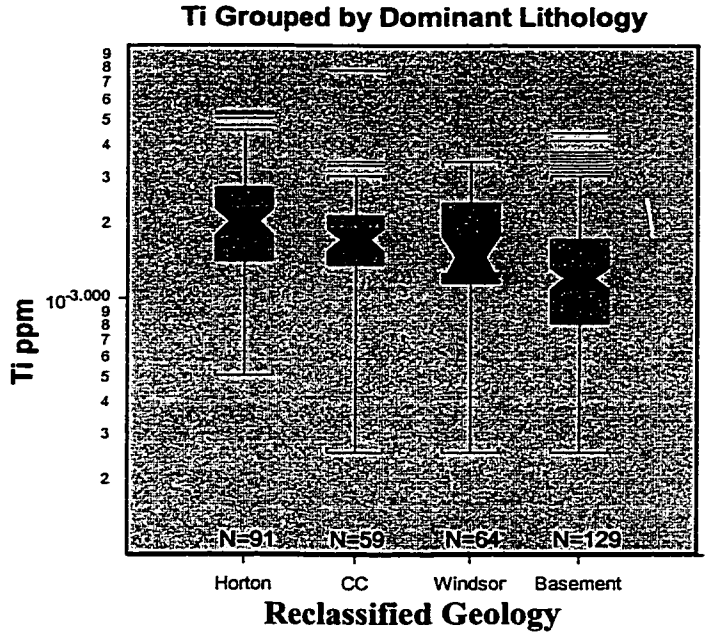
Ti Grouped by Dominant Lithology
Ti ppm
10-3.000
N=91
N=59
N=64
N=129
Horton
CC
Windsor
Basement
Reclassified Geology

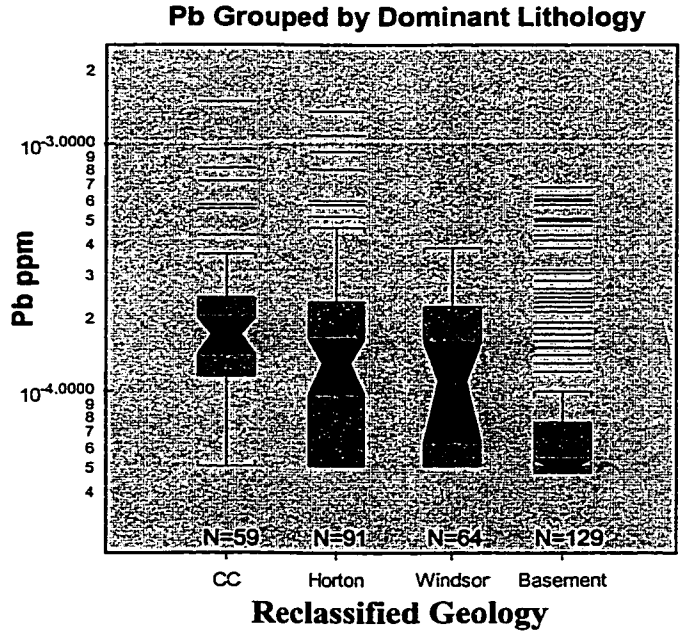
Pb Grouped by Dominant Lithology
Pb ppm
10-3.0000
10-4.0000
N=59
N=91
N=64
N=129
CC
Horton
Windsor
Basement
Reclassified Geology

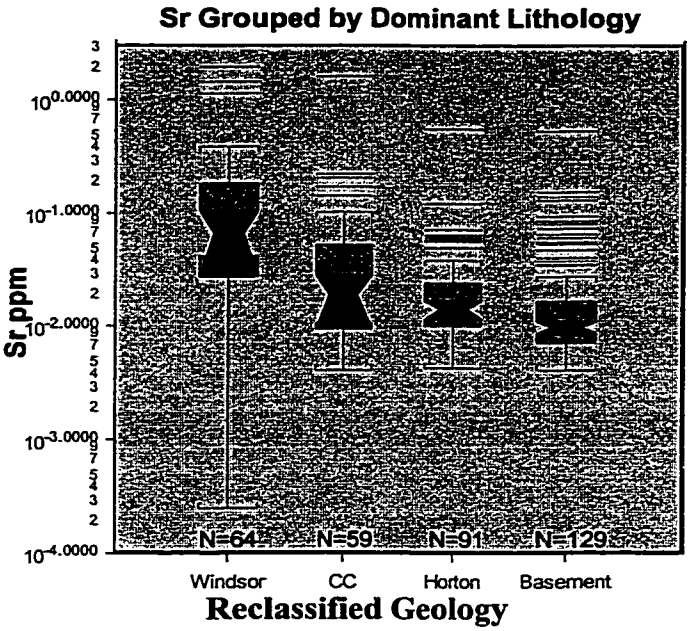
Sr Grouped by Dominant Lithology
Sr ppm
N=64
N=59
N=91
N=129
Windsor
CC
Horton
Basement
Reclassified Geology

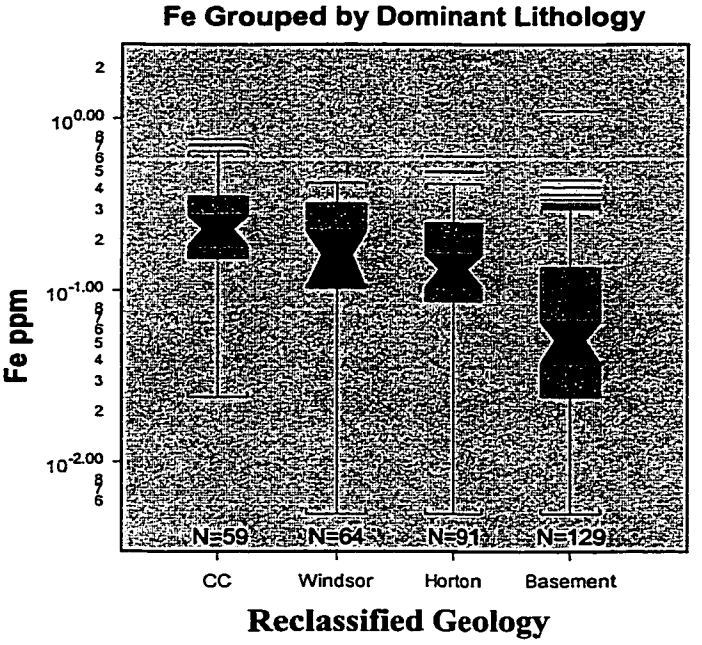
Fe Grouped by Dominant Lithology
Fe ppm
N=59
N=64
N=91
N=129
CC
Windsor
Horton
Basement
Reclassified Geology

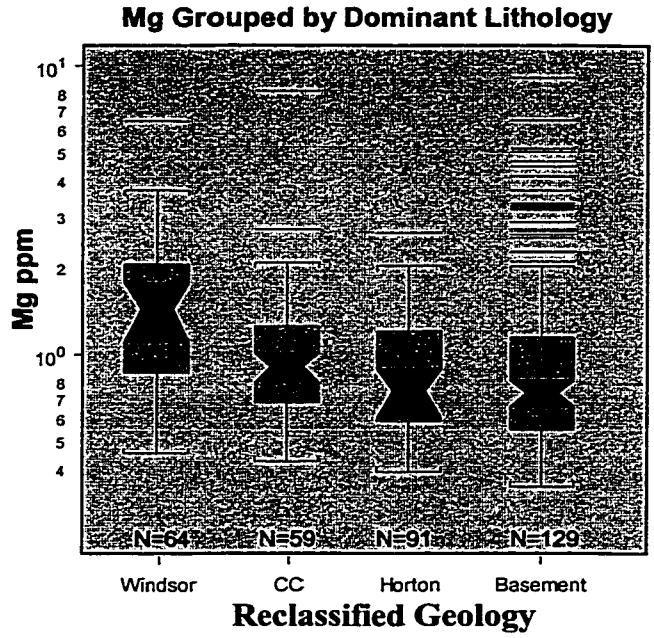
Mg Grouped by Dominant Lithology
Mg ppm
N=64
N=59
N=91
N=129
Windsor
CC
Horton
Basement
Reclassified Geology

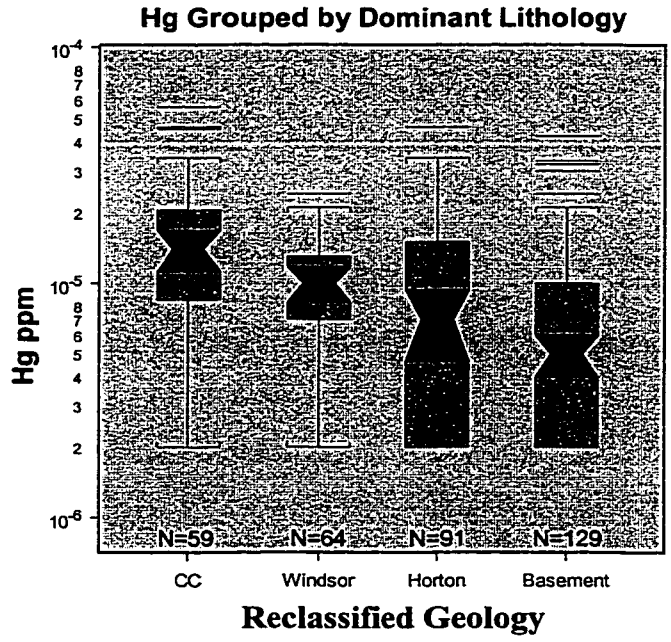
Hg Grouped by Dominant Lithology
Hg ppm
N=59
N=64
N=91
N=129
CC
Windsor
Horton
Basement
Reclassified Geology

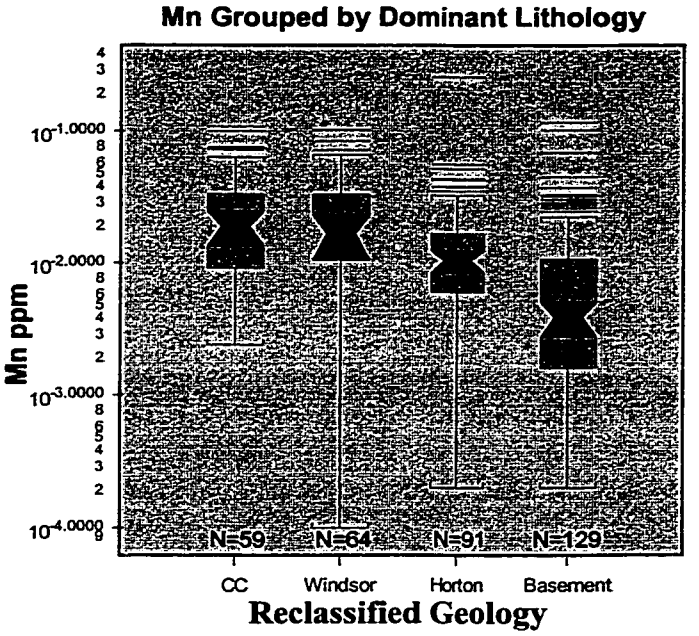
Mn Grouped by Dominant Lithology
Mn ppm
N=59
N=64
N=91
N=129
CC
Windsor
Horton
Basement
Reclassified Geology

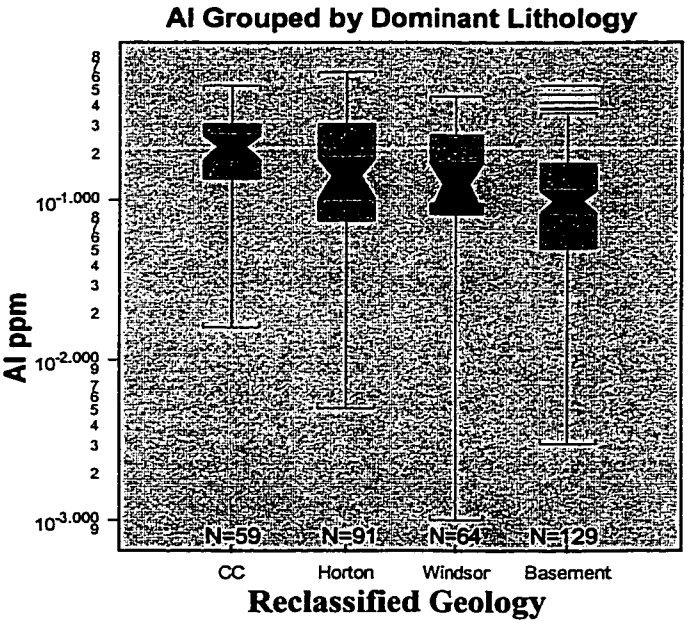
Al Grouped by Dominant Lithology
Al ppm
N=59
N=91
N=64
N=129
CC
Horton
Windsor
Basement
Reclassified Geology

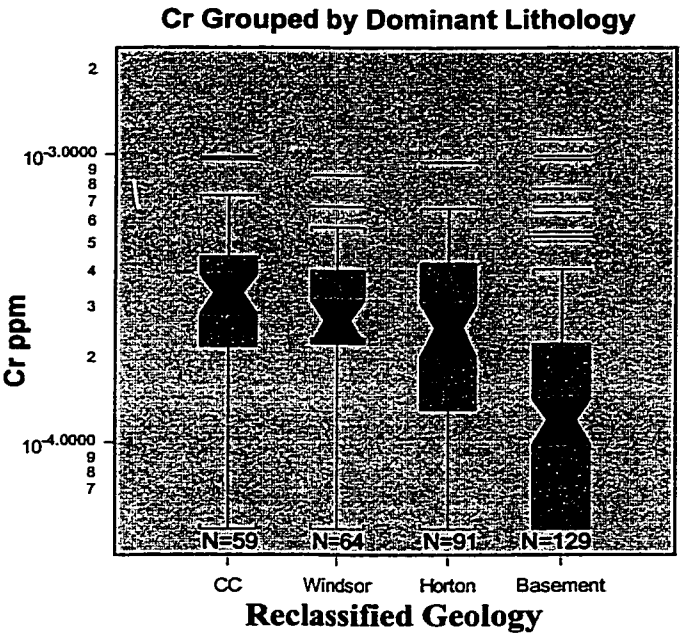
Cr Grouped by Dominant Lithology
Cr ppm
2
10-3.0000
9
8
7
6
5
4
3
2
10-4.0000
9
8
7
N=59
N=64
N=91
N=129
CC
Windsor
Horton
Basement
Reclassified Geology

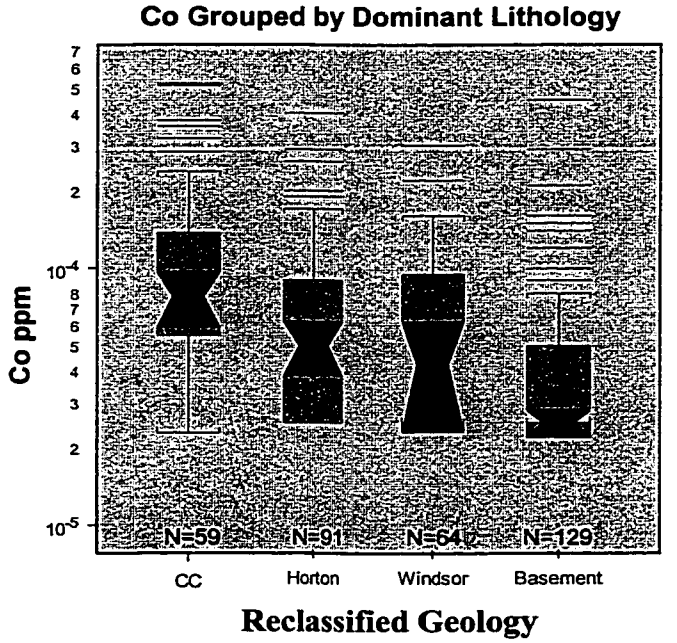
Co Grouped by Dominant Lithology
Co ppm
7
6
5
4
3
2
10-4
8
7
6
5
4
3
2
10-5
N=59
N=91
N=64
N=129
CC
Horton
Windsor
Basement
Reclassified Geology

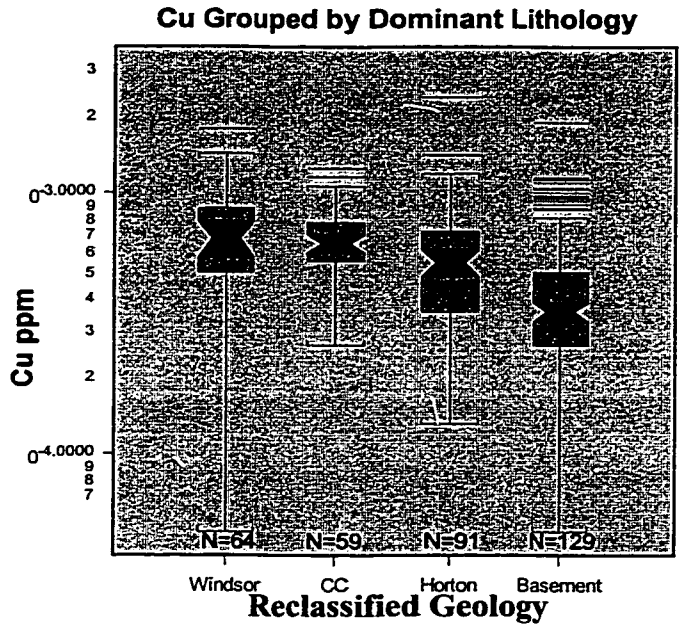
Cu Grouped by Dominant Lithology
Cu ppm
3
2
$0^{-3.0000}$
9
8
7
6
5
4
3
2
$0^{-4.0000}$
9
8
7
N=64
N=59
N=91
N=129
Windsor
CC
Horton
Basement
Reclassified Geology

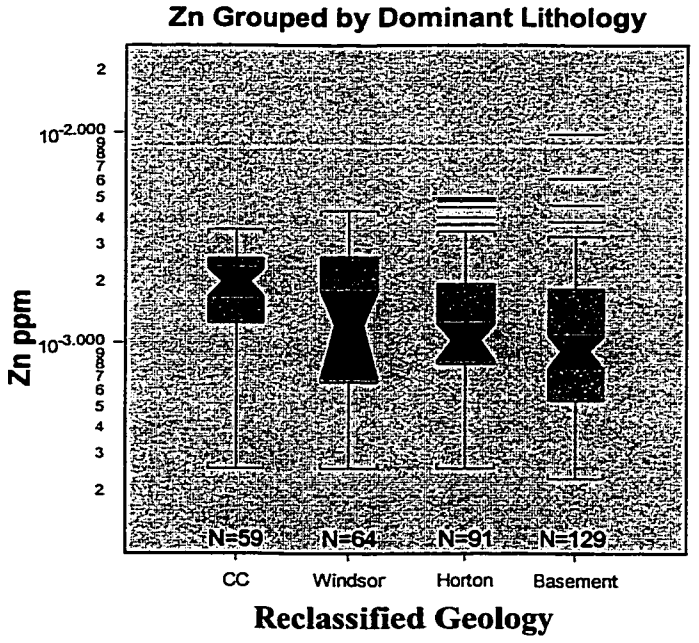
Zn Grouped by Dominant Lithology
Zn ppm
2
$10^{-2.000}$
9
8
7
6
5
4
3
2
$10^{-3.000}$
9
8
7
6
5
4
3
2
N=59
N=64
N=91
N=129
CC
Windsor
Horton
Basement
Reclassified Geology

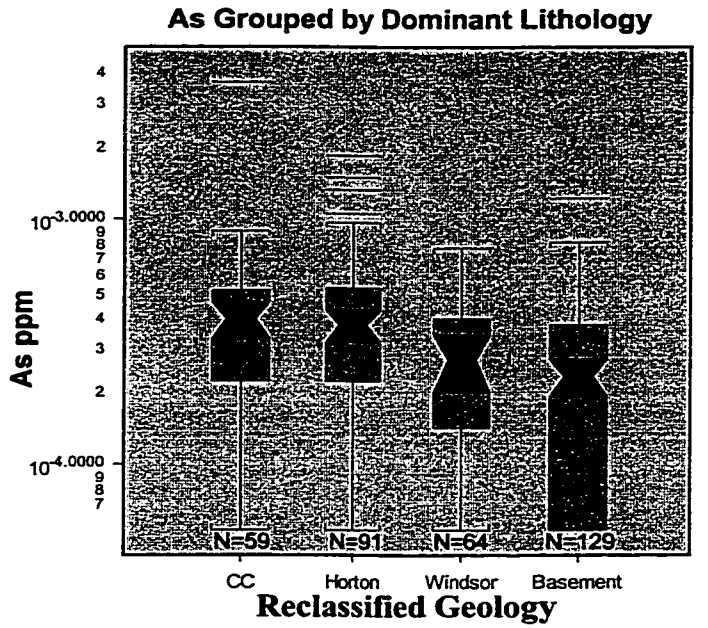
As Grouped by Dominant Lithology
As ppm
$10^{-3.0000}$
$10^{-4.0000}$
N=59
N=91
N=64
N=129
CC
Horton
Windsor
Basement
Reclassified Geology

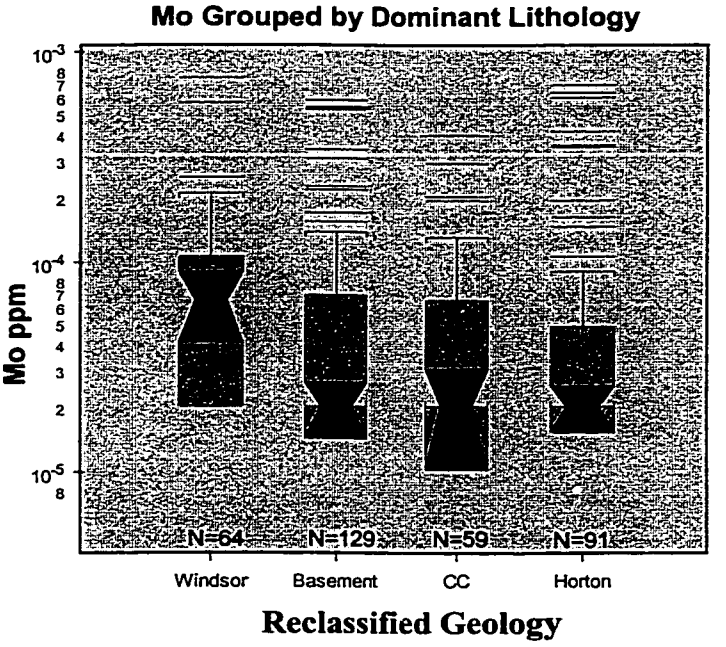
Mo Grouped by Dominant Lithology
Mo ppm
10^{-3}
10^{-4}
10^{-5}
N=64
N=129
N=59
N=91
Windsor
Basement
CC
Horton
Reclassified Geology

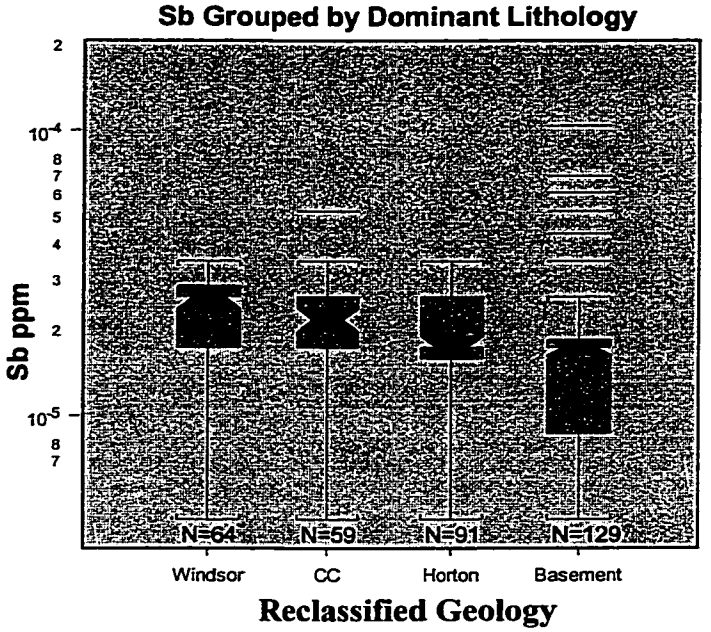
Sb Grouped by Dominant Lithology
Sb ppm
N=64
N=59
N=91
N=129
Windsor
CC
Horton
Basement
Reclassified Geology

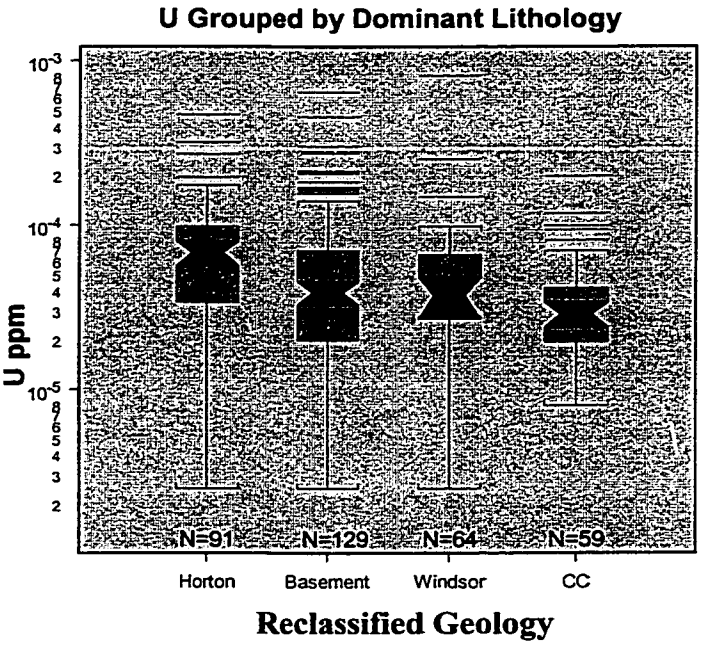
U Grouped by Dominant Lithology
U ppm
N=91
N=129
N=64
N=59
Horton
Basement
Windsor
CC
Reclassified Geology

Appendix F

Results of area cross tabulation and calculation of Yule's coefficient for metallic elements in the stream water and balsam fir twig surveys.

Comparison of Zn, using interpolated grids as the zones of influence

Area Cross Tabulation		Percentiles from Stream Water Survey						
		< 25 %	25%	50%	75%	90%	95%	98%
Percenitles From Balsam Fir Survey	< 25 %	17.55	35.23	36.65	34.09	10.47	0	0
	25%	20.98	34.63	42.45	32.67	0.73	0	0
	50%	55.04	39.55	37.45	23.3	6.34	1.66	2.85
	75%	40.3	30.62	15.1	13.48	7.41	1.85	1.84
	90%	16.9	16.85	7.61	5.5	1.52	4.55	0.94
	95%	1.71	2.62	0.85	0.49	0.11	0.38	0.84
	98%	0.41	0.94	0.26	0.05	0.05	0.11	0.31
	99%	0.51	2.2	0.73	0	0.02	0.21	0.67

Yules Coefficient		Percentiles from Stream Water Survey						
		< 25 %	25%	50%	75%	90%	95%	98%
Percenitles From Balsam Fir Survey	< 25 %	-0.2384	-0.1587	-0.1289	-0.0277	0.9584	0.941	0.8495
	25%	-0.2629	-0.1929	-0.0978	0.2145	0.9748	0.964	0.9063
	50%	-0.1477	-0.1629	-0.0383	0.2325	0.4547	0.3712	0.6447
	75%	-0.0493	-0.1124	-0.0084	0.2568	0.5154	0.4388	0.7585
	90%	0.1064	-0.0613	0.0577	0.374	0.5756	0.6682	0.8893
	95%	0.2181	-0.022	0.0954	0.4334	0.6165	0.7043	0.9172
	98%	0.2838	0.0107	0.1252	0.4621	0.6395	0.7238	0.9224

Comparison of Sr, using interpolated grids as the zones of influence

Area Cross Tabulation		Percentiles from Stream Water Survey						
		< 25 %	25%	50%	75%	90%	95%	98%
Percenitles From Balsam Fir Survey	< 25 %	65.78	42.09	30.04	14.73	5.58	1.74	0.16
	25%	52.79	41.08	28.88	16.88	3.79	2.2	0.12
	50%	33.55	52.54	45.53	32.41	1.78	6.17	0.89
	75%	4.51	17.67	26.49	15.35	3.65	1.3	6.34
	90%	0	1.41	11.12	8.8	3.14	1.59	0
	95%	0	0.21	3.74	4.45	6.1	2.84	0
	98%	0	0	2.18	1.74	0.72	0.88	0
	99%	0	0.02	2.69	1.48	0	0	0

Yules Coefficient		Percentiles from Stream Water Survey						
		< 25 %	25%	50%	75%	90%	95%	98%
Percenitles From Balsam Fir Survey	< 25 %	0.2486	0.2253	0.2171	0.2024	0.3859	0.6673	0
	25%	0.356	0.2988	0.2632	0.2763	0.4116	0.669	0.6518
	50%	0.5655	0.4434	0.3263	0.4004	0.3784	0.5741	0.4423
	75%	0	0.7253	0.4062	0.4064	0.2369	0	0
	90%	0	0.8423	0.4562	0.4825	0.3152	0	0
	95%	0	0.9213	0.2781	0.1854	0.1842	0	0
	98%	0	0.8814	0.1336	0	0	0	0

Comparison of Pb, using interpolated grids as the zones of influence

Area Cross Tabulation		Percentiles from Stream Water Survey						
		< 25 %	25%	50%	75%	90%	95%	98%
Percentiles From Balsam Fir Survey	< 25 %	67.32	32.31	51.91	11.94	2.34	0.78	0.16
	25%	39.72	38.56	39.89	27.8	6.68	2.03	1.39
	50%	22.29	60.11	37.27	41.82	9.18	3.66	1.19
	75%	12.36	30.28	22.13	5.3	5.05	4.29	0
	90%	0.62	2.4	0.46	2	0.1	1.94	1.26
	95%	0.06	1.08	0.47	1.38	1.71	1.32	0.79
	98%	0.04	0.12	0.25	0.83	1.12	0.96	0
	99%	1.84	0.1	3.83	1.97	0.36	0.15	0

Yules Coefficient		Percentiles from Stream Water Survey						
		< 25 %	25%	50%	75%	90%	95%	98%
Percentiles From Balsam Fir Survey	< 25 %	0.285	0.1261	0.3404	0.4267	0.5271	0.6691	0.9512
	25%	0.2887	0.0883	0.2	0.2649	0.3083	0.1968	0.1785
	50%	0.1951	0.0731	0.1068	0.3287	0.4124	0.3473	0.3756
	75%	0.3015	0.3422	0.4208	0.5185	0.5962	0.6387	0.649
	90%	0.2439	0.3842	0.3692	0.4399	0.4115	0.2981	0.0318
	95%	0.1178	0.3701	0.2574	0.2826	0.2226	-0.7773	0
	98%	0.0185	0.2956	0.0812	-0.087	-0.2154	0	0

Comparison of Mn, using interpolated grids as the zones of influence

Area Cross Tabulation		Percentiles from Stream Water Survey						
		< 25 %	25%	50%	75%	90%	95%	98%
Percentiles From Balsam Fir Survey	< 25 %	87.91	56.64	38.94	12.35	11.58	4.99	3.29
	25%	25.97	34.13	38.58	12.03	1.82	0.2	0
	50%	25.15	63.95	65.77	38.33	5.55	1.74	1.36
	75%	0	0.35	6.25	9.74	6.91	0.34	0
	90%	0	0.3	1.02	7.06	2.26	4.42	0.56
	95%	0	0.13	0.24	3.27	0.6	3.42	0.34
	98%	0	0.08	0.22	2.92	0	0	0
	99%	0	0.13	1.49	0.58	0	0	0

Yules Coefficient		Percentiles from Stream Water Survey						
		< 25 %	25%	50%	75%	90%	95%	98%
Percentiles From Balsam Fir Survey	< 25 %	0.3493	0.265	0.2019	0.0032	0.0435	0.043	0.2045
	25%	0.3737	0.2651	0.2739	0.1125	0.1106	0.0039	0.0201
	50%	0	0.7804	0.6257	0.4785	0.4448	0.2378	0.2646
	75%	0	0.7583	0.6864	0.5001	0.5839	0.3848	0.4058
	90%	0	0.7397	0.6218	0.4287	0.5421	0.4011	0.4437
	95%	0	0.6691	0.4081	0	0	0	0
	98%	0	0.5997	0.0215	0	0	0	0

Comparison of Mg, using interpolated grids as the zones of influence

Area Cross Tabulation		Percentiles from Stream Water Survey						
		< 25 %	25%	50%	75%	90%	95%	98%
Percentiles From Balsam Fir Survey	< 25 %	54.45	50.83	39.48	17.92	5.43	1.03	0.38
	25%	40.29	35.22	38.55	25.1	9.78	3.51	0.87
	50%	24.85	38.78	54.07	38.85	17.02	3.5	1.94
	75%	13.36	14.43	12.32	5.76	1.48	0.2	0.22
	90%	9.36	9.55	4.66	2.06	1.98	0.17	0.21
	95%	5.85	1.22	1.12	0.37	0.59	0.1	0.35
	98%	2.74	0	0.95	0.07	0.28	0.02	0
	99%	7	0	0.08	0.12	0.01	0	0

Yules Coefficient		Percentiles from Stream Water Survey						
		< 25 %	25%	50%	75%	90%	95%	98%
Percentiles From Balsam Fir Survey	< 25 %	0.0913	0.1348	0.1471	0.1154	-0.0144	-0.1204	-0.2164
	25%	0.0809	0.0939	0.0921	0.085	0.005	0.0026	-0.0726
	50%	-0.1787	-0.1642	-0.143	-0.0606	-0.0087	0.0812	0.0866
	75%	-0.2864	-0.2447	-0.1787	-0.0283	-0.0519	0.011	-0.0566
	90%	-0.4974	-0.3338	-0.2669	-0.0796	-0.049	0.0119	-0.1528
	95%	-0.6203	-0.4219	-0.4222	-0.2682	-0.3335	-0.2828	-0.2151
	98%	-0.7843	-0.6558	-0.5304	-0.4702	-0.2791	-0.1753	-0.1045

Comparison of Fe, using interpolated grids as the zones of influence

Area Cross Tabulation		Percentiles from Stream Water Survey						
		< 25 %	25%	50%	75%	90%	95%	98%
Percentiles From Balsam Fir Survey	< 25 %	76.09	38.39	21.48	2.75	0.02	0	0
	25%	32.51	62.28	56.31	33.23	1.78	4.32	0
	50%	9.34	34.69	50.75	43.97	2.22	5.47	0.11
	75%	4.8	7.1	15.5	19.72	6.61	6.92	1.64
	90%	0.32	6.49	10.55	2.56	1.09	1.86	0.54
	95%	0	2.78	0.01	1.81	0.05	0.28	1.62
	98%	0	0.17	0	1.64	0	0	0
	99%	0	0	0	0.19	0	0	0

Yules Coefficient		Percentiles from Stream Water Survey						
		< 25 %	25%	50%	75%	90%	95%	98%
Percentiles From Balsam Fir Survey	< 25 %	0.524	0.485	0.6666	0.9362	0	0	0
	25%	0.4777	0.3761	0.3823	0.4686	0.4545	0.5577	0.497
	50%	0.4236	0.338	0.3502	0.5014	0.4659	0.5334	0.4461
	75%	0.6973	0.2156	0.1827	0.338	0.3713	0.4774	0.38
	90%	0	0.208	0.4652	0.462	0.5229	0.6589	0.5653
	95%	0	0.5149	0.6951	0	0	0	0
	98%	0	0	0	0	0	0	0

Comparison of Cu, using interpolated grids as the zones of influence

Area Cross Tabulation		Percentiles from Stream Water Survey						
		< 25 %	25%	50%	75%	90%	95%	98%
Percentiles From Balsam Fir Survey	< 25 %	75.39	49.37	120.32	0	42.72	0	0
	25%	45.97	39.63	65.16	0	15.89	0	0
	50%	0	0	0	0	0	0	0
	75%	33.8	15.68	16.35	0	0	0	0
	90%	2.76	12.01	19.72	0	0	0	0
	95%	0	0	0	0	0	0	0
	98%	0.16	2.23	0	0	0	0	0
	99%	0.15	0	0	0	0	0	0

Yules Coefficient		Percentiles from Stream Water Survey						
		< 25 %	25%	50%	75%	90%	95%	98%
Percentiles From Balsam Fir Survey	< 25 %	-0.0558	-0.1319	-0.2504	-0.2504	0	0	0
	25%	-0.1064	-0.1889	0	0	0	0	0
	50%	-0.1064	-0.1889	0	0	0	0	0
	75%	0.369	0.0321	0	0	0	0	0
	90%	0.2625	0	0	0	0	0	0
	95%	0.2625	0	0	0	0	0	0
	98%	0	0	0	0	0	0	0

Comparison of Cr, using interpolated grids as the zones of influence

Area Cross Tabulation		Percentiles from Stream Water Survey						
		< 25 %	25%	50%	75%	90%	95%	98%
Percentiles From Balsam Fir Survey	< 25 %	96.68	0	41.58	16.16	18.68	6.94	2.41
	25%	104.65	0	37.8	24.06	8.75	9.07	0.45
	50%	101.39	0	23.17	10.34	5.93	0	0
	75%	39.07	0	7.83	0.15	0	0	0
	90%	31.25	0	3.06	1.58	0.12	0	0
	95%	2.22	0	2.01	0.61	0.9	0	0
	98%	0.08	0	1.57	0.74	1.22	0	0
	99%	0	0	0.03	1.05	1.62	0	0

Yules Coefficient		Percentiles from Stream Water Survey						
		< 25 %	25%	50%	75%	90%	95%	98%
Percentiles From Balsam Fir Survey	< 25 %	-0.1425	-0.1425	-0.1412	-0.2425	-0.2474	-0.605	-0.6857
	25%	-0.2096	-0.2096	-0.2475	-0.3013	-0.9947	-0.9888	-0.9824
	50%	-0.1957	-0.1957	-0.2531	-0.2523	0	0	0
	75%	-0.0935	-0.0935	-0.0432	-0.052	0	0	0
	90%	0.4568	0.4568	0.3706	0.3576	0	0	0
	95%	0.8381	0.8381	0.5585	0.4786	0	0	0
	98%	0	0	0.898	0.5835	0	0	0

Comparison of Co, using interpolated grids as the zones of influence

Area Cross Tabulation		Percentiles from Stream Water Survey						
		< 25 %	25%	50%	75%	90%	95%	98%
Percentiles From Balsam Fir Survey	< 25 %	63.51	67.71	32.99	12.54	0.03	0	0
	25%	28.2	51	52.34	20.03	17.81	5.76	0
	50%	35.88	30.9	41.91	18.37	1.27	4.72	3.16
	75%	17.76	9.68	17.23	27.03	8.08	3.13	0.97
	90%	2.32	2.34	4.43	7.46	2.82	2.2	1.26
	95%	0.44	1.91	1.84	2.19	0.01	0	0.29
	98%	0	0	0	0	0	0	0
	99%	1.75	0.09	0	0	0	0	0

Yules Coefficient		Percentiles from Stream Water Survey						
		< 25 %	25%	50%	75%	90%	95%	98%
Percentiles From Balsam Fir Survey	< 25 %	0.1995	0.3305	0.4116	0.9342	0.99	0.9842	0.9776
	25%	0.0467	0.197	0.2493	0.1819	0.4001	0.9822	0.9746
	50%	0.1118	0.2727	0.3793	0.3043	0.3527	0.5381	0.9853
	75%	0.2158	0.3058	0.3868	0.3992	0.5123	0.6748	0.8511
	90%	0.0086	0.0565	0.1257	0.0132	0.2108	0.4229	0.4845
	95%	-0.7662	-0.951	-0.9163	-0.9553	-0.9341	-0.8985	0
	98%	-0.7663	-0.9532	-0.92	0	0	0	0

Comparison of Ba, using interpolated grids as the zones of influence

Area Cross Tabulation		Percentiles from Stream Water Survey						
		< 25 %	25%	50%	75%	90%	95%	98%
Percentiles From Balsam Fir Survey	< 25 %	69.36	46.08	17.19	5.92	3.45	0	0
	25%	52.99	40.5	37.67	2.94	0.02	0.06	0
	50%	24.4	55.16	60.14	26.18	5.85	6.62	0.99
	75%	5.09	12.17	21.48	33.21	15.89	6.21	2.62
	90%	0.07	1.31	15.11	9.69	2.77	1.68	0.32
	95%	0	0	0.04	3.18	1.43	3	0.88
	98%	0	0	0	0	0	0	0
	99%	0	0	3.99	0.51	0	0.17	0.39

Yules Coefficient		Percentiles from Stream Water Survey						
		< 25 %	25%	50%	75%	90%	95%	98%
Percentiles From Balsam Fir Survey	< 25 %	0.353	0.4235	0.4058	0.3994	0	0	0
	25%	0.4771	0.4572	0.5724	0.5907	0.8535	0.8108	0.7466
	50%	0.5657	0.5492	0.5414	0.5118	0.4969	0.6334	0.6835
	75%	0.8847	0.7303	0.3892	0.3653	0.4483	0.5029	0.5681
	90%	0	0	0.5338	0.5489	0.6331	0.6655	0.7029
	95%	0	0	0.2258	0.3948	0.5498	0.7024	0.7636
	98%	0	0	0.2258	0.3948	0.5498	0.7024	0.7636

Comparison of Al, using interpolated grids as the zones of influence

Area Cross Tabulation		Percentiles from Stream Water Survey						
		< 25 %	25%	50%	75%	90%	95%	98%
Percenitles From Balsam Fir Survey	< 25 %	60.07	32.96	48.96	20.97	2.97	0.87	3.44
	25%	57.58	50.68	38.63	31.09	6.54	1.31	3.73
	50%	17.93	49.37	30.71	20.78	10.4	0.91	0.46
	75%	18.51	15.04	23.8	10.07	12.52	0.03	0.2
	90%	0	0.07	4.01	4.93	3.08	6.07	1.46
	95%	0	0	4.62	4.32	0.08	0	0
	98%	0	0	2.34	0.02	0	0	0
	99%	0	0	0	0	0	0	0

Yules Coefficient		Percentiles from Stream Water Survey						
		< 25 %	25%	50%	75%	90%	95%	98%
Percenitles From Balsam Fir Survey	< 25 %	0.165	0.0602	0.1491	0.2016	0.0407	-0.0581	-0.0102
	25%	0.244	0.1378	0.1408	0.2264	0.0399	-0.1427	-0.0822
	50%	0.1572	0.245	0.1949	0.2864	0.1801	-0.098	-0.2129
	75%	0	0.9112	0.4174	0.3929	0.4973	0.1206	0
	90%	0	0	0.1567	-0.614	0	0	0
	95%	0	0	-0.7013	0	0	0	0
	98%	0	0	0	0	0	0	0

Comparison of Sb, using interpolated grids as the zones of influence

Area Cross Tabulation		Percentiles from Stream Water Survey						
		< 25 %	25%	50%	75%	90%	95%	98%
Percenitles From Balsam Fir Survey	< 25 %	8.66	184.53	107.57	16.31	10	22.37	13.16
	25%	117.81	62.28	84.02	107.73	38.87	11.51	7.26
	50%	178.53	81.91	124.48	70.98	20.07	8.11	3.73
	75%	60.16	32.23	43.33	13.26	0.54	0.77	0.07
	90%	32	23.36	16.06	7.9	2.55	6.43	0.03
	95%	4.61	8.3	4.78	2.54	2.47	1.15	0
	98%	3.7	2.53	3.32	3.19	1.78	0.02	0
	99%	0.61	0.13	0.4	0	0	0	0

Yules Coefficient		Percentiles from Stream Water Survey						
		< 25 %	25%	50%	75%	90%	95%	98%
Percenitles From Balsam Fir Survey	< 25 %	-0.6423	0.0057	0.0856	-0.1579	-0.3439	-0.4435	-0.6217
	25%	-0.2751	-0.0965	-0.1496	-0.232	-0.2973	-0.4849	-0.7026
	50%	-0.1524	-0.1134	-0.1701	-0.1864	-0.1763	-0.5978	-0.4654
	75%	-0.0826	-0.0867	-0.0409	0.0207	0.0135	-0.6728	-0.565
	90%	0.0449	0.0062	0.0461	0.0746	-0.176	0	0
	95%	-0.0221	0.0654	0.0889	0.0218	-0.7577	0	0
	98%	-0.2952	-0.1456	0	0	0	0	0

Comparison of As, using interpolated grids as the zones of influence.

Area Cross Tabulation		Percentiles from Stream Water Survey						
		< 25 %	25%	50%	75%	90%	95%	98%
Percenitles From Balsam Fir Survey	< 25 %	49.84	54.82	37.15	14.33	2.38	0.01	0
	25%	57.06	39.01	52.6	10.89	1.48	4.62	0
	50%	39.54	29.14	52.29	31.22	9.22	10.09	1.23
	75%	1.96	11.81	14.14	21.95	5.23	2.81	5.96
	90%	10.41	9.73	3.73	5.56	2.1	0	0
	95%	0.77	1.92	0.66	1.92	2.51	0	0
	98%	0.05	1.38	0.42	0	4.34	0	0
	99%	0	0.54	0.03	0	0	0	0

Yules Coefficient		Percentiles from Stream Water Survey						
		< 25 %	25%	50%	75%	90%	95%	98%
Percenitles From Balsam Fir Survey	< 25 %	0.0893	0.2134	0.2859	0.4952	0.9402	0	0
	25%	0.1927	0.245	0.391	0.4617	0.4309	0.9803	0.9668
	50%	0.2804	0.204	0.3654	0.3721	0.3023	0.6616	0.6655
	75%	0.0252	-0.0367	0.1647	0.2399	-0.8646	-0.8171	-0.7097
	90%	0.4242	0.1948	0.3948	0.5185	-0.8691	0	0
	95%	0.7521	0.2262	0.4243	0.6287	-0.8126	0	0
	98%	0	-0.5942	-0.6436	-0.5901	-0.4719	0	0